TECHNICAL UNIVERSITY OF LIBEREC
Faculty of Mechanical Engineering

Design Optimization of Linear Vibratory Conveyors

Dissertation

Study programme: P2302 – Machines and Equipment
Study branch: 2302V010 – Machine and Equipment Design

Author: **M.A. Martin Sturm**
Supervisor: prof. Ing. Lubomír Pešík, CSc.

Liberec 2018

Prohlášení / Declaration

Byl jsem seznámen s tím, že na mou disertační práci se plně vztahuje zákon č. 121/2000 Sb., o právu autorském, zejména § 60 – školní dílo.

Beru na vědomí, že Technická univerzita v Liberci (TUL) nezasahuje do mých autorských práv užitím mé disertační práce pro vnitřní potřebu TUL.

Užiji-li disertační práci nebo poskytnu-li licenci k jejímu využití, jsem si vědom povinnosti informovat o této skutečnosti TUL; v tomto případě má TUL právo ode mne požadovat úhradu nákladů, které vynaložila na vytvoření díla, až do jejich skutečné výše.

Disertační práci jsem vypracoval samostatně s použitím uvedené literatury a na základě konzultací s vedoucím mé disertační práce a konzultantem.

Současně čestně prohlašuji, že tištěná verze práce se shoduje s elektronickou verzí, vloženou do IS STAG.

I have been notified that my dissertation is fully covered by Act No.121 / 2000 Sb. on copyright, especially § 60 - school work.

I am fully aware that the Technical University of Liberec (TUL) is not interfering with my copyright by using my dissertation for internal purposes.

If I use my dissertation or grant a license for its use, I am aware that I must inform TUL of this fact. In this case TUL has the right to seek that I pay the expenses invested in the creation of my dissertation to the full amount.

I declare that this dissertation is developed independently, using the cited literature and on the basis of consultation with the supervisor of this dissertation.

By the same time, I declare that the printed version of the dissertation work coincides with the electronic version uploaded in IS STAG.

Date:

Signature:

Thanks

This dissertation is based on knowledge, calculations, measurements and design activities combined during my doctoral studies at the Department of Machine Parts and Mechanisms, Faculty of Mechanical Engineering of the Technical University in Liberec and at the Department of Machine Parts and Mechanisms, Faculty of Mechanical Engineering of the University of Applied Science Zittau/Görlitz.

First and foremost, I like to express my sincere gratitude to my supervising Professor Ing. Lubomír Pešík, CSc., for his guidance, great support and encouragement throughout my PhD research studies. Without his guidance and persistent support this dissertation would not have been possible.

I like to extend my sincere thanks to my colleagues at the Faculty of Mechanical Engineering of the University of Applied Science Zittau/Görlitz, Dipl.-Ing. (FH) Hans-Armin Kammler for his generous assistance, determine the results of the various tests in conjunction with this dissertation and Dipl.-Ing. (FH) Wolfgang Meinck for his support and assistance, manufacturing necessary parts and helping to get things managed.

Last but not least I like to thank my family for their unconditional support, encouragement and love. Especially my wife and son gave strength to me and kept me laughing during the tough times of my PhD studies.

Annotation

STURM, M. Design Optimization of Linear Vibratory Conveyors. Liberec: Department of Machine Parts and Mechanisms, Faculty of Mechanical Engineering, Technical University of Liberec, 2018. 114 pages dissertation, leading: Prof. Ing. Lubomír PEŠIK, CSc.

This dissertation deals with the functional and performance optimization of vibratory conveyors in conjunction with the reduction of vibration to the ground with reference to the needs of practice. Based on an analysis of the current transport process of bulk materials, dynamical models are developed, enabling a systematic modification of the conveying process. With regards to the results of the developed modification possibilities, an efficient model for the optimum transport of the goods by simultaneous reduction of vibration transmission to the ground is developed.

To achieve the goal of this dissertation, a comprehensive dynamic analysis and optimization of the transport process is done, both with regard to the correct tuning of the vibratory conveyor and maintaining the required dynamic parameters, as well as with regard to the mechanical properties of the transported objects. Based on the results of the optimization dynamic parameters are proposed and measured. Some of them are implemented into functional samples in which the theoretical knowledge is verified by measurements of kinematic variables.

Keywords

Vibration technology, vibratory conveyors, vibration, modifying vibration, one-mass vibratory conveyor, two-mass vibratory conveyor.

Content

Prohlášení / Declaration 1
Thanks 2
Annotation 3
List of symbols, abbreviations and terms 6
List of Figures 11
List of tables 16
1 Introduction 17
2 Objective of the dissertation 20
3 Vibratory conveyors and their underlying systems 21
3.1 General conveyor designs 23
3.2 Vibratory conveyors for linear motion 25
4 Mechanical models of vibratory conveyors 28
4.1 Models for reciprocating oscillation of a one-mass system 28
4.1.1 Model for a linear conveyor of variant A 29
4.1.2 Model for a linear conveyor of variant B 32
4.2 Model for reciprocating oscillation of a two-mass system 35
4.3 Conveyed goods 39
4.4 Influence of the conveyed goods to vibratory conveyors 41
4.5 The power effect of the vibratory conveyor on the subsoil 42
5 Analysis and optimization of the transport process 44
5.1 Selection of a representative vibratory conveyor 44
5.2 Identification of dynamic parameters of the vibratory conveyor 45
5.2.1 Mass and inertia parameters 46
5.2.2 Springs and damping conditions 47
5.2.2 Natural frequencies of the conveyor 49
5.2.4 Analysis of the conveying element motion 51
5.2.5 Determination of the mass centre point and the centre of elasticity 54
5.2.6 Attitude of the conveyed goods 57
5.2.7 Vibration transmission to the ground 58

5.3 Analysis of dynamic parameters ... 59
5.3.1 Determined data of the vibratory conveyor ... 59
5.3.2 Amplitude and stiffness characteristics of the vibratory conveyor ... 62
5.3.3 Time and frequency characteristics of the vibratory conveyor ... 64
5.3.5 The power effect of the vibratory conveyor on the foundation ... 65
6 Improvement of the conveyor ... 67
6.1 Improvement of the one-mass system ... 67
6.1.1 Modification of the centre of elasticity ... 71
6.1.2 Modification by the use of guiding levers ... 73
6.1.3 Simulation of the modification by using guiding levers ... 74
6.1.4 Experimental determination and validation of the modification ... 75
6.1.5 Improvement of the conveying process ... 83
6.1.6 Transmission of Vibration to the ground after modification ... 83
6.2 Model of a two-mass system ... 84
6.2.1 Simulation of the conveying process ... 87
6.2.2 Experimental determination of the two-mass systems characteristic values ... 91
6.2.3 Effect of the conveyed goods on the two-mass system ... 99
6.2.4 Evaluation of the Two-mass system ... 104
6.2.5 Recommendations ... 104
7 Conclusion ... 107
Literature ... 109
List of Authors Publications ... 113
Appendix ... 114

List of symbols, abbreviations and terms

General symbols, abbreviations and terms

A	Discharge point for spring force A
B	Discharge point for spring force B
N	Carrier
O	Object
S	Inertial mass
V	Buffers
P	Floor
B	Vibration exciter

Latin symbols and terms

b	Damping coefficient	[kg s^{-2}]
b_{AS}	Damping coefficient in point A corresponding to distance “s”	[kg s^{-2}]
b_{BS}	Damping coefficient in point B corresponding to distance “s”	[kg s^{-2}]
b_x	Damping coefficient in x-direction	[kg s^{-2}]
b_y	Damping coefficient in y-direction	[kg s^{-2}]
b_z	Damping coefficient in z-direction	[kg s^{-2}]
f	Frequency	[Hz]
f_1	Natural frequency of mass 1 of a two-mass conveyor	[Hz]
f_2	Natural frequency of mass 2 of a two-mass conveyor	[Hz]
f_{ON}	Friction coefficient between objects and conveying element	
f_{VO}	Internal friction coefficient between object elements	
F	Force	[N]

F_0	Initial force	[N]
F_E	Excitation force	[N]
F_{P12}	Force of pneumatic spring between mass 1 and mass 2 of a two-mass conveyor	[N]
F_{R1}	Internal lever force corresponding to mass 1 of a two-mass conveyor	[N]
F_{R21}	Internal lever force corresponding to mass 2 and mass 1 of a two-mass conveyor	[N]
F_{TVO}	Friction force between object layers	[N]
F_{VOx}	Internal friction force of objects in x-direction	[N]
J_z	Mass moment of inertia in z-direction	[kg m²]
J_{Oz}	Mass moment of inertia of objects in z-direction	[kg m²]
k	Spring stiffness	[N m^{-1}]
k_{As}	Spring stiffness in point A corresponding to distance “s” of lever guided one mass conveyor	[N m^{-1}]
k_{Bs}	Spring stiffness in point B corresponding to distance “s” of lever guided one mass conveyor	[N m^{-1}]
k_{Ax}	Spring stiffness in x-direction point A	[N m^{-1}]
k_{Bx}	Spring stiffness in x-direction point B	[N m^{-1}]
k_{Az}	Spring stiffness in z-direction point A	[N m^{-1}]
k_{Bz}	Spring stiffness in z-direction point B	[N m^{-1}]
k_s	Spring stiffness corresponding to distance s of lever guided one mass conveyor	[N m^{-1}]
k_z	Total spring stiffness in z-direction	[N m^{-1}]
k_1	Spring stiffness corresponding to mass 1 of a two mass conveyor	[N m^{-1}]
k_{21}	Spring stiffness corresponding to mass 1 and mass 2 of a two mass conveyor	[N m^{-1}]
l	Length of the conveying element	[m]
m	Mass	[kg]
m_O	Mass of object	[kg]
m_1	Mass 1	[kg]
m_2	Mass 2	[kg]

m_3	Mass 3	[kg]
R_1	Lever corresponding to mass 1 of a two-mass conveyor	
R_{21}	Lever corresponding to mass 2 and mass 1 of a two-mass conveyor	
s_N	Displacement of objects	[mm]
s_1	Displacement of mass 1 of a two-mass conveyor	[mm]
s_2	Displacement of mass 2 of a two-mass conveyor	[mm]
s_{10}	Displacement amplitude of mass 1 of a two mass conveyor	[mm]
s_{20}	Displacement amplitude of mass 2 of a two mass conveyor	[mm]
s_{21}	Relative Displacement of mass 2 to mass 1 of a two-mass conveyor	[mm]
$\dot{s}$	Velocity	[mm]
$\ddot{s}_1$	Acceleration of mass 1 of a two-mass conveyor	[mm]
$\ddot{s}_2$	Acceleration of mass 2 of a two-mass conveyor	[mm]
$\ddot{s}_{21}$	Relative acceleration of mass 2 to mass 1 of a two-mass conveyor	[mm]
t	Time	[s]
T	Period of oscillation	[s]
w	Width of the conveying element	[m]
x	Displacement in x-direction	[mm]
x_m	1st amplitude of a free wave	[mm]
x_n	2nd amplitude of a free wave	[mm]
x_0	Displacement amplitude at the beginning of the motion in x-direction	[mm]
x_1	Displacement in x-direction corresponding to mass 1 of a two-mass conveyor	[mm]
x_2	Displacement in x-direction corresponding to mass 2 of a two-mass conveyor	[mm]
x_{21}	Relative displacement in x-direction corresponding to mass 1 and mass 2 of a two-mass conveyor	[mm]
$\dot{x}$	Velocity in x-direction	[m s^{-1}]
$\ddot{x}$	Acceleration in x-direction	[m s^{-2}]
$\ddot{x}_1$	Acceleration of mass 1 in x-direction of a two-mass conveyor	[m s^{-2}]

$\ddot{x}_2$	Acceleration of mass 2 in x-direction of a two-mass conveyor	[m s^{-2}]
z	Displacement in z-direction	[mm]
z_0	Displacement amplitude at the beginning of the motion in z-direction	[mm]
z_1	Displacement in z-direction corresponding to mass 1 of a two-mass conveyor	[mm]
z_{21}	Relative displacement in z-direction of mass 2 to mass 1 of a two-mass conveyor	[mm]
$\dot{z}$	Velocity in z-direction	[m s^{-1}]
$\ddot{z}$	Acceleration in z-direction	[m s^{-2}]
$\ddot{z}_1$	Acceleration of mass 1 in z-direction of a two-mass conveyor	[m s^{-2}]
$\ddot{z}_2$	Acceleration of mass 2 in z-direction of a two-mass conveyor	[m s^{-2}]

Greek symbols and terms

β	Angle of force transmission to mass for simplified model	[°]
β_{NS}	Angle of micro threw of objects	[°]
β_1	Angle of force transmission to mass 1 of a two-mass conveyor	[°]
β_2	Angle of force transmission to mass 2 of a two-mass conveyor	[°]
β_F	Angle of force transmission to mass	[°]
β_{PF}	Angle between force transmission point to mass centre point	[°]
δ	Damping constant	[s^{-1}]
η_A	Distance mass centre point to discharge point A in z-direction	[mm]
η_B	Distance mass centre point to discharge point B in z-direction	[mm]
η_{PF}	Distance mass centre point to force transmission point in z-direction	[mm]
Λ	Logarithmic decrement	
ξ_A	Distance mass centre point to discharge point A	[mm]
ξ_B	Distance mass centre point to discharge point B	[mm]
ξ_{PF}	Distance mass centre point to force transmission point in x-direction	[mm]
ρ	Length of radius vector of force to point of application for simplified model	[mm]

ρ_{PF}	Length of radius vector of force to point of application	[mm]
φ	Rotation angle corresponding to mass moment of inertia	[°]
$\ddot{\varphi}$	Angular acceleration	[° s^{-2}]
ω	Angular frequency	[s^{-1}]
ω_0	Free angular frequency	[s^{-1}]
ω_1	Free angular frequency of mass 1 of a two-mass conveyor	[s^{-1}]
ω_2	Free angular frequency of mass 2 of a two-mass conveyor	[s^{-1}]

List of Figures

Figure 1: Vibratory conveyors as part of assembly line 18

Figure 2: Linear vibratory conveyors 21

Figure 3: Transport of an object by a vibratory conveyor 22

Figure 4: Schematic representation of design variants (A, B, C, D) of vibratory conveyors 24

Figure 5: Vibratory conveyor with rectilinear motion 25

Figure 6: Clamp exciter vibrator on a vibratory conveyor reciprocating 26

Figure 7: Excitation model using a crank mechanism with an electric motor 27

Figure 8: Vibratory conveyor with linear motion in constructive variant A 28

Figure 9: Mechanical model of vibration conveyor with linear motion in the design of variant A 29

Figure 10: Simplified mechanical model of vibration conveyor with linear motion variant A 30

Figure 11: Amplitude over stiffness 3-D graph of a linear vibratory conveyor of variant A 31

Figure 12: Amplitude over time function of a linear vibratory conveyor of variant A 32

Figure13: Guided linear vibratory conveyor of variant B 33

Figure 14: Guided linear vibratory conveyor of variant B with flat springs 33

Figure 15: Mechanical model of vibration conveyor with linear motion in the design of variant B 34

Figure 16: Amplitude over time function of a linear vibratory conveyor of variant B 35

Figure 17: Vibratory conveyor with two masses of variant D 36

Figure 18: Mechanical model of the vibratory conveyor 36

Figure 19: General example of amplitudes of a two mass system 38

Figure 20: Simplified mechanical model of bulk goods being conveyed 40

Figure 21: Time course of dynamic forces transmitted to the conveyors frame and the floor 42

Figure 22: Vibros vibratory conveyor with eccentric drive 44

Figure 23: RFT calibration unit 46

Figure 24: Calibration signal 77.0 Hz 46

Figure 25: Conveying element and its coordinate system defined 46

Figure 26: Characteristic of helical springs of the conveyor in vertical direction 47

Figure 27: Characteristic of helical springs of the conveyor in horizontal direction 48

Figure 28: Time function of acceleration in vertical direction on free oscillation 48

Figure 29: Resonances with sensor position z- and z-direction 50

Figure 30: Resonances with sensor position x- and z-direction 50

Figure 31: Resonances with sensor position x- and y- direction and horizontal excitation 50

Figure 32: Resonances with sensor position x- and z- direction and vertical excitation 51

Figure 33: Operation condition 52

Figure 34: Motion of reference marks 53

Figure 35: Amplitudes in z-direction of reference marks 54

Figure 36: Photographical determination of mass centre point 55

Figure 37: 3D-CAD model of the conveying element 55

Figure 38: Centre of elasticity and mass centre point 56

Figure 39: Recorded motion of an example good 57

Figure 40: Recorded spectrum of vibrations to the ground from 0 – 100 Hz 58

Figure 41: Example for excitation over resonance 59

Figure 42: Mechanical model of the examined conveyor 60

Figure 43: Amplitude over stiffness for the rotation of the linear vibratory conveyor 63

Figure 44: Rotation component of the amplitude in point A of the conveyor 64

Figure 45: Graph amplitude over time for the motion of the linear vibratory conveyor 65

Figure 46: Corresponding stiffness k_{Az} and for k_{Bz} non-rotation condition 68

Figure 47: Corresponding stiffness and k_{Bz} for the selection of test springs 70

Figure 48: Selected spring type for the installation in point A 70

Figure 49: Selected spring type for the installation in point B 71

Figure 50: Spring with spacer 71

Figure 51: Graph amplitude over time for the motion of the modified linear vibratory conveyor 72

Figure 52: Graph amplitude over time – outline influence of rotation 72

Figure 53: Mechanical model variant B of the analysed conveyor 73

Figure 54: Graph amplitude over time for the motion of the simulated linear vibratory conveyor variant B 74

Figure 55: One-mass vibratory conveyor with modified springs 75

Figure 56: Frequencies determined for excitation in x-direction, sensor situated in the geometrical centre of the conveying element 76

Figure 57: Frequencies determined for excitation in x-direction, sensor situated next to the hand-over point of the conveying element 76

Figure 58: Frequencies determined for excitation in y-direction, sensor situated in the geometrical centre of the conveying element 77

Figure 59: Frequencies determined for excitation in y-direction, sensor situated next to the hand-over point of the conveying element 77

Figure 60: Frequencies determined for excitation in z-direction, sensor situated in the geometrical centre of the conveying element 77

Figure 61: Frequencies determined for excitation in z-direction, sensor situated next to the hand-over point of the conveying element 78

Figure 62: New centre of elasticity 79

Figure 63: Excitation frequency of the modified vibratory conveyor 80

Figure 64: Motion of reference marks 81

Figure 65: Amplitudes in z-direction of reference marks after modification 82

Figure 66: Recorded motion of an example good after the modification 83

Figure 67: Recorded spectrum of vibrations to the ground from 0 – 100 Hz after the modification 84

Figure 68: Observed mechanical model of a two-mass linear vibratory conveyor 85

Figure 69: Amplitude over frequency function of the two-mass swing system 86

Figure 70: Amplitude over time function of the implemented two-mass swing system 87

Figure 71: Function model of a two-mass vibratory conveyor 88

Figure 72: Components of mass m_2 89

Figure 73: Components of mass m_1 89

Figure 74: Components of mass m_3 90

Figure 75: Graph amplitude over time for the two-mass conveyor model 90

Figure 76: Two-mass linear vibratory conveyor test model 92

Figure 77: Electromagnetic exciter and its technical data 92

Figure 78: Frequencies determined for excitation in x-direction of the conveying element mass m_2 93

Figure 79: Frequencies determined for excitation in z-direction of the conveying element mass m_2 94

Figure 80: Frequencies determined for excitation in x-direction of mass m_1 95

Figure 81: Frequencies determined for excitation in z-direction of mass m_1 95

Figure 82: Operation controller of 2-mass linear vibratory conveyor on 50 % operation power 96

Figure 83: Excitation frequency during operation in x-direction of the conveying element mass m_2 96

Figure 84: Excitation frequency during operation in x-direction of mass m_1 98

Figure 85: Graph amplitude over time of the tested real two-mass conveyor 98

Figure 86: Amplitude over frequency function of the tested two-mass swing system and its optimum operation point and its presumed amplitude tolerance range 99

Figure 87: Amplitude s_{10} for empty conveying element and added masses 100

Figure 88: Amplitude s_{20} for empty conveying element and added masse 101

Figure 89: Amplitude s_{20} for empty and loaded conveying element 102

Figure 90: Goods on conveying element mass m_2 during test 102

Figure 91: Excitation frequency during operation in x-direction of the conveying element mass m_2 including 5.0 Kg mass element 103

Figure 92: Pneumatic spring element 105

Figure 93: Effective force F_{p12} caused by a pneumatic spring element 106

List of tables

Table 1: Second field-driven asynchronous motors 22

Table 2: Design variants of vibratory conveyors 23

Table 3: Resonance frequencies after modification of the system and comparison with original values 78

Table 4: Centre of elasticity after modification of the system and comparison with original value 79

Table 5: Comparison of angles and amplitudes before and after the modification 82

Table 6: Tolerances based on DIN 7168-1 91

Table 7: Calculated amplitudes s_{10} and s_{20} for different masses on the conveying element m_2 100

1 Introduction

Vibration technology since many years is part of production plants in the automotive industry, electronic industry, food industry and other industries. The greatest expansion has been achieved at the time, when it started being used for the transport of various materials and for other special operations, which include for example, mixing or compaction. For decades, vibrating devices are used in many heavy-duty areas, especially in the mining and construction industries, which are the sectors with high demands regarding intended vibrations and the avoidance of unwanted vibrations [2].

Additionally, vibration technology started to be used in areas with strict hygienic conditions, such as the food industry and the medical industry. Experts dealing not only with the correct function and with sufficient delivery capacity of the conveyors, but also with the reduction of the transmission of vibrations to the surroundings and thus limiting the noise generated. Although this research has been ongoing for many years, it remain difficulties in the design and determination of optimum parameters of dynamic vibratory conveyors with regard to their mechanical nature or the mechanical nature of the transported objects. Operational problems concerning also the functional reliability and performance stability, as well as adverse effects of vibration and noise to the working environment.

These important requirements to vibratory conveyors operating in resonance regions are additionally influenced by changes of the goods to be conveyed during the transport process. The number and thus the mass of the parts and eventually their material cause changes. These factors generating considerable problems, because production lines are generally designed for the steady and continuous supply of components or materials. Therefore, it is necessary to ensure smooth transport performance [3].

Interlocking dynamic parameters influencing the natural frequencies and appropriate vibration shapes are decisive for the vibration service.

Desired function and optimal performance of vibratory conveyors can be provided by changing the dynamic parameters so that the system remained dynamic in the resonance range even while changing the number of parts transported or weight of conveyed material. This problem can be solved in principle by changing the weight and inertia of moving masses parameters or changing the stiffness of resilient links. In terms of practical use, prioritize measures can be used to regulate inertial effects [4].

For an optimum operation of vibratory conveyors, also low emission of vibrations into the ground and surroundings has to be guaranteed. To minimize the dynamic effects, methods for primary dynamic forces can be applied, consisting of balance respectively absorber mechanisms, including the transported materials. Methods of dynamic vibration suppression on the conveyor frame or its vibro-isolation to the surroundings must be taken under

consideration. Particular of these measures are dealt with in this dissertation, to optimize the design and the performance of linear conveyors.

Nowadays, the use of vibration technology is practice in many sectors of industrial production. It is an integral part of production and assembly lines as a means for transporting components to place processing or assembling. Without such machinery today mining, metallurgical, processing plants and other primary engineering cannot even be imagined [7, 29].

Vibratory conveyors are often deployed in large groups and are part of automated manufacturing and assembly processes (figure 1)

Source: [33]

Figure 1: Vibratory conveyors as part of assembly line

Extensive application of vibratory conveyors in industrial plants leading to efforts to improve their function and eliminate the problems in conjunction with them. Much effort is dedicated to the optimum adjustment of geometrical parameters, which depends on many factors, such as mechanical properties of the transported objects, their size, the friction against the conveying surface and the frequency of oscillation of the conveying element [13].

There is a constant effort of producers to increase transport capacity and reduce the energy intensity of the whole transport process by operating vibratory conveyors on the resonance range. However, this requirement sets high demands to the correct tune of the dynamic conveyor system. The main problem for a successful solution is to change the total charge weight of transported objects during the transport process, which significantly affects the stability of the operating resonance range. This leads to variations in transport performance and reliable operation of the conveyor [22, 27].

In practice, vibratory conveyors are often situated in production-assembly plants, operating in a number of many tens and various structural variants. Problems therefore arising not only in the requested capacity, the function and stability of performance of the conveyors, but also in lowering the quality of the working environment of the operating personnel due to

the transmission of unwanted dynamic forces into the floor and supporting the building structure [14].

The topic of the dissertation came up due to urgent needs in practice on a linear vibratory conveyor of VIBROS s.r.o, Příbram (CZ).

2 Objective of the dissertation

The main target of the dissertaion is to determine design methods and selected structural measures for building linear vibratory conveyors in a way that their application achieving operational reliability, sufficient and uniform performance during transport of objects and bulk materials. Guaranteeing this, the transmission of dynamic forces into the floor hast to be kept on a minimum level.

The chosen methods of treatment of the topic is based on the identification of the dynamic parameters of the existing representative vibratory conveyor dynamic analysis and optimization of its dynamic parameters in the design and manufacture of functional samples of selected measures and evaluate their contribution to practice.

The dissertation is divided into four parts [21].

The first part deals with linear vibratory conveyor systems and their parameters. The basic dynamic parameters are defined, directly affecting the function and performance of vibratory conveyors transport. Their identification is performed with selected and representative types of conveyors on the basis of measurements of kinematic quantities.

In the second part, dynamic characteristics are analysed in terms of their effect on the function and performance parameters of the conveyors. With regard to significant nonlinearity of computational models for solving dynamic conditions, numerical methods are applied to vibratory conveyors of the simplest cases.

The third part is devoted to proposals of structural measures for functional and performance optimization operation of vibratory conveyors. They are defined procedures for determining parameters of a specific modification of the centre of elasticity and a proposal of a guide mechanism of the conveying element. The main attention is focused on the elimination of depending tunes of the system, to harmonise the motion of the transported objects. Achieving this goal, significantly increases operational reliability and increasing transport performance.

The fourth part of the dissertation deals with systems limiting the transmission of undesirable vibrations to the surroundings. The problems is solved by the use of vibration absorbers. In this part of the dissertation, structural solutions are introduced in the form of functional samples of selected proposals from the previous chapter and their implementation into a demonstration model. Conclusion of the chapter is devoted to the measurement of kinematic quantities of optimized vibration conveyor and evaluate the effectiveness of selected structural measures for functional and performance optimization.

3 Vibratory conveyors and their underlying systems

Nowadays, various manufacturers of vibratory conveyors existing worldwide. This offers a wide field of applications in different industries to transport parts or in heavy industry to transport and sorting of bulk materials. The main advantage of vibratory conveyors are structural modesty and low overall maintenance requirements. This definition, however, is more concerned with just vibratory conveyors used in heavy industry. The use of vibratory conveyors in buildings and assembly halls, showing over the time its main drawbacks associated with the vibration and noise [8].

This dissertation assumes the term vibratory conveyor only as such a device which allows to transport an object in a horizontal direction or additionally also in the vertical direction upwards. Other facilities are considered chutes, screens, compactors, mixers etc. and their problems are not intended to be solved, although some calculation procedures, mechanical models of dynamic systems, simulation of operating conditions, etc. would probably be beneficial. Despite this separation from the machines using a vibration technique, vibratory conveyors are a wide range of devices which are characterized by different mechanical systems and design configurations (figure 2).

Source: [34], [35], [36], [37]

Figure 2: Linear vibratory conveyors

According to the nature of the design and the main carrier of the oscillatory motion of objects, vibratory conveyors are divided in linear and screw conveyors.

Vibratory conveyors are fundamentally different from other transport systems. Conventional devices for transport purposes usually characterized by a continuous motion of the object transported along the conveying element (carrier) while vibratory conveyors include the transported objects, components or bulk material, to a periodic motion having a main component of transport way without contact with the carrier.

The trajectory of oscillation of the carrier respectively the conveying element can be easily determined by looking to a certain point of the transport surface during operation.

In operation, a vibratory conveyor from a mechanical point of view is always a repeated oblique litter object in order to transfer (figure 3) [30].

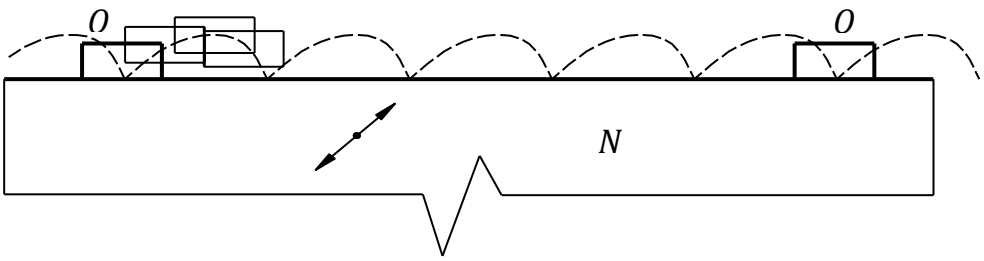

Source: [18]

Figure 3: Transport of an object by a vibratory conveyor (Carrier motion N, Object O)

Amplitude and frequency of conveying elements are obviously the main parameters for correct function and sufficient output of a conveyor. In addition to these variables, it is necessary to define the angle of the direction vector of the oscillatory motion of the conveying element relative to the main direction of the objects transported, or to the horizontal plane. This angle is called the elevation.

Other important factors effecting the function and performance of vibratory conveyors are mechanical properties of the conveyed objects, such as surface and shape of the object and the transport surface of the conveying element. It can be imagined, that the physical transport friction between the object and the surface of the conveying element takes a fundamental role [30].

For linear conveyors driven by exciter induction motors are commonly using the following frequency (Table1).

Table 1: Second field-driven asynchronous motors

Frequency [Hz]	Speed [min^{-1}]	Motor embodiments
12	720	Eight poles
16	960	Six poles
24	1440	Four pole
50	3000	Two poles

Source: Own table

The elevation angle, which generates the direction of the goods is always determined for a given application due to the significant influence of the shape and the material of the conveyed parts, its material and its surface. In practice, an elevation angle between 15° and 35° is chosen. This range is based on practical experiments. As bigger the angle, as lower the frequency of excitation has to be chosen [15].

3.1 General conveyor designs

The designs of basic vibratory conveyors such as shown in figure 2 generally containing the following components and properties:

- Conveying element,
- Inertial mass,
- Frame,
- Floor,
- Elasticity of the conveying element to the frame,
- Guide mechanism between the conveying element and frame,
- Elasticity of the conveying element to the inertial mass,
- Guide mechanism between the conveying element and inertia,
- Vibration exciter attached to a conveying element,
- Vibration exciter to the inertial mass,
- Vibration exciter between the carrier and inertia,
- Buffers.

Linear vibratory conveyors in technical practice are operated in a large number of design variants and combinations. Most frequently used states are shown in table 2.

Table 2: Design variants of vibratory conveyors

Common design variants	A	B	C	D
Conveying element (carrier) *N*	X	X	X	X
Inertial mass *S*			X	X
Buffers *V*			X	X
Floor *P*	X	X	X	X
Springing and damping bond *PT* between carrier *N* and floor *P*	X	X		
Guiding mechanism *VM* between carrier *N* and Floor *P*		X		
Springing and damping bond *PT* between carrier *N* and inertia *S*			X	X
Guiding mechanism *VM* between carrier *N* and inertia *S*				X
Vibration exciter *B* connected to the carrier *N*	X	X	X	
Vibration exciter *B* connected to inertia *S*				X

Note: X - The above objects are part of structural variants of a vibratory conveyor
Source: Own source

The individual structural variants A through D are mainly used in technical practice and can be identified on real products.

Conveying elements of vibratory conveyors often are designed like pipes, cylindrical or conical drums as well as rectangular channel. The guiding mechanism of the carrier relative to the frame or inertia, often is designed as parallelogram due to the simplicity and reliability of this kind of construction.

Flexible binding between conveying element and frame or inertia often is conducted by leaf springs or helical springs. The inertia mass is resiliently linked on one side to the carrier and the other side to the frame. This is preferably applied for generating a certain form of motion to the conveying element or minimizing the transmission of undesirable vibrations to the frame and the surroundings. Besides that, stabilization of tuning is another issue for the use of an inertia mass.

Frames of vibratory conveyors consists of a welded or a cast construction and are often supported in form of rubber springs with a relatively high rigidity. In some cases, frames are connected to the floor by rigid links, for example by means of screw anchors. In this cases, no rubber sprigs are installed [2].

Eccentric drives or electromagnetic vibration exciters realize excitation. External vibration exciters are inherently imbalanced rotors and can be connected to the conveying element or the inertial mass. Electromagnetic oscillation exciter are usually connected exciting a spring. The split core on one side is attached to the inertial mass and the second side to the conveying
element [11, 20].

Four typical individual state of the art design variants of one-mass and two-mass linear vibratory conveyors are schematically shown in figure 4.

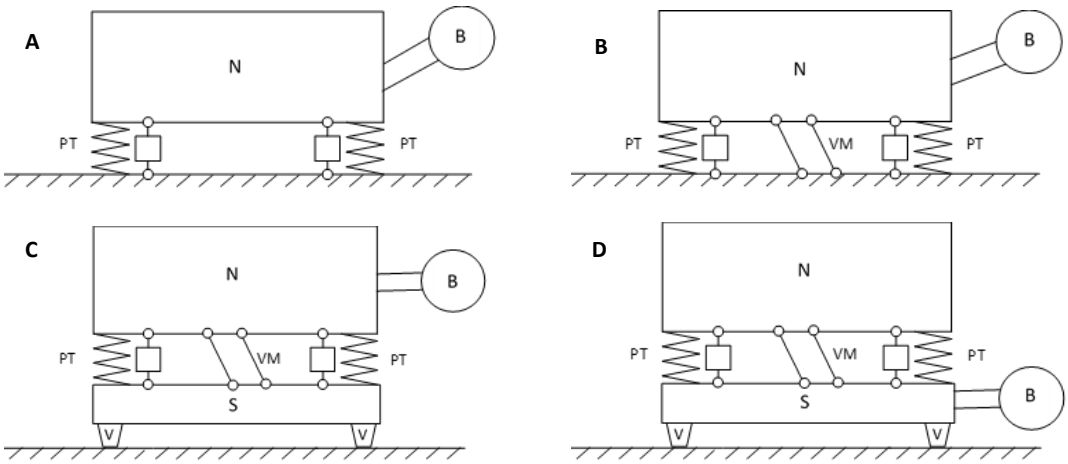

Source: Own source

Figure 4: Schematic representation of design variants (A, B, C, D) of vibratory conveyors: N – conveying element, S – additional mass, V - buffers, PT – springing and damping bond, VM – guiding mechanism, B – drive

The fundamental division of vibratory conveyors can be found in the character of the main traffic motion of the objects transported, which can be linear or helical. From this point of view, vibratory conveyors can be divided into linear conveyors and screw conveyors. In both designs, the structural variants are similar. In technical practice, linear conveyors variant occurs mostly in A to D, but variant C has only low importance. The general configurations A, B and D is given special attention.

3.2 Vibratory conveyors for linear motion

Vibratory conveyors with linear motion (Figure 5) used for the transport of small articles or bulk material in a number of industries. All of the above-mentioned embodiments A to D are common.

Source: [38]

Figure 5: Vibratory conveyor with rectilinear motion

The conveying element mainly meets the requirements for transportation. In addition it can be supplemented with a sieve for sorting, or a tube where the material is transported in an enclosed space to significantly reduce dust.

The surface of the conveying element, which is in contact with the goods to be conveyed, must be made of wear-resistant material. In addition, the coefficient of friction between the surface and the conveyed material must be taken into account. Correctly chosen conveying surfaces will last for the life time of a conveyor [29].

The conveying element (carrier) is attached to the frame or inertia of a guide mechanism that defines the kinematics of the conveyor. Springing and damping binding of the carrier to the frame or the inertia using steel helical springs or leaf springs. Leaf springs can be used in the conveyor structure as guide mechanism, since the spring and damper bond exhibits pliability almost exclusively in the perpendicular direction to the longitudinal of the leaf spring. Therefore, the position of the carrier relative to the frame or the inertia is unambiguously defined [12].

The spring and damper bond of the inertial mass to the frame is normally performed by helical springs. The frame of vibratory conveyors is supported by levelling aids or secured for example using screw anchors to the floor.

Source: [39]

Figure 6: Clamp exciter vibrator on a vibratory conveyor reciprocating

External vibration exciter (figure 6) for reciprocating conveyors are attached to a carrier or to the inertial mass. Often they are duplicated so that the force effect generates a harmonic force in one direction. The amplitude of the driving force depends on the eccentricity and the angular velocity of the rotating masses. Suitable controllers adjust angular velocity sometimes for desired infinitely variability. This determines the excitation frequency, the amplitude of the driving force, the size of the displacement and the frequency of the oscillatory motion of the conveying element. The amplitude depends on the relationship between excitation and the natural frequency of the dynamic vibration conveyor system. Most conveyors are operated in the natural frequency, when the energy consumption of the device is minimal [6].

If the conveying element is equipped with two exciters connected duplicated to the carrier, the resulting excitation force in the vertical plane of symmetry of the vibration conveyor is generated. This enables the main direction of oscillatory motion of the carrier, without respect to the frame or inertia bound guide mechanism. For the design variants A to D, that principle is presupposed.

The spring linkage and mass distribution media along with the transported objects must meet this solution, to minimize rotation around the transverse axis of the carrier. Given a stable structural design, when a relatively long carrier has a large moment of inertia to said axis, said condition is approximately satisfied. This also requires that the resulting excitation force pass through the centre of gravity (mass centre point) close enough to support the centre of elasticity of its bond to the frame. Nevertheless, it can be expected that the individual points of the conveying element will move along ellipses, which will affect the operation form of the conveyor. These simplified systems are mainly used for bulk materials and the transport process may be carried to their desired mix [25].

To stabilize the motion of the carrier which is connected to inertia (Figure 4, B to D), requires that the inertial mass shows a small angular displacement to an axis perpendicular to the vertical plane of symmetry of the vibratory conveyor.

This requirement can be ensured sufficiently using a large inertia mass to said axis and by the same time a sufficient stiffness and damping of strong bonds inertial mass to the frame. It is necessary respectively recommended, to respect the resonance range of the dynamic system of the vibratory conveyor. Especially when driving a vibratory conveyor by a reciprocating drain exciter, oscillations can occur during the shutdown sequence and crossing the area of resonance will result in a significant increase in the amplitude. The entire machine will vibrate very strong [16].

Another frequently used option of excitation is the drive by an electric motor crank mechanism. The electric motor is mounted on the frame and through a belt drive a crank mechanism, whose piston rod is resiliently mounted to the conveying element creates the motion (figure 7).

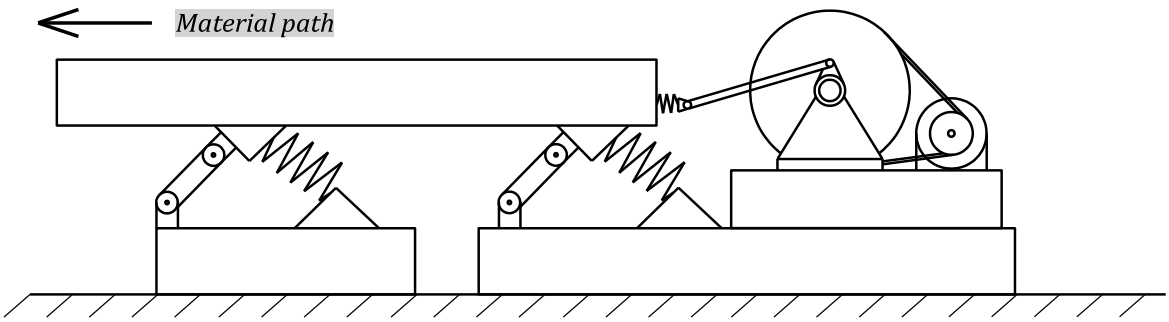

Source: [17]

Figure 7: Excitation model using a crank mechanism with an electric motor

4 Mechanical models of vibratory conveyors

The basis of each kinematic and dynamic analysis of mechanical systems is a properly and correctly assembled mechanical model, which enables not only to determine its properties, but also to simulate operational processes. In addition, it is also possible to monitor the impact and dynamic parameters on their behaviour [1].

For vibratory conveyors, mechanistic models for the determination of equations of motion and their solutions, allowing functional and performance optimization of the transport process, can be used. Subsequently, mechanical models and equations of motion for the most common structural variants of linear vibratory conveyors and screw motion conveyors can be assembled [18]. With the reduction of inertial effects and parameters of springing and damping characteristics of the system, a generalized mechanical model is provided. So it is possible to optimize the transport process for both types of vibratory conveyors [6, 7]. The solved mechanical models of vibratory conveyors have to be evaluated. The object properties do not affect the dynamic attitude of the monitored dynamic systems. This assumption can be accepted only in cases, when the transported objects are part of the nominal value of the total weight. Due to the possible diversity of the objects, their dynamic properties will be discussed and integrated into the mechanical model in subsequent chapters.

4.1 Models for reciprocating oscillation of a one-mass system

One-mass linear vibratory conveyors corresponding to the in chapter 3.1 described variant A consisting of a conveying element which is connected to the base frame by four helical springs. Two eccentric drives are connected directly to the conveying element under a certain angle to the horizontal line. The eccentric dives turning clockwise (left drive in direction of material flow) and anti-clockwise (right drive in direction of material flow). These drives are self-centring and so a motion across the main forwarding direction is eliminated.

One-mass linear conveyors are designed to forward bulk goods such as stones respectively small rocks, sand and mixtures of these materials.

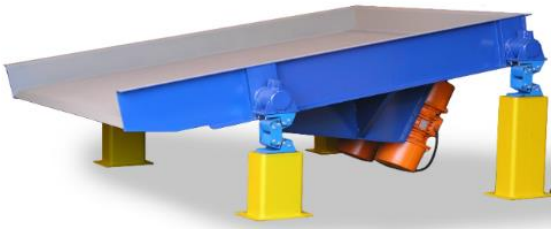

Source: [35]

Figure 8: Vibratory conveyor with linear motion in constructive variant A

4.1.1 Model for a linear conveyor of variant A

Corresponding to the conveyor variant A as shown in figure 8, the following general mechanical model can be of this conveyor type can be generated:

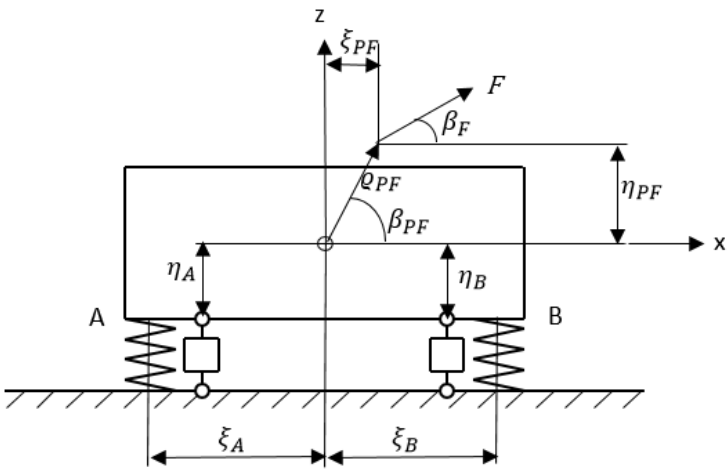

Source: Own source

Figure 9: Mechanical model of vibration conveyor with linear motion in the design of variant A

Based on this mechanical model, the following general equations can be build [24]:

$$J_z = m \cdot \xi_A \cdot \xi_B \tag{1}$$

Assuming $\xi_A = \xi_B$, equation (1) can be converted to

$$J_z = m \cdot \xi^2 \tag{2}$$

Based on this assumption, the following equations can be set up:

$$m\ddot{x} + (k_{Ax} + k_{Bx}) \cdot z + \left[(k_{Ax} - k_{Bx})\frac{\xi}{2}\right] \cdot \varphi = F_0 \cdot \cos(\omega Ft) \tag{3}$$

$$m\ddot{z} + (k_{Az} + k_{Bz}) \cdot z + \left[(k_{Az} - k_{Bz})\frac{\xi}{2}\right] \cdot \varphi = F_0 \cdot \sin(\omega Ft) \tag{4}$$

$$J_z\ddot{\varphi} + \left[(k_{Az} - k_{Bz})\frac{\xi}{2}\right] \cdot z + \left[(k_{Az} - k_{Bz})\frac{\xi^2}{4}\right] \cdot \varphi = -F_0 \cos\beta F \cdot \rho PF sin\beta PF + \\ +F_0 \sin\beta F \cdot \rho PF cos\beta PF \tag{5}$$

Converted into the matrix form, the following matrices can be built

a) For the mass

$$M = \begin{bmatrix} m & 0 & 0 \\ 0 & m & 0 \\ 0 & 0 & J_z \end{bmatrix} \tag{6}$$

b) For the stiffness of the springs

$$K = \begin{bmatrix} k_{Ax} + k_{Bx} & 0 & -\eta_A k_{Ax} - \eta_B k_{Bx} \\ 0 & k_{Az} + k_{Bz} & \xi_A k_{Az} + \xi_B k_{Bz} \\ -\eta_A k_{Ax} - \eta_B k_{Bx} & \xi_A k_{Az} + \xi_B k_{Bz} & \eta_A^2 k_{Ax} + \eta_B^2 k_{Bx} + \xi_A^2 k_{Az} + \xi_B^2 k_{Bz} \end{bmatrix} \tag{7}$$

The mechanical model described in figure 9, enables three degrees of freedom, i.e. a longitudinal motion in x-direction, a second longitudinal motion in z-direction and a rotation around the mass centre point, depending on the situation and effective direction of the excitation force and the centre of elasticity of the system. To ensure a pure linear motion under the intended excitation angle, it is necessary to avoid any kind of rotation around the mass centre point on this type of linear vibratory conveyor. As soon as a rotation takes place, the motion of the conveyed goods will be influenced in an unintended way, causing a suboptimal motion of the goods and a potential malfunction of the conveyor [5].

A mayor influence in this model comes from the damping conditions. To exemplify this point, the following simplified model is introduced:

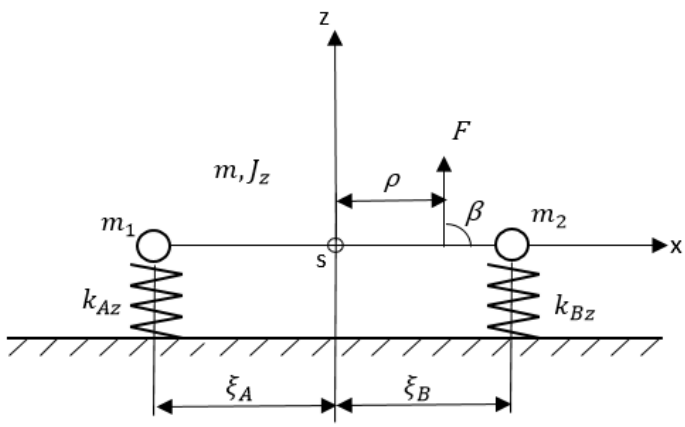

Source: Own source

Figure 10: Simplified mechanical model of vibration conveyor with linear motion variant A

In this model, the influence of the situation and effective direction of the excitation force as well of the horizontal components of the motion is neglected. For this model, the following equations can be formed for the values in z-direction:

For the displacement

$$z = z_0 \cdot \sin(\omega t), \tag{8}$$

for the velocity

$$\dot{z} = z_0 \omega \cdot \cos(\omega t) \tag{9}$$

and for the acceleration

$$\ddot{z} = -z_0 \omega^2 \cdot \sin(\omega t). \tag{10}$$

The velocity which is linked to the damping in the dynamic calculation of the system, represents the first derivation of the displacement and is the only component including a cosine function. For systems with very low damping, as given on a linear vibratory conveyor of the variant A, the following equations then can be formed:

$$k_{Az} z_0 \sin(\omega t) + k_{Bz} z_0 \sin(\omega t) - m x_0 \omega^2 \sin(\omega t) = F_0 \cdot \sin(\omega F t) \tag{11}$$

$$k_{Az} z_0 + k_{Bz} z_0 - m z_0 \omega^2 = F_0 \tag{12}$$

$$k_{Az} \xi_A + k_{Bz} \xi_B - F_0 \rho = 0 \tag{13}$$

By the use of a numerical model, based on the equations (11) to (13), the following graph for amplitude over stiffness in z-direction will be received:

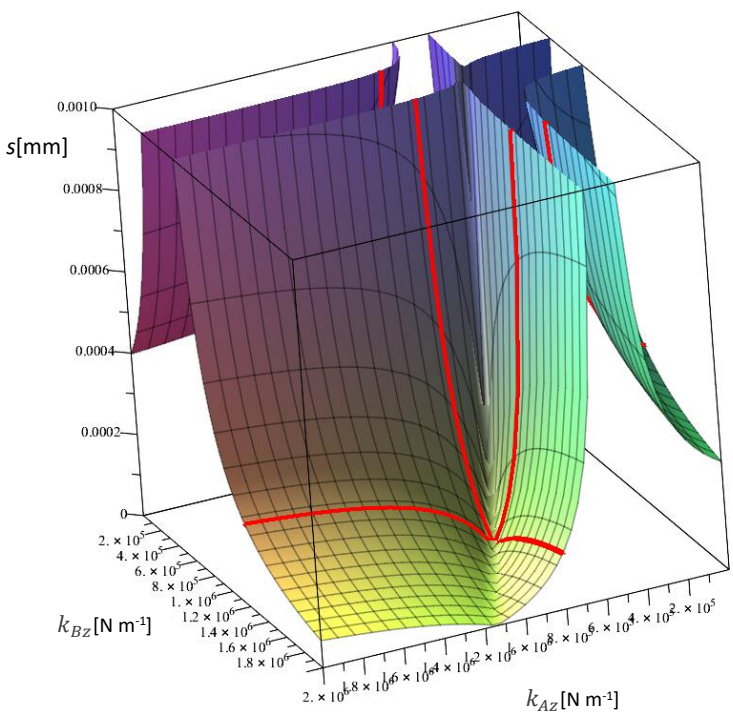

Source: Own source

Figure 11: Amplitude over stiffness 3-D graph of a linear vibratory conveyor of variant A

The graph shows the area of no-rotation, where the valley between the stiffness k_{AZ} and k_{BZ} is situated. The intended amplitudes of the system can be selected by following the particular lines through the valley. In addition, a graph for amplitude over time can be build, using the results from the above calculation as shown in figure 12:

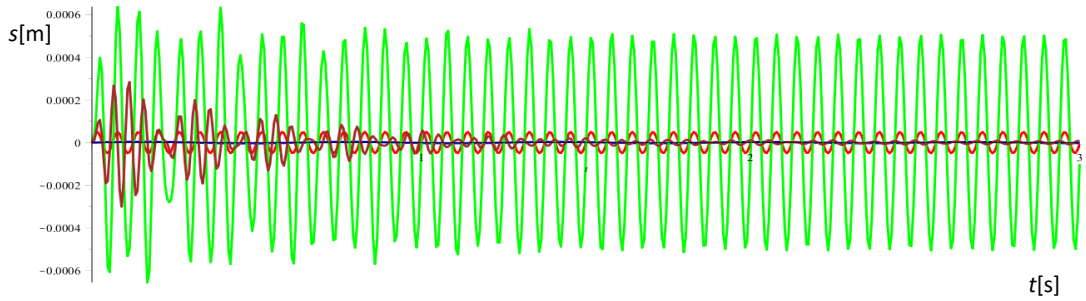

Source: Own source

Figure 12: Amplitude over time function of a linear vibratory conveyor of variant A

In this graph, the red line represents the excitation in z-direction, the green line shows the amplitude in z-direction, the blue line demonstrates the amplitude in x-direction and the brown line stands for the rotation of the system under the selected conditions. It can be seen, that the brown line for the selected case is nearly in line with the blue line. So the rotation can be avoided by the correct selection of parameters of such a system.

Transmitting these conditions into the general model shown in figure 9, a conveyor variant A with pure linear motion and no rotation around its mass centre point can be designed.

4.1.2 Model for a linear conveyor of variant B

Corresponding to the conveyor variant B as shown in figure 12, the following type of linear vibration conveyor can be found in practice. Here two possibilities for the transmission of the excitation force are typical. The first possibility is, that the conveying element is driven by an exciter with eccentric disk, mounted to the frame of the conveyor. The force is transmitted by a crank mechanism to the conveying element under a certain angle, 90° to the angle of the guiding levers. This type of design is shown in figure 13. For this kind of excitation, typically only one electric motor is sufficient.

Source: [40]

Figure 13: Guided linear vibratory conveyor of variant B

An alternative option is the installation of eccentric drives as shown in figure 6 directly to the conveying element. The direction of the excitation force then has to be given by the angle of fixation of the drives to the conveying element, comparable to variant A. In this case typically two counter-rotating exciters are installed to the conveying element, avoiding unwanted motion of the goods to be conveyed across the mayor conveying direction. Often on linear vibratory conveyors of variant B, flat springs replacing a system of helical spring and guiding levers. The design in that case is simpler and the intended effects are the same. An example is shown in figure 14.

Source: [41]

Figure 14: Guided linear vibratory conveyor of variant B with flat springs

For this type of linear vibratory conveyor, the following general mechanical model can be developed:

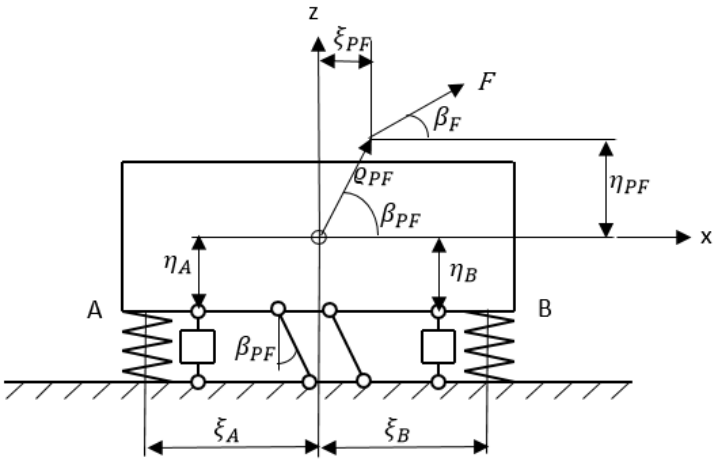

Source: Own source

Figure 15: Mechanical model of vibration conveyor with linear motion in the design of variant B

For the particular application as vibratory conveyor of variant B as shown in figure 17 and 18 specifications can be made to ensure the intended motion of the goods:

The angle of force vector to the horizontal β_{PF} in its application is identical to the angle of the force vector effecting the mass centre point and the horizontal β_F.

$$\beta_{PF} = \beta_F \tag{14}$$

Applying the excitation force directly to the vertical situation of the mass centre, the following definition can be made:

$$\eta_{PF} = 0 \tag{15}$$

Which results in the conclusion:

$$\varrho_{PF} = 0 \tag{16}$$

The angle of the force vector effecting the mass centre point and the horizontal β_{PF} is identical to the angle between the vertical and the lever mechanism. Additionally the assumptions for the relation of ξ_A to ξ_B and J_z are identical to the model of variant.

Based on these assumptions, equations (3) of variant A can be formed:

$$J_z\ddot{\varphi} + \left[(k_{Az} - k_{Bz})\frac{\xi}{2}\right] \cdot z + \left[(k_{Az} - k_{Bz})\frac{\xi^2}{4}\right] \cdot \varphi = 0 \tag{17}$$

In this mechanical model the rotation around the mass centre point is eliminated by the use of the levers. The remaining motion is linear and corresponds to the excitation force angle β_F.

Converting the remaining equations (3) and (4) into matrix form, the following matrices can be build

c) For the mass

$$M = \begin{bmatrix} m & 0 \\ 0 & m \end{bmatrix} \tag{18}$$

d) For the stiffness of the springs

$$K = \begin{bmatrix} k_{Ax} + k_{Bx} & 0 \\ 0 & k_{Az} + k_{Bz} \end{bmatrix} \tag{19}$$

The amplitude over time graph will show the following characteristic:

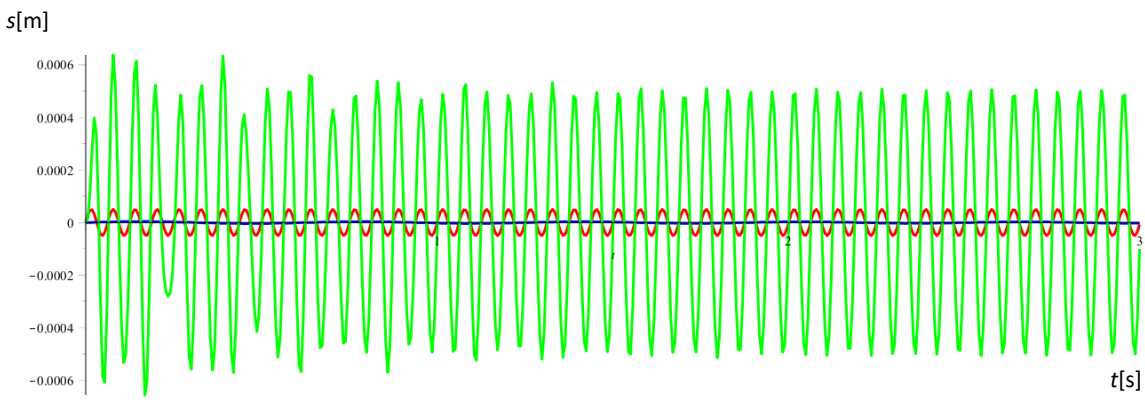

Source: Own source

Figure 16: Amplitude over time function of a linear vibratory conveyor of variant B

The red line represents the excitation in z-direction, the green line shows the amplitude in z-direction and the blue line demonstrates the amplitude in x-direction.

Linear vibratory conveyors of variant B are less sensitive to slight differences in spring stiffness and a change of the mass centre of the goods to be conveyed during the real conveying process.

In case of critical applications with sudden changes of loads respectively masses, especially on only one side of a conveying element, variant B supplies the much more change resistant conveying motion compared to variant A.

4.2 Model for reciprocating oscillation of a two-mass system

The assembly of the following two-mass vibratory conveyor consists of three principal parts, the conveying element build as a conveying trough, represented by character m_2 , the excited mass with the drive, represented by character m_1 and a supporting element, fixed to the ground [2,9].

Both masses are connected by the use of springs. In this case, helical springs are chosen. The excitation of m_1 is done by an eccentric drive, installed to excite the mass 90° to the lever R_1 [5]. The springs with their particular stiffness are defined as k_1 and k_{21} . The damping of the system is neglected. Mass m_1 is connected to the ground by levers under an angle β_1 , mass m_2 is connected to mass m_1 by levers under an angle β_2 . The levers enabling a defined guidance of the masses motion. Figure 17 shows the mechanical model of this two-mass conveyor.

Source: [42]

Figure 17: Vibratory conveyor with two masses of variant D

The corresponding dynamic model of a two-mass linear vibratory conveyor based on the design principle shown in figure 17 is shown in the following figure 18 [17].

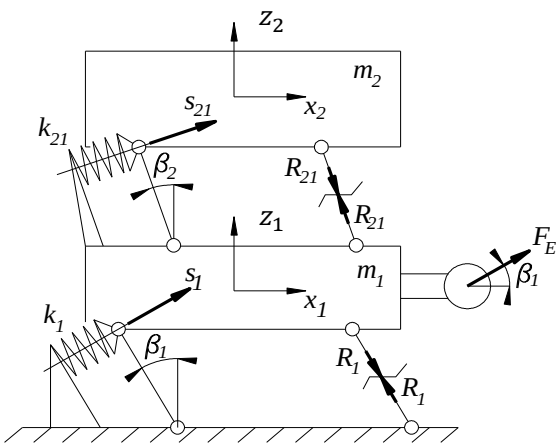

Source: Own source

Figure 18: Mechanical model of the vibratory conveyor

Based on the mechanical model shown in figure 18, the following equations are formed [10]:

$$m_1\ddot{x}_1 + k_1x_1 - k_{21}x_{21} - F_{R1}\sin\beta_1 + F_{R21}\sin\beta_2 = F_E\cos\beta_1 \,, \tag{20}$$

$$m_1\ddot{z}_1 + k_1 z_1 - k_{21} z_{21} - F_{R1}\cos\beta_1 + F_{R21}\cos\beta_2 = F_E \sin\beta_1 \,, \tag{21}$$

$$m_2\ddot{x}_2 + k_{21} x_{21} - F_{R21} sin\beta_2 = 0 \,, \tag{22}$$

$$m_2\ddot{z}_2 + k_{21} z_{21} - F_{R21}\cos\beta_2 = 0 \,, \tag{23}$$

Summing up the equations (20) and (22), (21) and (23) as well as (22) and (23), the following equations can be formed:

$$m_1\ddot{x}_1 + k_1 x_1 - F_{R1}\sin\beta_1 + m_2\ddot{x}_2 = F_E\cos\beta_1 \,, \tag{24}$$

$$m_1\ddot{z}_1 + m_2\ddot{z}_2 + k_1 z_1 - F_{R1}\cos\beta_1 = F_E\sin\beta_1 \,, \tag{25}$$

$$(m_2\ddot{x}_2 + k_{21}x_{21})cos\beta_2 + (m_2\ddot{z}_2 + k_{21}z_{21})sin\beta_2 = 0 \,. \tag{26}$$

Merging equation (24) and (25), the equation can be formed as

$$\frac{m_1\ddot{x}_1 + k_1 x_1 + m_2\ddot{x}_2}{sin\beta_1} + \frac{m_1\ddot{z}_1 + k_1 z + m_2\ddot{z}_2}{cos\beta_1} = F_E\,\frac{\cos\beta_1}{\sin\beta_1} + F_E\,\frac{\sin\beta_1}{\cos\beta_1}, \tag{27}$$

and after converting equation (27)

$$(m_1\ddot{x}_1 + m_2\ddot{x}_2 + k_1 x_1)\cos\beta_1 - (m_1\ddot{z}_1 + m_2\ddot{z}_2 + k_1 z_1)\sin\beta_1 = F_E \,, \tag{28}$$

Splitting up the motion of x_2 and $z_2$into the components, the following form can be written

$$(m_1\ddot{x}_1 + m_2\ddot{x}_1 + m_2\ddot{x}_{21} + k_1 x_1)\cos\beta_1 - (m_1\ddot{z}_1 + m_2\ddot{z}_2 + m_2\ddot{z}_{21} + k_1 z_1)\sin\beta_1 = F_E \,, \tag{29}$$

$$(m_2\ddot{x}_1 + m_2\ddot{x}_{21} + k_{21}x_{21})cos\beta_2 + (m_2\ddot{z}_1 + m_2\ddot{z}_{21} + k_{21}z_{21})sin\beta_2 = 0 \,. \tag{30}$$

The levers guide the motion of each of the two masses between floor and mass m_1 and between mass m_1 and mass m_2. Therefore the coordinate vectors with the characters x and z can be merged and replaced by character s [19].

Then the equations (29) and (30) can be formed as

$$m_1\ddot{s}_1\cos^2\beta_1 + m_2\ddot{s}_1\cos^2\beta_1 + m_2\ddot{s}_{21}\cos\beta_2\cos\beta_1 + k_1 s_1\cos^2\beta_1 + m_1\ddot{s}_1\sin^2\beta_1 + m_2\ddot{s}_1\sin^2\beta_1 + +m_2\ddot{s}_{21}\sin\beta_2\sin\beta_1 + k_1 s_1\sin^2\beta_1 = F_E \,, \tag{31}$$

$$m_2\ddot{s}_1\cos\beta_1\cos\beta_2 + m_2\ddot{s}_{21}\cos^2\beta_2 + k_{21}s_{21}\cos^2\beta_2 + m_1\ddot{s}_1\sin\beta_1\sin\beta_2 + m_2\ddot{s}_{21}\sin^2\beta_2 + +k_{21}s_{21}\sin^2\beta_2 = 0 \,. \tag{32}$$

with

$$s_{21} = s_2 - s_1 \tag{33}$$

After simplifying the equations (31) and (32), the final equations of motion for the analysed conveyor model are

$$(m_1 + m_2)\ddot{s}_1 + m_2\ddot{s}_{21}(\cos\beta_2\cos\beta_1 + \sin\beta_2\sin\beta_1) + k_1 s_1 = F_E \,, \tag{34}$$

$$m_1\ddot{s}_1(\cos\beta_2\cos\beta_1 + \sin\beta_2\sin\beta_1) + m_2\ddot{s}_{21} + k_{21}s_{21} = 0\,. \tag{35}$$

For the further analysis of the dynamic model, three cases are of particular interest:

- Case one with $\beta_1 = \beta_2$,
- Case two with $\beta_1 = 0$ and
- Case three with $\beta_2 = 0$.

For case one with $\beta_1 = \beta_2$, equation (31) can be converted step by step

$$(m_1 + m_2)\ddot{s}_1 + m_2\ddot{s}_{21} + k_1 s_1 = F_E\,, \tag{36}$$

$$m_1\ddot{s}_1 + m_2\ddot{s}_1 + m_2\ddot{s}_2 - m_2\ddot{s}_1 + k_1 s_1 = F_E\,, \tag{37}$$

$$m_1\ddot{s}_1 + m_2\ddot{s}_2 + k_1 s_1 = F_E\,, \tag{38}$$

to the final form

$$m_1\ddot{s}_1 + k_1 s_1 - k_{21}(s_2 - s_1) = F_E\,. \tag{39}$$

Equation (32) is transformed by the same way into the final form

$$m_2\ddot{s}_2 + k_{21}(s_2 - s_1) = 0. \tag{40}$$

For case two with $\beta_1 = 0$, the equations are

$$(m_1 + m_2)\ddot{s}_1 + m_2\ddot{s}_{21}cos\beta_2 + k_1 s_1 = F_E\,, \tag{41}$$

$$m_2\ddot{s}_1 cos\beta_2 + m_2\ddot{s}_{21} + k_{21}s_{21} = 0. \tag{42}$$

For case three with $\beta_2 = 0$, the following equations can be formed

$$(m_1 + m_2)\ddot{s}_1 + m_2\ddot{s}_{21}cos\beta_1 + k_1 s_1 = F_E\,, \tag{43}$$

$$m_2\ddot{s}_1 cos\beta_1 + m_2\ddot{s}_{21} + k_{21}s_{21} = 0. \tag{44}$$

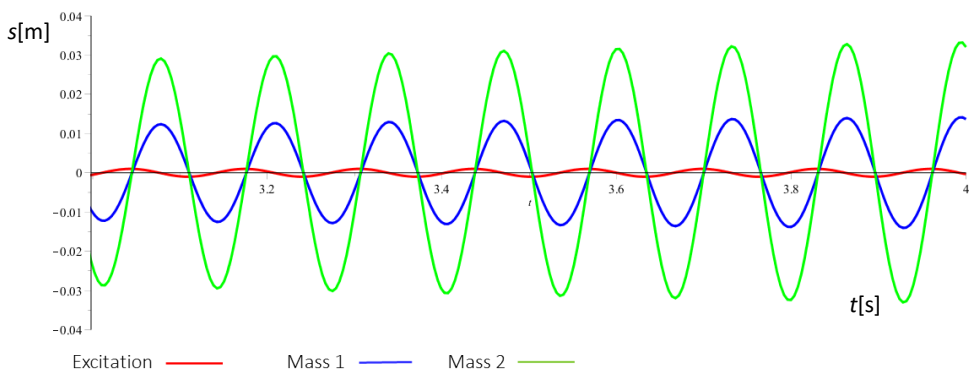

Source: Own source

Figure 19: General example of amplitudes of a two mass system

4.3 Conveyed goods

The conveyed object of the vibratory conveyors must have some mechanical and physical properties, relate to its material, shape, dimensions, etc. For example, the object must have a solid state. There must be physical friction between the conveying element and the object.

Linear vibratory conveyors are mainly used to transport small parts and loose materials. As a rule, minor parts immediately after initial contact with the conveying surface of the oscillating conveying element are disposed so that they are not permanently stacked during transport. They have to be integrated into a mechanical model by their total weight m_0, the experimentally determined moment of inertia J_{Oz} and the coefficient of friction f_{ON} relative to the individual surface of the conveying element.

The situation changes, as soon as the transported goods having the nature of bulk material or components remaining during the transport in the layers. In this case, the object will be loaded to the mechanical model also by its total weight m_0 and moment of inertia J_{Oz}, but the coefficient of friction must be considered not only between the object and the carrier f_{ON}, but also in the contact surfaces between the layers of the object itself f_{VO} .

It is obvious that in many cases the identification of these parameters is very difficult. The replacement mechanical model of the object in a simplified solution is based on the definition of the layers and the coefficient of friction f_{VO} between them (shown in figure 20).

Under the simplistic assumption that two layers will exist, the layers are volumetric and each layer or particles of the transported object are not able to climb, it will be possible to express the condition for the transport of the layers of material without the relative displacement of the shape.

$$F_{VOx} \leq F_{TVO} \tag{45}$$

and

$$-\ddot{s}_N cos\beta_{NS} \leq (g + \ddot{s}_N sin\beta_{NS}) f_{VO}. \tag{46}$$

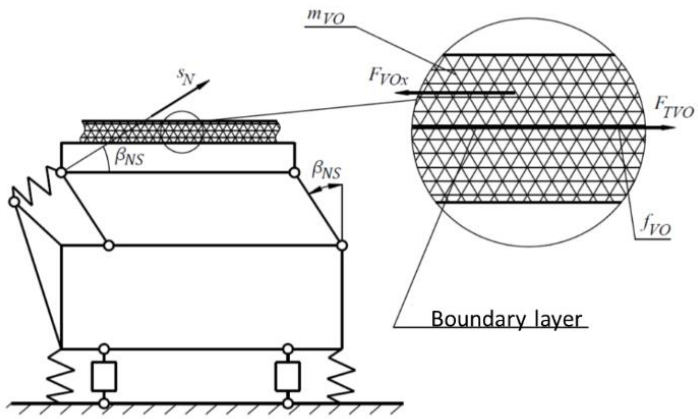

Source: [18]

Figure 20: Simplified mechanical model of bulk goods being conveyed

Unless the conditions (45) and (46) are met, there is a permanent slip of the transported objects or layers of conveyed bulk material and the intended effect of the vibration transport is lost.

In this case, the transport process is significantly disturbed and mixing, tumbling or compaction occurs simultaneously. The issue of the process is not the subject of dissertation, and therefore it will be further assumed that conditions (45) and (46) are fulfilled for the ongoing considerations.

For the functional reliability and conveying performance, the magnitude of the coefficient of friction between the transported object and the conveying element is decisive in terms of friction. As it will be explained below, the friction coefficients and properties associated with the coherence of an object playing a very important role and influence conveying process.

Dynamic parameter analysis will be performed based on time courses of the kinematic quantities of the carrier and the transported objects. Particular attention will be given to frequency dependencies. In dynamic analysis, it is recommended that vibratory conveyors operate in the resonant area of their major natural frequency, which minimizes the energy demands on their operation. Therefore, when observing the influence of changes in dynamic parameters on the oscillation of the conveying element, it is necessary to evaluate the possible deviation from its optimal tuning, i.e. from the resonant state [15].

The dynamic parameters of the vibratory conveyor, which have a significant effect on its function and conveying performance, considering in particular the weight of the conveyed objects m_0 and the quantities describing the springs and the dampers as well as the inertia bonds, stiffness, and friction coefficients. The criteria for assessing this effect will be the amplitude of the oscillating motion of the conveying element.

The influence of geometric parameters, elevation angle and climb angle are of importance for transport performance. Geometric links are directly associated with frictional bonds that are given by the coefficient of friction between the transported object and the carrier surface of the carrier.

The analysis of vibration conveyors also includes the determination of their dynamic force effects that act on the floor and cause its vibration and the associated noise load of operation.

4.4 Influence of the conveyed goods to vibratory conveyors

The mass parameters and the texture of the goods to be conveyed on a vibratory conveyor will influence the motion of the conveyer in any of the representative variants A to D. However, the individual influence to each of the variants will show different effects.

The common relation between mass, stiffness and natural frequency on the of an oscillating system is described in the equation

$$\omega = \sqrt{\frac{k}{m}} \tag{47}$$

Assuming that the frequency of excitation of the conveyor is matching the natural frequency of the system, the stiffness and the mass will have to be in a ratio that keeps the vibratory conveyor in its optimum performance condition.

The stiffness of the springs can be chosen in a way that an average object-mass is considered to be permanently part of the conveyor and can be added to the mass of the conveying element being excited. In addition, it will be necessary to determine the maximum and the minimum mass level of the goods to be conveyed, to keep the efficiency of the conveyor and to avoid damages by overloading the system.

The mass of the goods will have additional effects, depending on the area of mass concentration on the conveying element. Especially vibratory conveyors of variant A will react extremely critical to single sided mass concentrations, due to the week guidance of the conveying element to its frame. The mass immediately will influence the situation of the mass centre of the conveying element and the conveying process will not be running on its optimum. In the worst case created by overloading the system on one single side of the conveying element, the conveying process will stop and damages can affect the structure.

On guided conveying elements like in variants B to D, the influence of the mass mainly is reduced to an effect on the capacity of the conveyor. The guiding mechanism compensates the displacement of the mass centre point up to a certain range. In any case it is necessary even on guided mechanisms to define the optimum mass to be conveyed and to determine an individual tolerance range.

The average mass of the objects to be conveyed can easily calculated by using equation (47), the tolerance range can be determined easiest by evaluation tests of a system with reference to its capacity and the transmission of vibrations to the environment.

4.5 The power effect of the vibratory conveyor on the subsoil

It is significant for the operation of the vibratory conveyor, to analyse its force effect causing vibration of the floor and the associated surrounding noise. Vibratory conveyors are usually deployed to assembly lines in large numbers.

In terms of ground forces transfer and associated noise, vibration conveyor operations are very unfavourable and operators are making great efforts to unwanted floor vibrations and often blocking the entire building.

Particularly unfavourable phenomena are disturbances that represent an increase in the dynamic forces of a group of machines or devices operating at the same or very close operating frequency.

Avoidance of such a phenomenon is only possible with the perfect vibration isolation of each individual vibratory conveyor.

Dynamic forces that are transmitted to the conveyor frame, in basic design variants are given by the forces of rubber springs forming an elastic bond between the inertia mass and the frame against the floor.

Figure 21 shows an example for the result of calculating the time course of dynamic forces and subsoil for a representative vibratory conveyor and the optimal weight of the loaded objects.

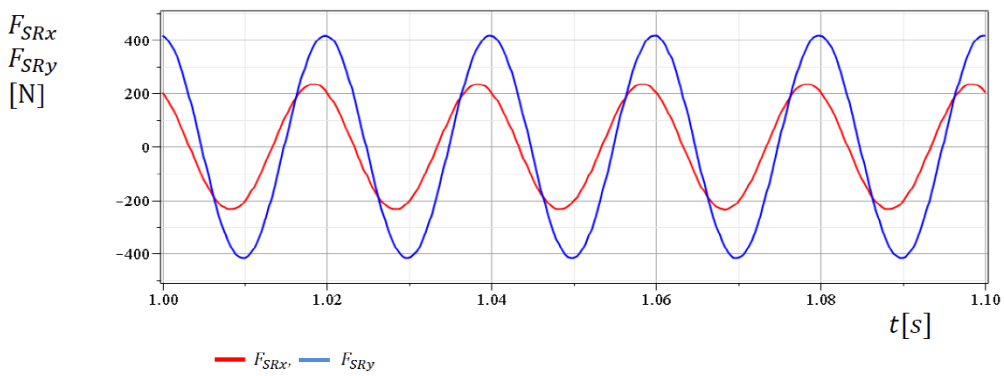

Source: [18]

Figure 21: Time course of dynamic forces transmitted to the conveyors frame and the floor

The amplitude of the dynamic force acting on the vibratory conveyor on its subsoil is relatively large, depending on the variant of the conveyor and the chosen conditions. The group effect of the devices can be expected to give rise to vibrations of the floor and the whole building. In case of excessive vibration, which could damage the health of the operator, anti-vibration and noise protection often are implemented.

5 Analysis and optimization of the transport process

The initial step in the process of optimizing a system is the detailed und structured analysis of the existing system with reference to all impacts of the existing design. In case of a linear vibratory conveyor, these impacts are manly influenced by the design, but also by influences of the location, the conveyor is operating in. Optimizing of the transport process can also be influenced by eliminating vibrations, transmitted to the floor, the conveyor is situated on. These vibrations can cause negative effects to the building by creating unwanted resonances. By the same time, the transmission of vibration forces to the ground costs energy, which could be used for the increase of efficiency of the conveying process. A detailed analysis of design and motion of a representative vibratory conveyor is done in the following chapters.

5.1 Selection of a representative vibratory conveyor

The linear vibratory conveyor to be analysed and improved is manufactured by the Czech company VIBROS s.r.o, Příbram and the type designation is PVA 050.012 P. It consists of the conveying element which is connected to the base frame by four helical springs, so it is a typical variant A conveyor. Two eccentric drives are connected directly to the conveying element under an angle of 30° to the horizontal line. The eccentric dives turning clockwise (left drive in direction material flow) and anti-clockwise (right drive in direction of material flow). These drives are self-centring and so a motion across the main forwarding direction is eliminated. Figure 22 shows the side view of the conveyor with the top cover of the left eccentric drive opened. So the eccentric mechanism of the drive can be seen. The conveyor is designed to forward bulk goods such as stones respectively small rocks, sand and mixtures of these materials.

Source: Own source

Figure 22: Vibros vibratory conveyor with eccentric drive

The technical specification of the linear conveyor are follows [23, 32]:

Length of conveying element:	1200.00 mm
Width of conveying element:	500.00 mm
Drive:	2 x 400 V/50 Hz, 3 Ph, 0.55 kW
Operating frequency:	16.00 Hz
Angle of drive axis to vertical α:	30°
Maximum displacement (90° to drive axis):	10.00 mm
Maximum acceleration (90° to drive axis):	100.00 m s^{-2}
Delivery rate:	1.00 kg s^{-1}
Oscillating weight:	268.00 kg

5.2 Identification of dynamic parameters of the vibratory conveyor

It is expected, that a uniform motion over the full length or the conveying element will be generated, to enable a smooth transport of the bulk goods to the hand over point of the conveyor. This will be necessary for an efficient supply of the goods, avoiding any kind of blocking respectively bottle neck effect by goods not conveyed properly close to the hand over point.

The first step to get necessary information on the linear vibratory conveyor is the determination of the resonance frequencies and the corresponding directions of their appearance. Therefore, a test series is established, using the following test equipment [17]:

- Piezo-sensors type 4508, brand Brüel & Kjær
- Connecting wire to analyser
- 4-channel analyser type 3050, brand Brüel & Kjær
- Software “Pulse Labshop V.19”

The sensor has to be fixed to the test object by an adhesive wax that enables the operator to place the sensor to different positons of the conveyer.

The sensors are calibrated using a calibration unit on 77.00 Hz calibration frequency brand RFT in advance of the trials.

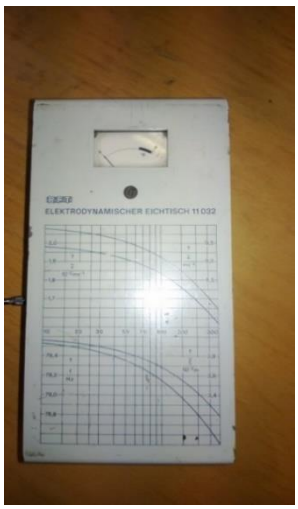

Source: Own source

Figure 23: RFT calibration unit

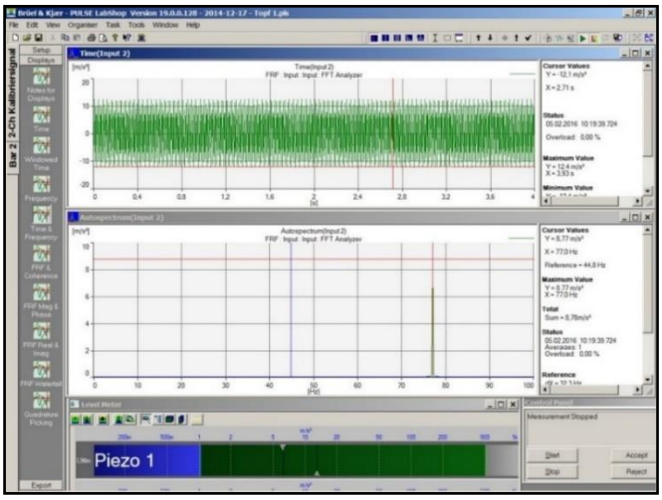

Source: Own source

Figure 24: Calibration signal 77.00 Hz

For the description of the effective direction of the resonance frequencies, the coordinate system shown in figure 4 is defined.

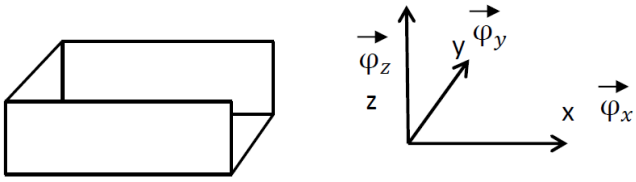

Source: Own source

Figure 25: Conveying element and its coordinate system defined

5.2.1 Mass and inertia parameters

The linear vibratory conveyor consist of the conveying element with the eccentric exciters and the frame made of steel profiles, which are fixed to the ground. The total mass of the moving parts, i.e. the conveying element including the two exciters is 268.00 kg, while the mass of each exciter is 55.00 kg. The conveying element without exciters has a mass of 158.00 kg. The frame of the conveyor is a welded design made of steel, having a total mass of 49.00 kg. The mass of each of the four springs is 1.73 kg. The average mass of the goods to be conveyed has to be determined due to the fact that no information on that matter is available.

In a first step, the conveyor is analysed by testing the empty system. Based on the result of the analyses, data for the integration of mass influences will be developed.

The coupling of the conveying element to the frame of the conveyor consists of the following elements:

- Four cylindrical pipes of 80.00 mm length and 63.00 mm diameter, welded to the conveying element
- Four cylindrical pipes of 80.00 mm length and 63.00 mm diameter, welded to the frame
- Four helical springs

No additional guiding mechanism exists and no dampers are installed. The full motion generated by the exciters fixed to the conveying element, is transmitted by the four springs to the frame.

5.2.2 Springs and damping conditions

In a test, the vertical stiffness (in direction of the spring centre axis) is determined. This is done by using a special test equipment, where single helical springs can be loaded along their centre line with a pre-defined force. The data are recorded manually and as result, the following value is calculated form 4 trials:

Vertical stiffness per single spring k_v : 84326 N m^{-1}

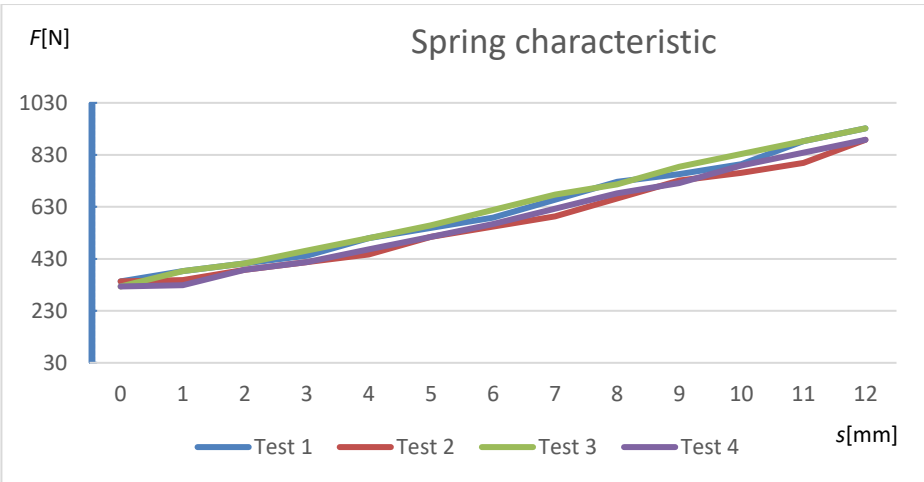

Source: Own source

Figure 26: Characteristic of helical springs of the conveyor in vertical direction

In a second test, the horizontal stiffness (across the spring centre axis) of the helical springs is determined by using a special equipment, which enables an even horizontal tensile load to the conveying element. The data again are recorded manually and the result is divided by four, to get the following result per spring:

Horizontal stiffness per single spring k_h: 33583 N m^{-1}

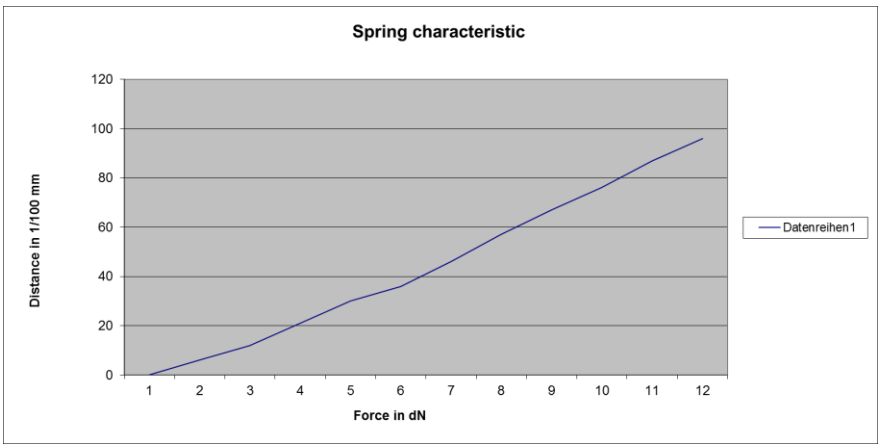

Source: Own source

Figure 27: Characteristic of helical springs of the conveyor in horizontal direction (own source)

The damping of the system is determined by using the method of the logarithmic decrement. For this method, the time function of acceleration is analysed, using the free oscillation of the system.

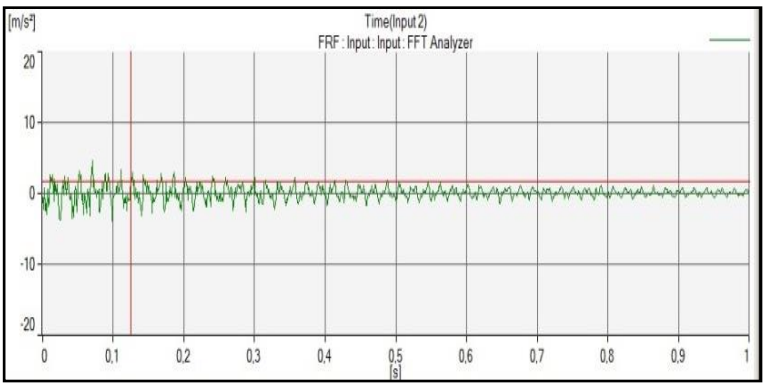

Source: Own source

Figure 28: Time function of acceleration in vertical direction on free oscillation

The necessary equations for the calculation of the logarithmic decrement Λ are

$$\Lambda = ln\frac{x_m}{x_n} \tag{48}$$

Alternatively Λ can be calculated as well using the equations

$$\Lambda = \frac{2\cdot\pi\cdot\delta}{\sqrt{\omega_0^2-\delta^2}} \tag{49}$$

and

$$\Lambda = \delta \cdot T \tag{50}$$

with

$$\delta = \omega_0 \cdot b \,. \tag{51}$$

The values for x_m and x_n in x-direction and in z-direction can be determined from the respective recorded graph. Melting and adjusting the equations (48) and (50), the damping can be determined:

$$\omega_0 \cdot b \cdot T = ln \frac{x_m}{x_n} \tag{52}$$

For the calculation of b, the equation can be formed to the final term:

$$b = \frac{ln \frac{x_m}{x_n}}{\omega_0 \cdot T} \tag{53}$$

The determined values now can be fit into equation (53) and as result a relatively low damping is in x-direction and z-direction is calculated, showing the following values:

Damping of the conveyor in x-direction:

$$b_x = b_y = 654.60\ kg\ s^{-1}$$

Damping of the conveyor in z-direction

$$b_z = 588.80\ kg\ s^{-1}$$

Dividing the results by four, the damping per spring can be determined:

$$b_x = b_y = 163.65\ kg\ s^{-1}$$

and

$$b_z = 147.20\ kg\ s^{-1}$$

The major target of a vibratory conveyor is the efficient transport of the goods to be conveyed. High damping would have a strong negative effect on the amplitude and the acceleration of the goods and so directly on the output of the conveyor. In addition, based on the conclusion done with the help of equation (9), the potential rotation around the mass centre point of the conveying element would be increased having higher damping. The values meet the expectation for this type of linear conveyor, matching variant A.

5.2.2 Natural frequencies of the conveyor

To get the necessary information on the resonance frequencies corresponding to the coordinate system of the conveying element, two piezo sensors are used for parallel in combination with two channels of the analyser.

Therefor the frequency spectrum is analysed, taking one sensor a reference to one fix position and moving the second sensor to different positions, representing all six degrees of freedom of the coordinate system of the conveying element. The excitation step by step then is done manually in the six directions of freedom and the date are recorded. Figures 29 to 32 intended to give representative outline of the testing.

Source: Own source

Figure 29: Resonances with sensor position z- and z- direction

Source: Own source

Figure 30: Resonances with sensor position x- and z- direction

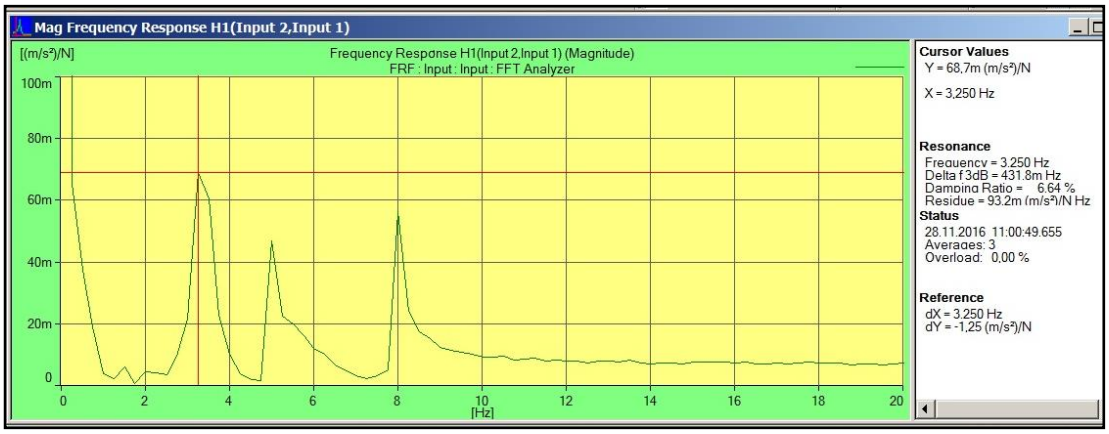

Source: Own source

Figure 31: Resonances with sensor position x- and y- direction and horizontal excitation

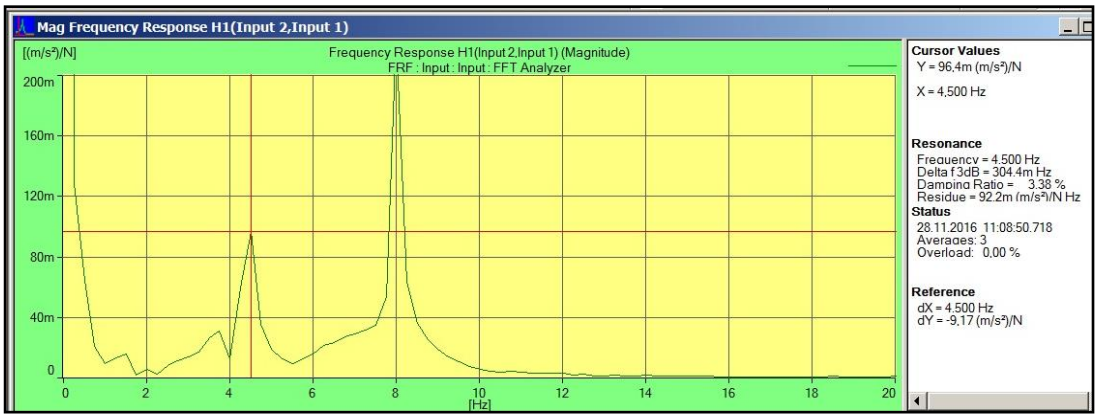

Source: Own source

Figure 32: Resonances with sensor position x- and z- direction and vertical excitation

As result of this analysis the following resonance frequencies are identified:

- Resonance in x- direction (conveying direction): 3.25 Hz
- Resonance in y-direction (across conveying direction): 3.25 Hz
- Resonance in z-direction (vertical): 4.25 Hz
- Rotation around x-axis (A): 3.50 Hz
- Rotation around y-axis (B): 8.00 Hz
- Rotation around z-axis (C): 5.25 Hz

This analysis already shows, that none of the natural frequencies matching the intended excitation frequency of 16.00 Hz. It can be presumed, that the conveyor will not provide the optimum conveying capacity.

5.2.4 Analysis of the conveying element motion

As next step of the system analysis, the motion of the linear conveyor under working conditions is checked. Therefore, the conveyor drive is started and the operation frequencies are determined. It is expected to find the operation frequency of 16.00 Hz of the excitation drive as described in the manual of the conveyor. Of additional interest is, if any resonance frequencies can be identified and what the occurrence of these frequencies will be during the operation.

As shown in figure 33, the 16.50 Hz signal is clearly traceable and none of the resonance frequencies appearing on the graph. The difference to the intended operation frequency can be explained by an inaccuracy of the transformer and is not deeper analysed.

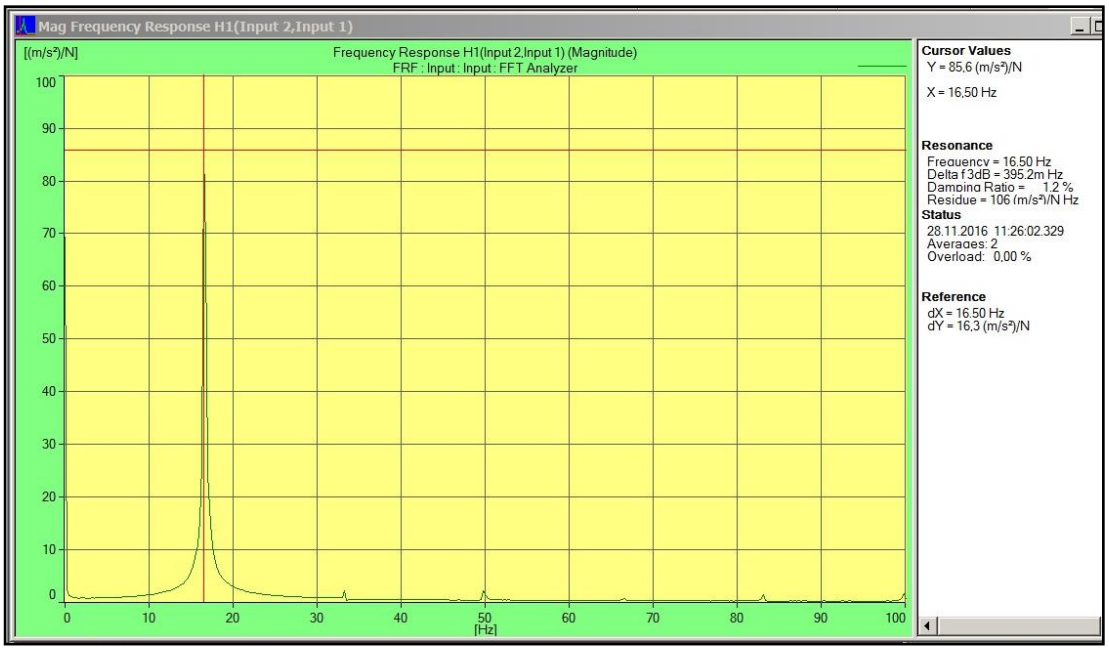

Source: Own source

Figure 33: Operation condition

Running the conveyor, it becomes obvious, that the motion over the full length of the conveying element is not the same at any point. Putting a piece onto the conveying element, for example a screw, it can be seen, that the good is moving with a small amplitude and a quick forward motion into the direction of the hand over point.

Approximately in the middle of the conveying element, i.e. after 600.00 mm, the amplitude in z-direction is bigger than in the beginning and the forward motion is significantly slower. Close to the hand-over point of the conveying element, the amplitude in z-direction is very strong and the forward motion of the good is only very slow. Repeating the test with different testing objects, having different masses and centre points, the general motion characteristic is confirmed. Some of the objects even get thrown backward close to the hand over point.

Therefore, the motion of the conveying element at three significant positions of the conveying element is analysed, by using reference marks which are photographed with slow shutter speed. As significant positions are identified a position close to the back, the approximate centre and a point close to the hand-over position of the conveying element. The marks are fixed to the side frame of the conveying element. Then the angles of the motion to the horizontal line are determined by graphic analysis. The results are taken from figure 34.

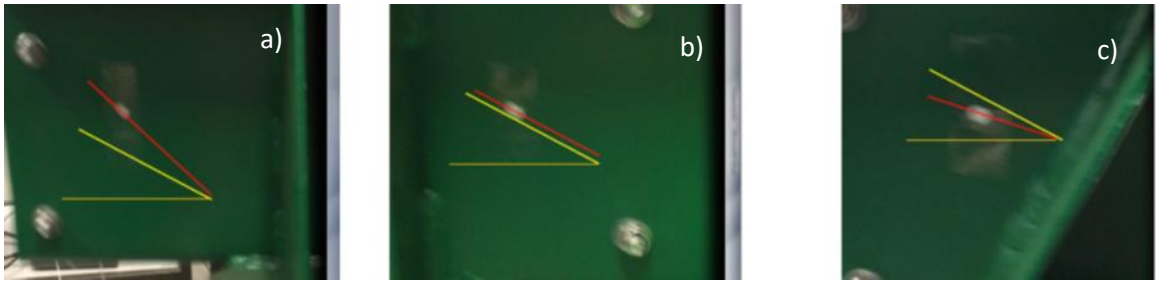

Source: Own source

Figure 34: Motion of reference marks
a) close to hand-over point, b) close to conveying element centre c) close to back side

Legend corresponding to figure 34:

- The orange Line represents the horizontal (parallel to x-direction)
- The yellow line represents the angle of excitation of 30°
- The red line represents the motion of the considered reference mark

The evaluation of the test shows the following results:

- The motion of reference mark “a” takes place under 42° to the horizontal i.e. +12° to the excitation direction
- The motion of reference mark “b” takes place under 30° to the horizontal i.e. the excitation direction
- The motion of reference mark “c” takes place under 18° to the horizontal i.e. -12° to the excitation direction

The different amplitudes in z-direction in each measured points is of particular interest. The increase of that component of the motion causes the most significant obstacle of a smooth transport of the goods to be conveyed.

For the analysis of the amplitude in z-direction, the pictures used in figure 34 are supplied with individual scales and the amplitude is directly measured out of the picture. This well-established photogrammetric method needs a known reference figure to determine the requested dimensions. This reference is the diameter of the reference dots used for the test of 5.00 mm diameter. Figure 35 indicates the results of the analysis.

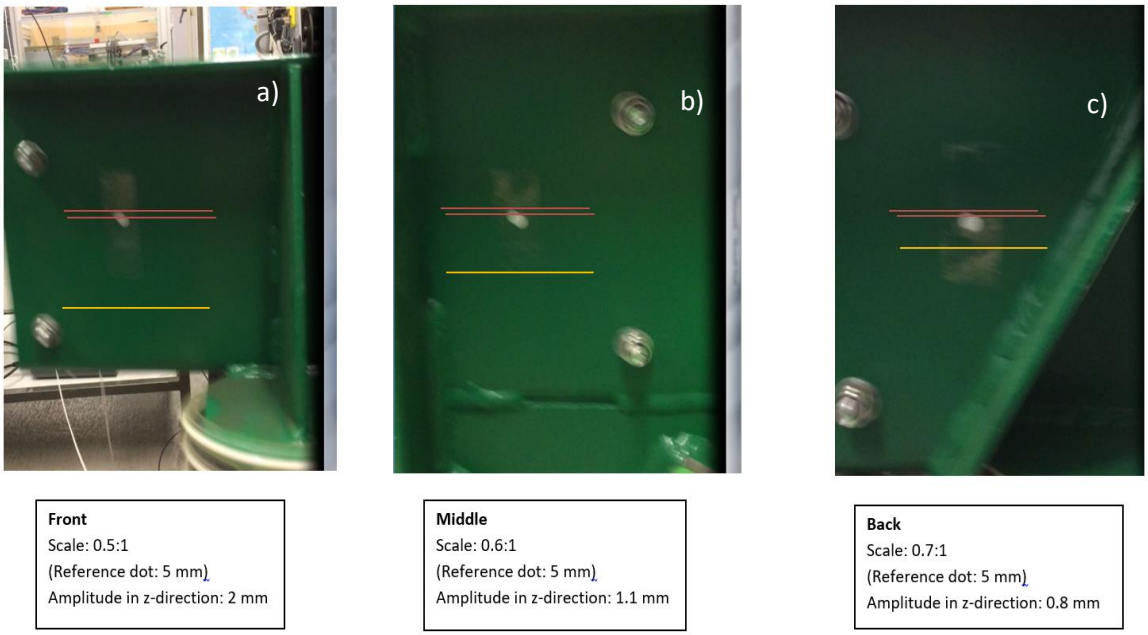

Source: Own source

Figure 35: Amplitudes in z-direction of reference marks

It is demonstrated, that the motion of the conveying element is not like it should be. As reason for this is suspected, that the centre mass point and the centre of elasticity of the conveying element is not situated in the geometrical centre of the system, in line with the force vector of the excitation. A detailed analysis to identify the influence factors will be done further on.

5.2.5 Determination of the mass centre point and the centre of elasticity

A first rough confirmation of the assumption, that geometrical centre point and mass centre point in x-direction are not identical, can be done by visualizing the mass conditions based on figure 22. The result of this simple method is visualized in figure 36. The geometrical centre point is situated in the middle of the conveying element, i.e. half way in x-direction between the helical springs. The geometrical distance between the spring-centres is 1070.00 mm, so the half distance is 535.00 mm.

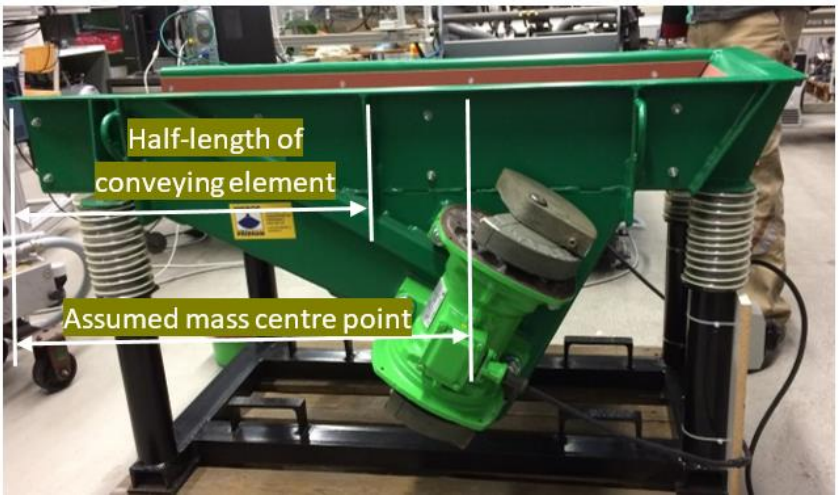

Source: Own source

Figure 36: Photographical determination of mass centre point

A precise determination of the mass centre point and the distance to the geometrical centre in x-direction will be done based on the 3-D CAD model of the conveying element including the eccentric drives fixed to it.

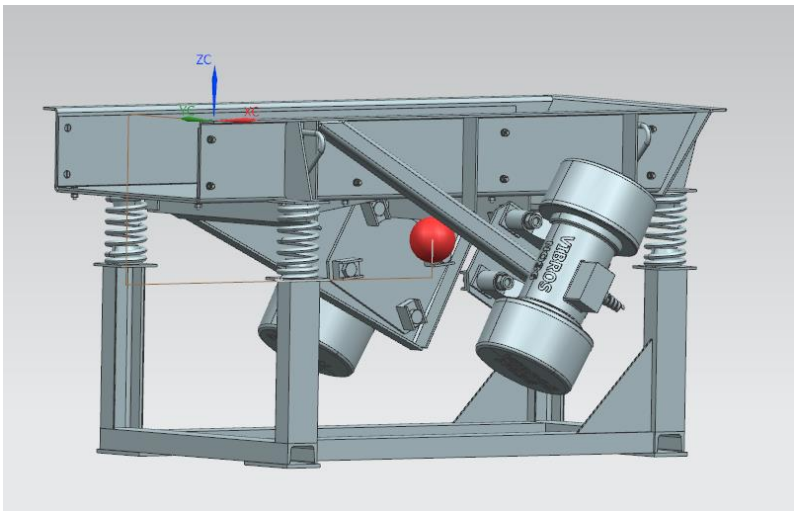

Source: Own source

Figure 37: 3D-CAD model of the conveying element

The red sphere shows the position of the mass centre point. Corresponding to the Cartesian coordinate system shown in figure 37, the mass centre point of the conveying element has the following position:

x-direction: 833.25 mm

y-direction: 300.00 mm (centre line)

z-direction: - 286.50 mm

Based on the CAD model it is demonstrated, that the assumption of a difference of geometrical and mass canter point in x-direction exists on the conveyor. The geometrical centre point can be found at 665.00 mm length and the mass centre point has its position in x-direction at 833.25 mm from the hand over point.

To create a smooth and uniform motion in all areas of the conveying element, the mass centre point has to be brought in-line with the force vector of the excitation.

The second important point to be found, is the centre of elasticity of the vibratory conveyor. To guarantee a uniform motion of the conveying element in all areas, it is necessary that the mass centre point and the centre of elasticity are both situated in line with force vector of the system. The centre of elasticity must be determined practically in x- and z-direction on the conveyor. Therefor a force is put to the conveying element in different zones, first in x-direction and the in z-direction. As soon as the force only results in a pure linear motion, the positional centre is identified. Figure 38 shows the result of this experimental determination.

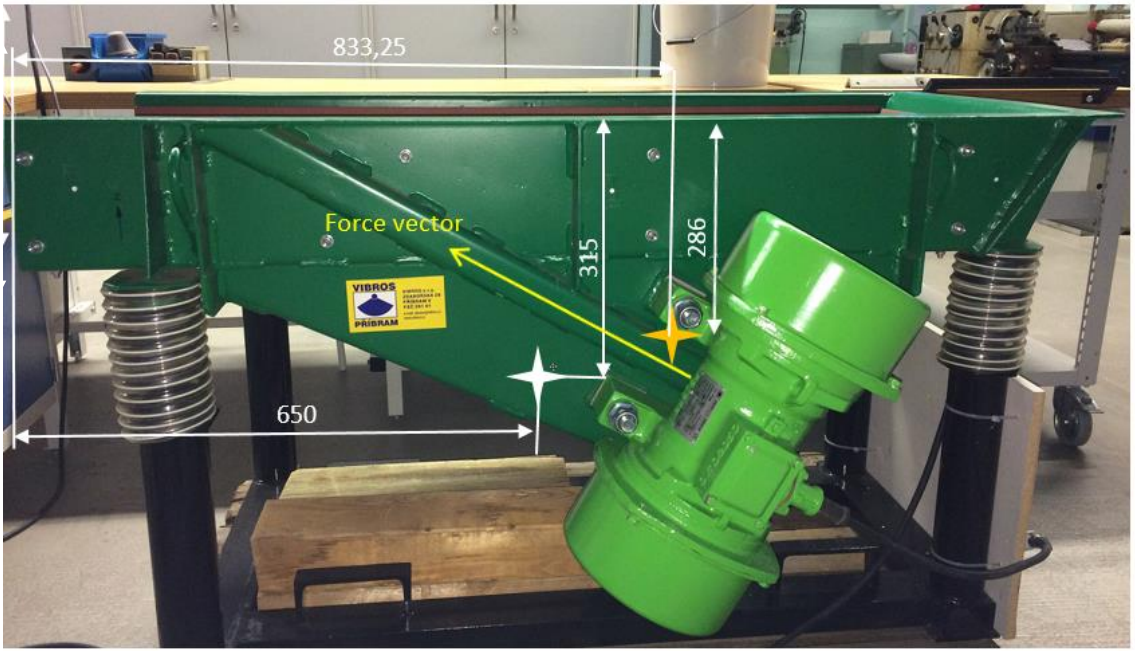

Source: Own source

Figure 38: Centre of elasticity (white) and mass centre point (orange)

Immediately it is visible, that the force vector of the excitation force is not in- line with the centre of elasticity and the mass centre point of the system, which explains the present un-uniform motion of the conveying element.

Based on this perception, an engineering design will be developed to solve the problem.

5.2.6 Attitude of the conveyed goods

Due to the motion of the conveyor causing different amplitudes under different angles on the conveying path, the conveyed good are accelerated differently during their way from the end to the hand-over point of the conveying element. At the backside of the conveying element, the goods are accelerated under an angle of 18°, which supplies a smooth and relatively quick in x-direction oriented motion. The motion more and more receives a component in z-direction, as more the goods are getting conveyed into the direction of the hand-over point of the conveying element. Simultaneously, the decrease of the goods speed in x-direction can be detected. Approximately, on the half way between the geometrical centre and the hand-over point of the conveying element, the motion of the goods starts to get very turbulent. The acceleration in z-direction moves the goods to more than the double amplitude compared to the start point of the motion. By the same time, the conveying speed lowers significantly. Bulk material is strongly segregated in this zone. Additionally, a blocking effect can be identified, caused by goods remaining in this part of the conveying element. New material from the back of the conveyer will be retained. The Last quarter of the distance between geometrical centre and hand-over point converts into a bottleneck.

A video demonstrating the effect enclosed in appendix 4 of the dissertation. Figure 39 will give an impression of the described effect.

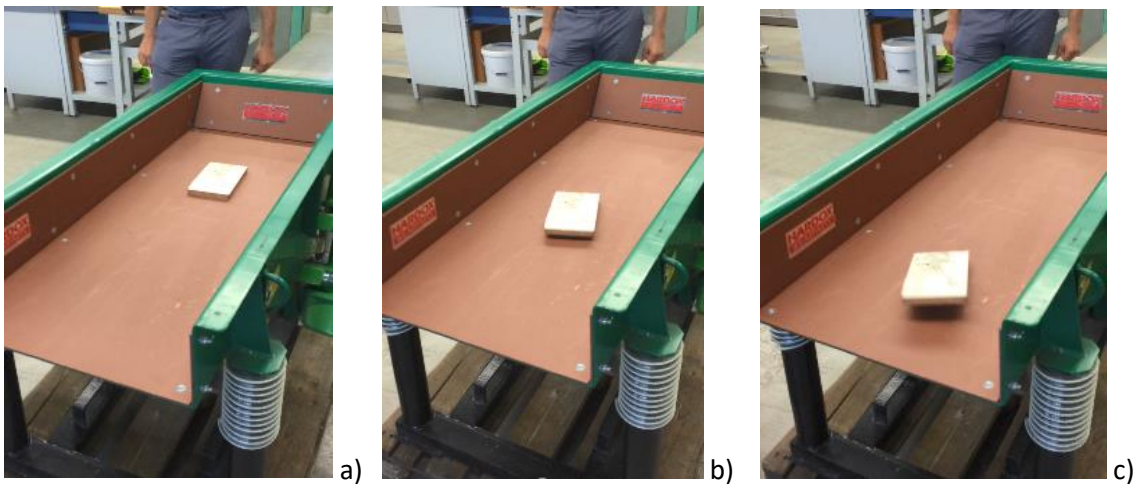

Source: Own source

Figure 39: Recorded motion of an example good. Position a) near the start point, b) in the area of the geometrical centre and c) close to the hand-over point of the conveying element

5.2.7 Vibration transmission to the ground

To get the necessary information on the vibration forces transmitted to the ground during the operation of the vibratory conveyor, one sensor is fixed to the frame.

It is oriented in z-direction and situated in the approximate geometrical centre of one of the two traverse steel bars to record the full spectrum of the vibrations transmitted by the conveying element. Operating the conveyor in a real situation, the frame will be fixed to the ground by heavy-duty screws and no damping elements are foreseen to be placed between the frame and the ground. The result of this installation method is the direct and undamped transmission of the full vibration. Due to the relevance of vibration signals up to 100.00 Hz, the recorded spectrum shown in figure 40 is cut off at this value.

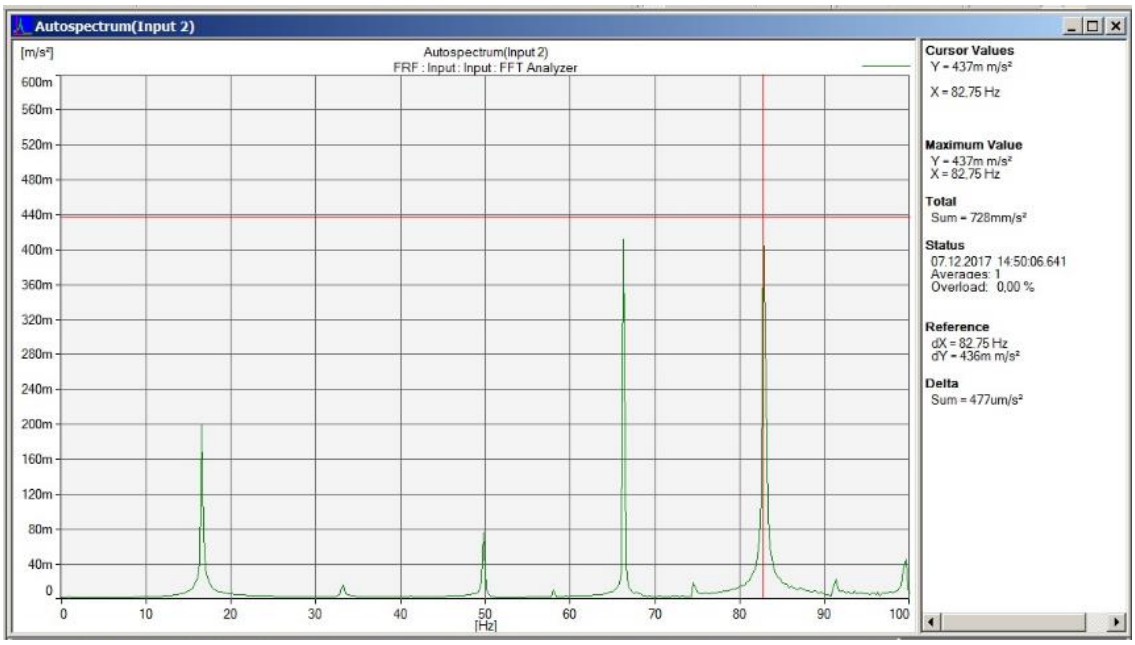

Source: Source Own source

Figure 40: Recorded spectrum of vibrations to the ground from 0 – 100 Hz

The excitation frequency of 16.50 Hz is clearly identified. In addition the multiples of the excitation frequency can be found. However, the third multiple of 66.00 Hz and the fourth multiple of 82.50 Hz are the signals showing the highest acceleration values. The first multiple value of 33.00 Hz and the second multiple value of 49.50 Hz are proportionally low to the strength of the original excitation signal. Additional, very week signals showing multiples of the half frequency, beginning with 57.75 Hz, but these frequencies will have no significant effect to the subsoil.

5.3 Analysis of dynamic parameters

Comparing the natural frequencies to the excitation frequency of the linear vibratory conveyor it is obvious that the conveyor is not working in its optimum capacity range. Due to the relation between the frequency ω_0, the mass of the conveyor m and the stiffness of the springs k, the optimum excitation frequency ω_E would have to match the natural frequency in z-direction of $2\pi f_{0x}$, which is 26.70 s^{-1} . However, based on the 16.00 Hz excitation frequency, the value for $\omega_E = 100.53$ s^{-1}. This means the system is running over resonant in an area high above the optimum working point of the system. In figure 43 the effect is shown in a graph amplitude over frequency.

For a further general optimisation of the conveyor, the system has to be modified in a way that the natural frequency ω_0 and the excitation frequency ω_E will get closer or under the best conditions will become identical. This is not part of this dissertation work.

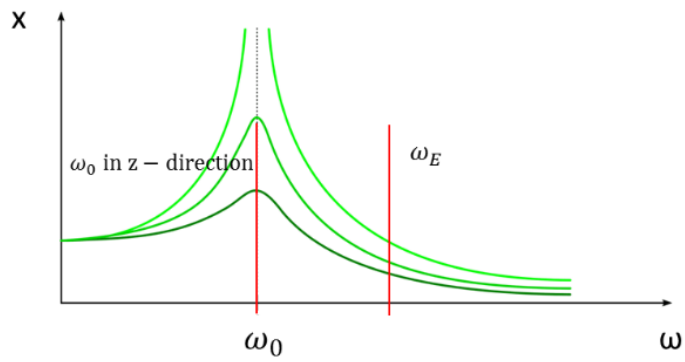

Source: Own source

Figure 41: Example for excitation over resonance

5.3.1 Determined data of the vibratory conveyor

Analysing the motion of the conveyor, it will be of interest to harmonize the vertical motion in particular over the full length of the conveyor. Therefor the general mechanical model figure 42 presented in chapter 4.1 of the conveyor is taken as base for a model of the real vibratory conveyor.

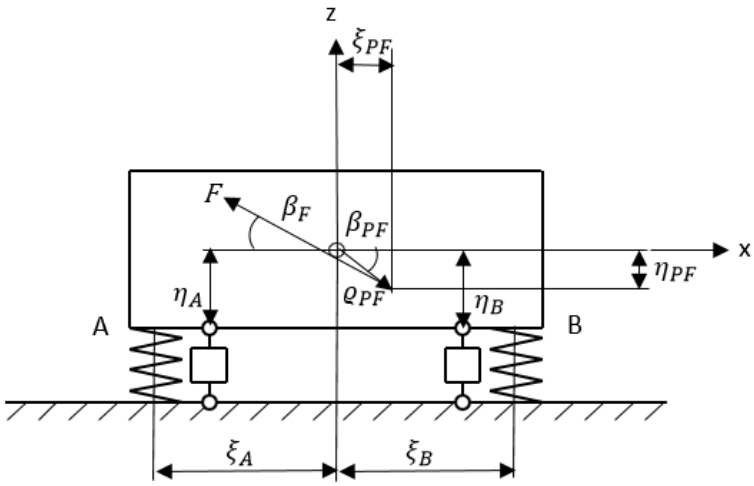

Source: Own source

Figure 42: Mechanical model of the examined conveyor

To generate a harmonic and even motion over the full length of the conveyor in a later step, it is necessary to find the correct parameters to avoid a rotation around the mass centre point of the system. The necessary values can be determined by analysing the CAD-drawing, certain values from the tests and measured dimensions to calculate the dynamic parameters. Later these values will be used to calculate the displacement of the centre of elasticity and to simulate the modified motion by using the mathematical software "Maple".

The result of the analysis is a maximum acceleration of 40.60 m s^{-2}. For the calculation of the effective force, this value has to be lowered to the effective value of acceleration, dividing the value by $\sqrt{2}$. The effective acceleration is 28.70 m s^{-2}.

Based on the Formula

$$F_E = m \cdot a, \tag{54}$$

the result for the effective force on the force vector is

$$F_E = 268.00\ kg \cdot 28.70\ m\ s^{-2}$$

$$F_E = 7692\ N = 7.70\ kN$$

The moving mass *m* of the linear vibratory conveyor is 268 kg. The mass moment of inertia in z-direction can be calculated based on the equation:

$$J_Z = m \cdot (\frac{1}{3} l^2 + \frac{1}{12} w^2), \tag{55}$$

where *l* represents the length and *w* the width of the conveying element. This results in:

$$J_Z = 268.00\ kg \cdot (\frac{1}{3} 1.40\ m^2 + \frac{1}{12} 0.006\ m^2)$$

$$J_Z = 175.00\ kg\ m^2$$

The distances between the points A respectively B and the mass centre point m of the conveyor are:

$$\xi_A = 603.25\ mm$$

$$\xi_B = 468.75\ mm$$

The total mass of the conveying element of 268.00 kg can be distributed to the spring fixation points A and B as follows:

$$m_A = 117.20\ kg$$

and

$$m_B = 150.80\ kg$$

The distance between mass centre point s and force transmission point is

$$\rho_{PF} = 105.00\ mm.$$

The angle β_{PF} between the horizontal crossing the point of application and the radius vector ρ_{PF} is

$$\beta_{PF} = 36.20°.$$

The angle between the excitation force and the horizontal crossing the point of application to the conveying element is

$$\beta_F = 30°.$$

The vertical distance η_A and η_B between the mass centre and the fixation point of the springs is

$$\eta_A = \eta_B = 111.00\ mm.$$

The stiffness in x-direction of each spring pair in A and B is

$$k_{Ax} = k_{Bx} = 67166\ N\ m^{-1}.$$

Based on these data, a numerical analysis can be done by the use of the mathematical software “Maple”. This analysis will show the characteristics of the present motion of the vibratory conveyor and will give ideas for the modification of the system.

5.3.2 Amplitude and stiffness characteristics of the vibratory conveyor

Based on the method described in chapter 4.1.1, the calculated and determined values are fit into the general equations (3), (4) and (5). In addition, the damping of the system has to be considered on the real conveyor. This is done by extending the equations by the terms corresponding to the damping of the system as follows:

$$m\ddot{x} + (k_{Ax} + k_{Bx}) \cdot x + [(k_{Ax} - k_{Bx})\xi_A + (k_{Ax} - k_{Bx})\xi_B] \cdot \varphi + (b_{Ax} + b_{Bx}) \cdot \dot{x} + \\ +[(b_{Ax} - b_{Bx})\xi_A + (b_{Ax} - b_{Bx})\xi_B] \cdot \dot{\varphi} = F_0 \cdot \cos(\omega Ft) \tag{56}$$

$$m\ddot{z} + (k_{Az} + k_{Bz}) \cdot z + [(k_{Az} - k_{Bz})\xi_A + (k_{Az} - k_{Bz})\xi_B] \cdot \dot{\varphi} + (b_{Az} + b_{Bz}) \cdot \dot{z} + \\ +[(b_{Az} - b_{Bz})\xi_A + (b_{Az} - b_{Bz})\xi_B] \cdot \dot{\varphi} = F_0 \cdot \sin(\omega Ft) \tag{57}$$

$$J_z\ddot{\varphi} + [(k_{Az} - k_{Bz})\xi_A + (k_{Az} + k_{Bz})\xi_B] \cdot z + [(b_{Az} + b_{Bz})\xi_A + (b_{Az} + b_{Bz})\xi_B] \cdot \dot{z} + \\ +[(k_{Az} - k_{Bz})\xi_A^2 + (k_{Az} - k_{Bz})\xi_B^2] \cdot \varphi + [(b_{Az} + b_{Bz})\xi_A^2 + (b_{Az} + b_{Bz})\xi_B^2] = \\ = -F_0 \cos\beta F \cdot \rho PF sin\beta PF + +F_0 \sin\beta F \cdot \rho PF cos\beta PF \tag{58}$$

Finally all equations are converted into matrix form. For the mass matrix and the damping matrix, the equations will stay identical to equations (6) and (7). For the damping, the following matrix has to be created:

$$B = \begin{bmatrix} b_{Ax} + b_{Bx} & 0 & -\eta_A b_{Ax} - \eta_B b_{Bx} \\ 0 & b_{Az} + b_{Bz} & \xi_A b_{Az} + \xi_B b_{Bz} \\ -\eta_A b_{Ax} - \eta_B b_{Bx} & \xi_A b_{Az} + \xi_B b_{Bz} & \eta_A^2 b_{Ax} + \eta_B^2 b_{Bx} + \xi_A^2 b_{Az} + \xi_B^2 b_{Bx} \end{bmatrix} \tag{59}$$

As result of the numerical calculation under use of the software “Maple”, the graph figure 43 for the relation amplitude over Stiffness in z-direction for the rotation of the system can be found:

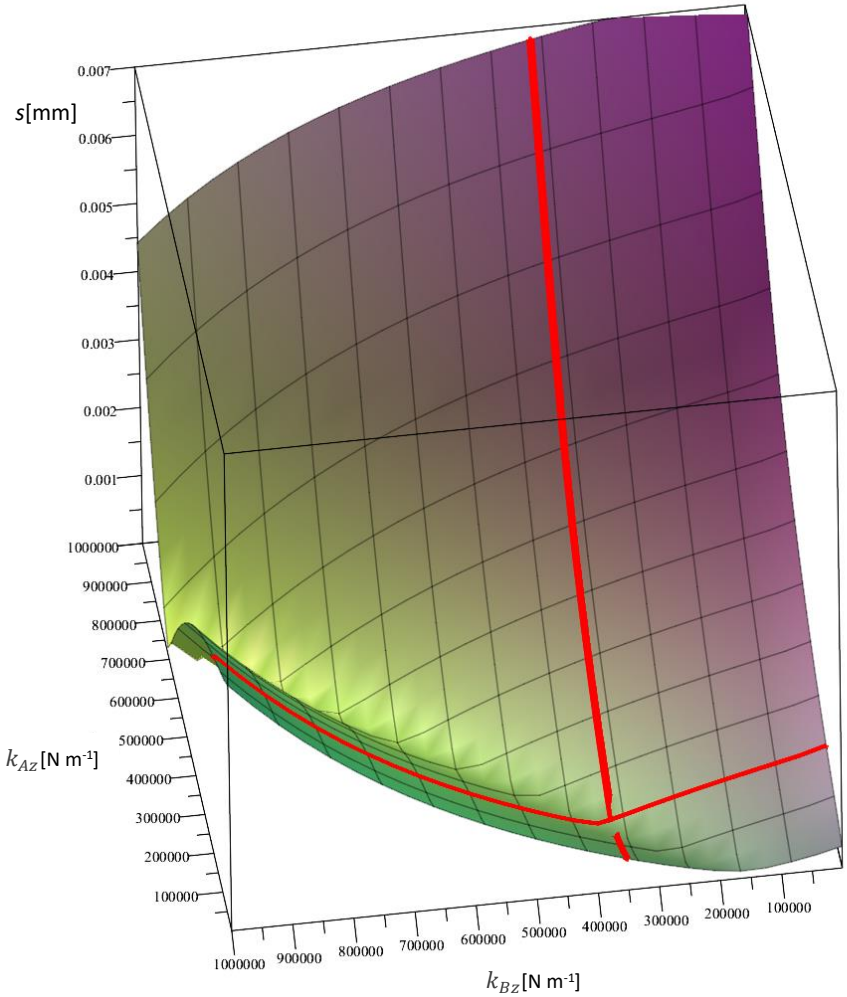

Source: Own source

Figure 43: Amplitude over stiffness for the rotation of the linear vibratory conveyor

The valley of the graph represents the zone, where no rotation of the system will take place. Following that valley, the stiffness k_{Ax} and k_{Bx}can be found, where no rotation of the vibratory conveyor will take place. Looking on the stiffness of the springs installed, each pair of springs installed in point A and B represents a value of 168652 N m^{-1}. Following the graph, k_{Bx} is situated in the area of no rotation while the amplitude for k_{Ax} corresponds to an amplitude of approximately 1.00 mm. That means, the rotating component of the motion in point A has an additional effect of 0.90 mm compared to point B. The graph figure 44 illustrates this effect.

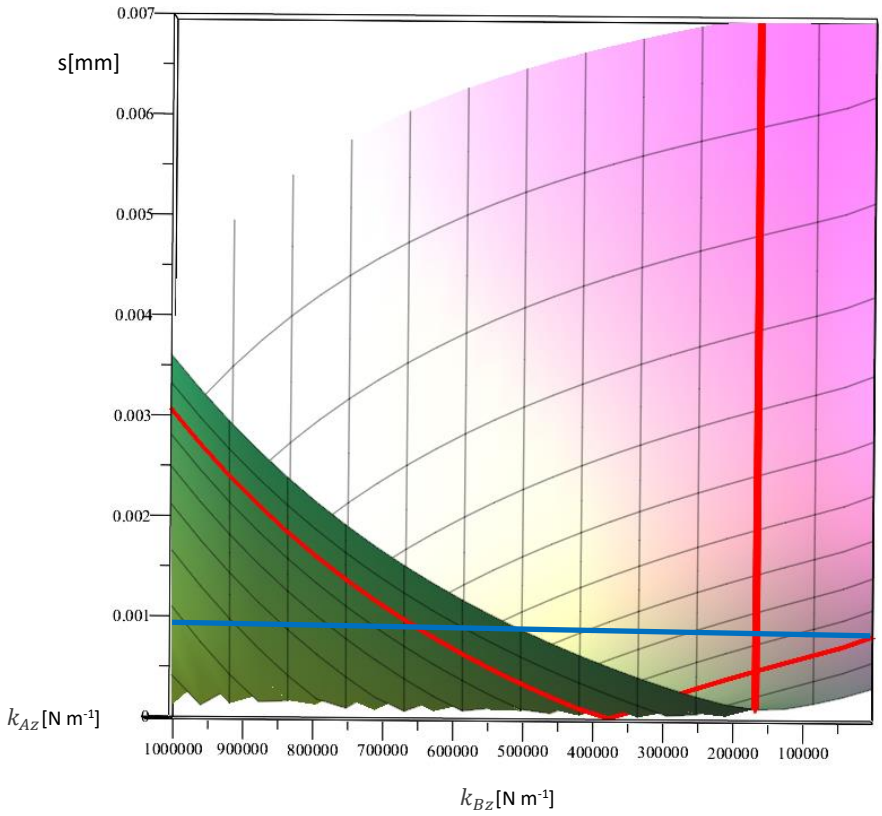

Source: Own source

Figure 44: Rotation component of the amplitude in point A of the conveyor (blue line)

Calculation and graph confirming the experience made during testing the system. So the equations are verified as useful tool for the general analysis of linear vibratory conveyors of variant A. In a further step, the calculation model will be used for the determination of spring pairs, elimination the rotation component of the conveyor.

5.3.3 Time and frequency characteristics of the vibratory conveyor

As a cross check and to verify the calculation for amplitude over time, an additional calculation and numerical simulation is done for the relation amplitude over time.

This graph shows the time function of the different components of the motion for the excited system, i.e. The Amplitude of the excitation, the x-component of the amplitude, the z-component of the amplitude and the rotation component of the amplitude. The rotation component should ideally be zero respectively very close to zero to enable a smooth linear conveying motion. A significant rotation component will confirm the effect calculated already for the model amplitude over stiffness. The result of the numerical calculation of the “Maple” software id shown in figure 45.

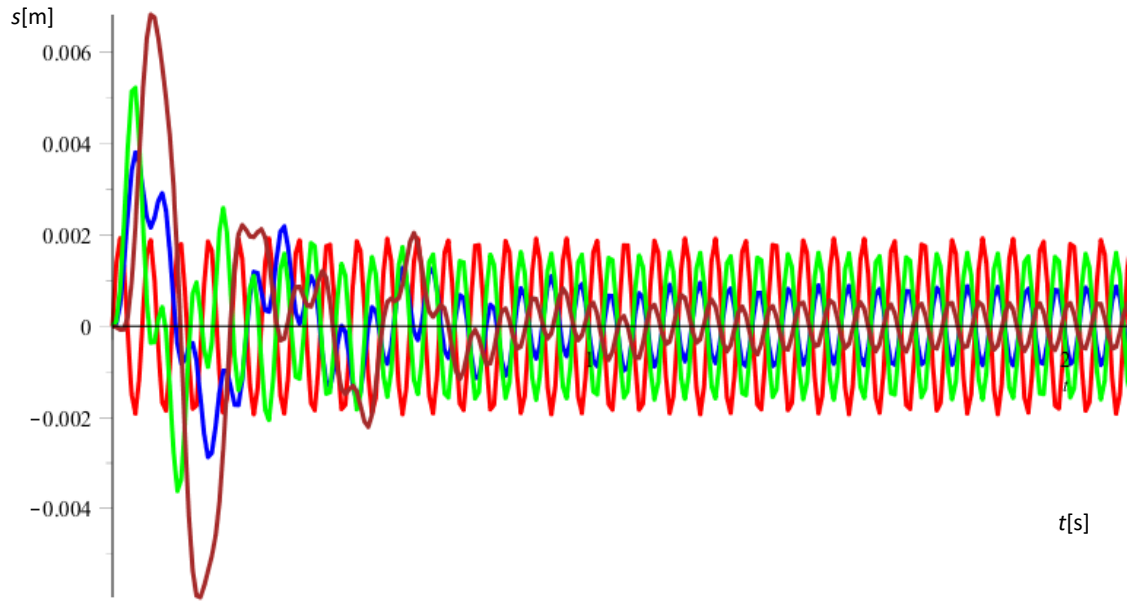

Source: Own source

Figure 45: Graph amplitude over time for the motion of the linear vibratory conveyor.

In this graph, the red line represents the excitation, the blue line demonstrates the amplitude in x-direction, the green line shows the amplitude in z-direction and the brown line stands for the rotation of the system under the selected conditions. The expected results are shown in this graph, corresponding to the experiences made during the operation tests of the conveyor.

In the further steps, both simulations will be used for the identification and selection of appropriate springs for the optimisation of the linear vibratory conveyor.

5.3.5 The power effect of the vibratory conveyor on the foundation

In all previous analysis of the linear vibratory conveyor, the effect of the transmission of vibration to the ground has been neglected. Due to the principle of design of this tested conveyor of variant A it can be determined, that the system has a very low damping due to its nature. No dampers are installed between conveying element and frame due to the fact, that the primary target of conveying good guaranteeing a certain capacity could not be put into reality under technical acceptable conditions.

Increasing the damping between the conveying element and the frame, to reduce vibration transmission to the ground, would result a lower conveying capacity and as already demonstrated in equation (9) a increasing rotation of the conveying element, which in any case has to be avoided.

The frame of the existing conveyor is welded of steel profiles, which are foreseen to be fixed to the ground by heavy duty screws. No rubber damper is foreseen to be situated between the frame and the ground.

An integration of rubber elements could help to lower the amplitude of the transmitted vibrations to the ground, but no significant effect would be perceptible. A disadvantage of this potential approach to solve the problem is the direct effect on the stiffness of the whole system. The operation conditions regarding the intended motion will change and a loss of capacity compared to an optimised system will occur.

One favourable solution to segregate the transmission of vibration without the loss of conveying capacity is the compilation of a vibratory conveyor of variant A into a conveyor of variant D. This possibility and its effect will be followed as option for the improvement of the conveyors motion by simultaneous reduction, if possible even elimination of the transmission of vibration to the environment of the conveyor.

6 Improvement of the conveyor

This chapter deals with the possibilities of optimising the motion characteristic of linear vibratory conveyors. Based on the already set up models for the optimisation of the motion and so by the same time the increase of conveying capacity of one-mass conveyors, the possibilities and limitations for linear conveyors of variant A and B will be proposed verified by testing and validated with reference to their potentials and limitations in the first step.

In the second step, a two-mass conveyor system will be analysed, as well with regards to its possibilities and limitations, but with particular focus on the possibility of elimination of vibration transmission to the ground. The proposed mechanical model of such a system will be simulated, verified and validated by testing. To do the verification, a representative function model is presented, build and tested.

6.1 Improvement of the one-mass system

The target is to influence the motion of the linear vibratory conveyor based on the described mechanical model. Therefor the centre of elasticity must be moved, which will be demonstrated using the two alternative possibilities,

a) Modifying the vertical springs stiffness k_v
b) Modifying the distances ξ_A or/and ξ_B or
c) Modifying the mass

Putting the focus on the capacity, the balance conditions and the possibilities of modification of the reviewed conveyor, a modification of the mass by fixing additional mass elements to the hand-over point of the conveyor cannot be preferred.

The modification of the distances ξ_A or ξ_B will effect a major redesign and structural changes to the vibratory conveyor. In addition the system will become more rotation sensitive when the vertical brackets of the frame will be positioned closer to each other. As soon as the goods to be conveyed will come in contact with the conveying element, the rotation effect will increase supplemental and the modification will become counterproductive and under the worst condition totally useless.

To keep the compact and rigid design of the linear vibratory conveyor, the best possible solution to modify the conveyors motion would be a re-location of the centre of elasticity. This can be done based on equations (56) to (58), respectively their matrix forms.

Keeping the mass conditions of the conveying element untouched and ensuring the damping conditions staying competitive to the presently existing once, a solution will be found by changing the stiffness conditions of the springs in the points A and B of the conveyor.

Keeping the focus on this modification possibility, three options of influencing the situation of the mass centre point with a simultaneous elimination of the rotation part of the motion are generally possible:

- Changing the stiffness k_{Az} by replacing the springs in point A
- Changing the stiffness k_{Bz} by replacing the springs in point B
- Changing the stiffness k_{Az} and the stiffness k_{Bz} by replacing all springs in points A and B

The first option, keeping the stiffness $k_{Az} = 158652$ N m^{-1} constant on a modified system, would be a practicable possibility. Looking to the graph amplitude over stiffness, the corresponding value of k_{Bz} can easily be identified:

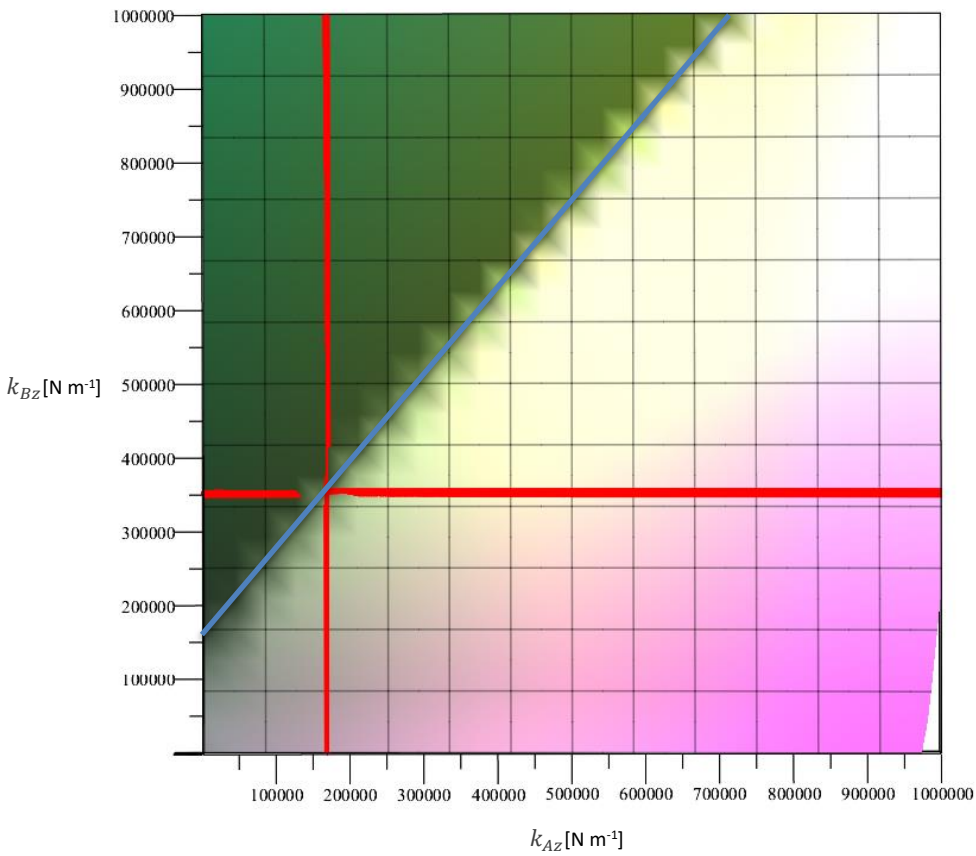

Source: Own source

Figure 46: Corresponding stiffness k_{Az} and k_{Bz} for non-rotation condition (blue line = neutral zone)

For the selected stiffness $k_{Az} = 168652$ N m^{-1}, a value for $k_{Bz} = 352000$ N m^{-1} is shown in the graph. Finding springs with this stiffness characteristic, the existing springs in point B just have to be replaced and the conveying element is expected to generate a pure linear motion with no rotation components.

Using the same graph it can be determined, that a modification of stiffness k_{Az} by simultaneous retention of stiffness k_{Bz} cannot be realised. The stiffness of the new springs in point A would become so low, that the conveyor could not realise a technical useful motion anymore.

Any stiffness modification of both springs along the blue line would be possible as well. However, it is recommended to select stiffness values not below approximately $k_{Az} = 80000$ N m^{-1}, to keep the system and the conveying process reliable.

One important decision factor for the method of the modification is the availability of standard springs. To match the target of implementing an efficient and cost effective solution with less as possible special solutions into reality, the test application for the existing linear vibratory conveyor has to be done by the use of standard springs.

A deep investigation on springs with the requested stiffness shows, that no standard springs for the planned modification are available on the European market for the case, that the springs used in point A remain in the system. Based on the proposed method of following the non-rotation zone in the amplitude over stiffness graph, suitable springs can be identified. For the verification and validation test of the proposed method, the following springs have been identified and installed:

- Two spring with 51000 N m^{-1} stiffness to reach a total stiffness of $k_{Az} =$ 102000 N m^{-1} installed in point A
- Two spring with 124000 N m^{-1} stiffness to reach a total stiffness of $k_{Bz} =$ 248000 N m^{-1} installed in point B

This combination will comply very closely with the requirements, as shown in figure 47:

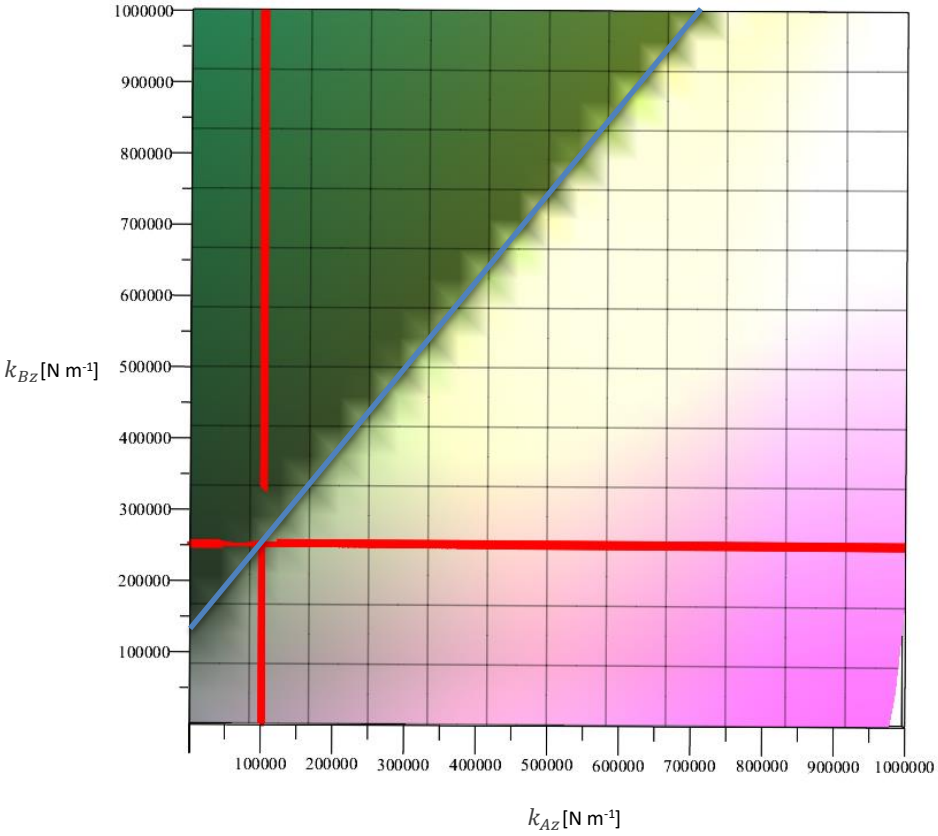

Source: Own source

Figure 47: Corresponding stiffness k_{Az} and k_{Bz} for the selection of test springs (blue line = neutral zone)

Based on that correlation, spring pairs with the specification shown in figure 48 and 49 are implemented to the linear vibratory conveyor:

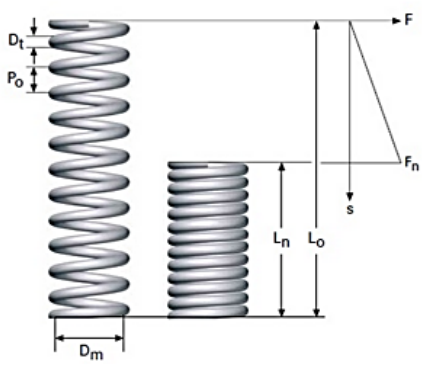

Dimensions and characteristics	
Part number	6908
Dt	12
Di	70
Dm	82
L0	200
nt	8.7
Po	26
Ln	130.6
Fn	3546
c	51
Ändutförande	1
Mtr	EN 10270-1-SM

Source: Lesjöfors AB

Figure 48: Selected spring type for the installation in point A

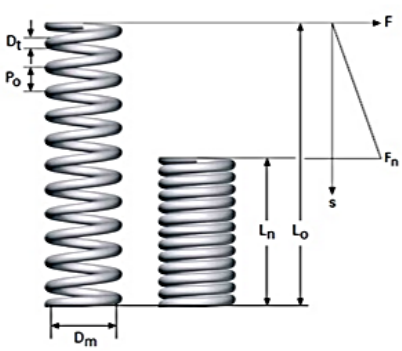

Dimensions and characteristics

Part number	6938
Dt	14
Di	70
Dm	84
L0	150
nt	6.6
Po	26,6
Ln	107
Fn	5341
c	124
Ändutförande	1
Mtr	EN 10270-1-SM

Source: Lesjöfors AB

Figure 49: Selected spring type for the installation in point B

The new springs having different length´. To avoid an inclination of the conveying element, a spacer is installed directly to the frame of the vibratory conveyor. The new conditions are shown in figure 50.

Source: Own source

Figure 50: Spring with spacer

6.1.1 Modification of the centre of elasticity

The effect of the modification using the new springs with a total stiffness of

$$k_{Az} = 102000\ N\ m^{-1}$$

and

$$k_{Bz} = 248000\ N\ m^{-1}$$

Can be simulated by the use of the numerical calculation model and the software "Maple" again. Replacing the original springs by the new springs, the graph for amplitude over time will have the characteristic, shown in figure 51:

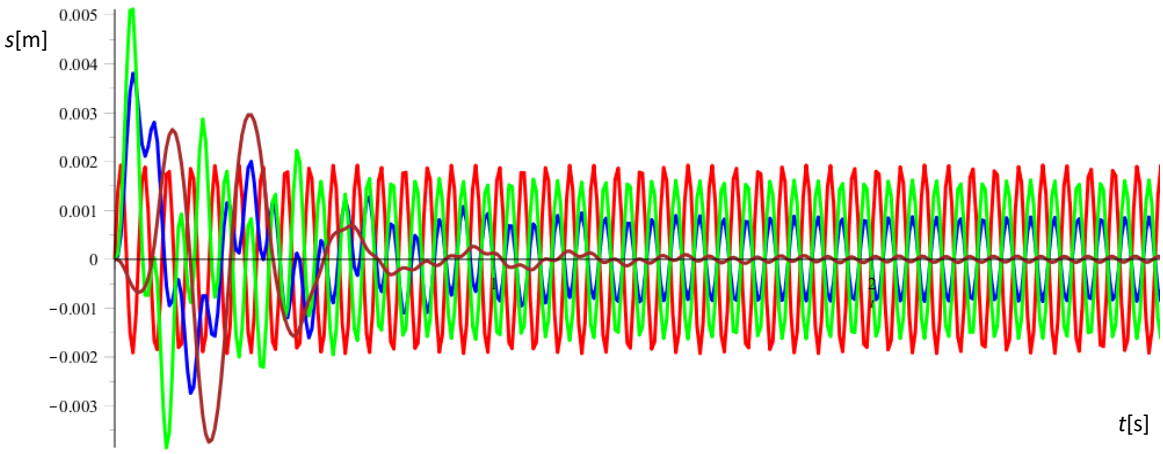

Source: Own source

Figure 51: Graph amplitude over time for the motion of the modified linear vibratory conveyor

Based on this simulation, the positive effect on the modification can be seen. Again, the red line shows the excitation, the blue line demonstrates the amplitude in x-direction, the green line shows the amplitude in z-direction and the brown line stands for the rotation of the system. This rotation is in a very low and acceptable tolerance range now. The influence of the rotation on the total motion is now in the area of only +/- 0.1 mm as shown on the outline figure 52.

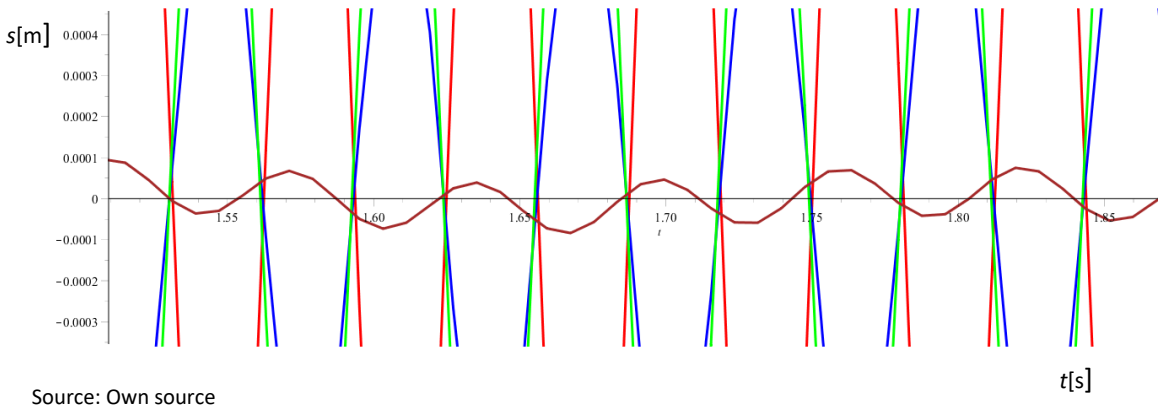

Source: Own source

Figure 52: Graph amplitude over time – outline influence of rotation

Based on this simulation, a test series for the determination of the new natural frequencies and the operation conditions is realised.

6.1.2 Modification by the use of guiding levers

In chapter 4.1.2, the general dynamic model of a linear vibratory conveyor is already introduced. In this chapter, the potential effects of such a guiding mechanism to the analysed vibratory conveyor are simulated. Figure 53 shows the mechanical model of the conveyor, with integrated guiding levers.

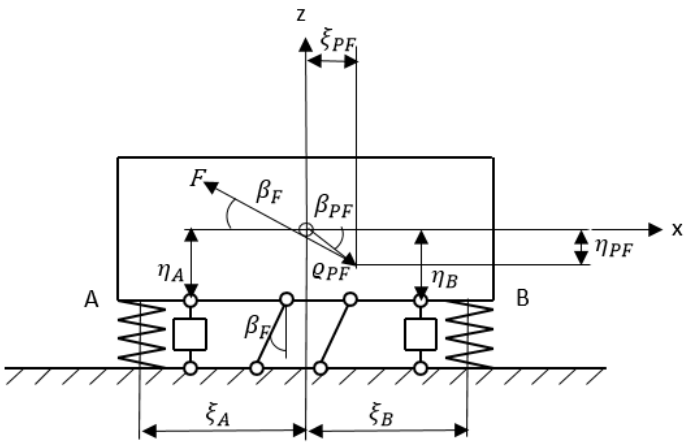

Source: Own source

Figure 53: Mechanical model variant B of the analysed conveyor

The mechanical model corresponds to the model presented in figure 15. All assumptions made for the general dynamic model in equations (14) to (17) are valid for the analysed conveyor.

Assuming that the change of the angle β_F during the operation is very small, the following assumption can be done:

$$\beta_F \ll 0 = const. \tag{60}$$

For that case, the coordinate vectors with the characters x and z can be merged and replaced by character s. Doing this, the equations (3) und (4) can be merged to

$$m\ddot{s} + (k_{As} + k_{Bs}) \cdot s = F_0 \cdot (\omega F t). \tag{61}$$

The stiffness k_{As} and k_{Bs} will have to be determined by the equation

$$k_s = \sqrt{k_x^2 + k_z^2}, \tag{62}$$

With the value of

$$k_s = \sqrt{(67166\ N\ m^{-1})^2 + (163000\ N\ m^{-1})^2} = 176296\ N\ m^{-1}$$

Taking the influence of the damping into consideration, equation (61) has to be extended to its following final form

$$m\ddot{s} + (k_{As} + k_{Bs}) \cdot s + (b_{As} + b_{Bs}) \cdot \dot{s} = F_0 \cdot (\omega F t). \tag{63}$$

The systems now is reduced to one degree of freedom, having a general expressiveness for linear vibratory conveyors of variant B.

6.1.3 Simulation of the modification by using guiding levers

The values from the analysed conveyor are transmitted to the numerical simulation model for the determination of the amplitude over time, which already is applied to the variant A conveyor. A simulation of the amplitude over stiffness will not be necessary, due to the reduction of three degrees of freedom to only one degree of freedom. The results of the simulation are shown in figure 54.

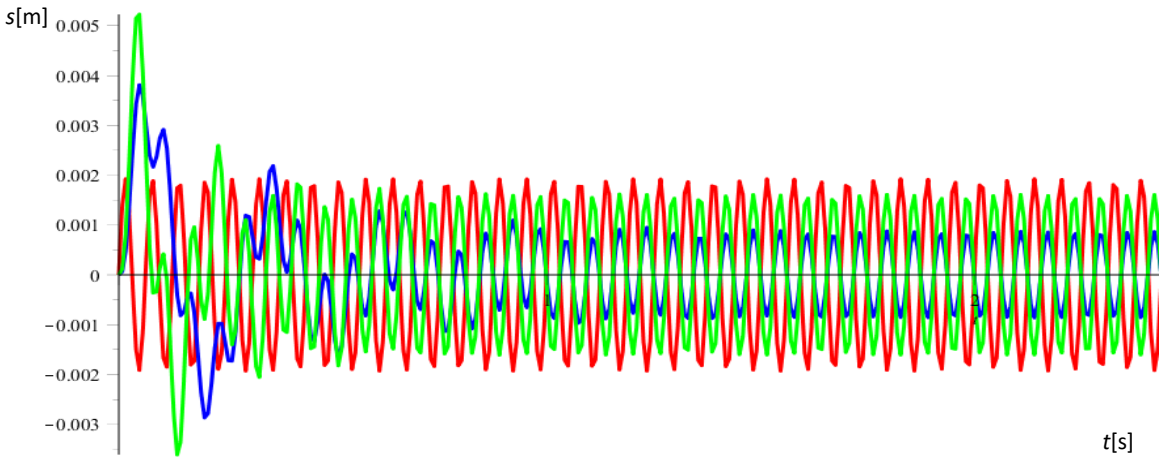

Source: Own source

Figure 54: Graph amplitude over time for the motion of the simulated linear vibratory conveyor variant B

Again the red line shows the excitation, blue line demonstrates the amplitude in x-direction and the green line shows the amplitude in z-direction. Due to the condition of only one remaining degree of freedom caused by the lever arm system, no rotation of the conveying element takes place.

The additional benefit of a solution with lever arms compared to a conveyor of variant A is less sensitivity and dependence on the individual stiffness of the springs mounted in point A and B of the conveyor. As well, sudden changes of the mass of transported objects do not have a big influence to the vibratory conveyor with reference to the motion characteristic over its length. The levers enabling a restricted guidance of the conveying element, with and without conveyed goods.

Due to the difficult modification possibilities of the analysed linear vibratory conveyor and the lack of influence to the reduction of vibration to the ground, this solution is identified as proper solution to optimise a linear vibratory conveyor but will not be verified and evaluated by tests.

For new designs of linear vibratory conveyors, used in insensitive environments with reference to vibration transmission, variant B conveyors can be recommended and the numerical simulation presented is of general use.

6.1.4 Experimental determination and validation of the modification

Based on the calculations done in chapter 6.1, the springs presented in figure 48 and 49 and the spacer shown in figure 50 are implemented. The total stiffness k_{Az} close to the hand over point of the linear vibratory is now lowered to 102000 N m^{-1} while the total stiffness k_{Bz} close to the back end of the conveyor is increased up to 248000 N m^{-1}. The result of the modification is shown in figure 55:

Source: Own source

Figure 55: One-mass vibratory conveyor with modified springs

A first simple test, exciting the system manually close to the hand over point and at the back end of the vibratory conveyor supplies the effect of different reaction amplitudes on both sides compared to the original condition.

To get detailed information of the effects of the modification, a series of tests is set up with the target to determine

- Resonance frequencies and operation frequencies of the new system
- Effects to the motion of the conveying element
- Effects to the transmission of vibrations to the ground

Due to the sudden defect of one force sensor, the determination of the necessary values is done by the use of one single sensor, covering the surface stepwise in all three dimensions.

In the first step, the resonance frequencies in x-, y- and z- direction are determined. The results are shown in figures 56 to 61:

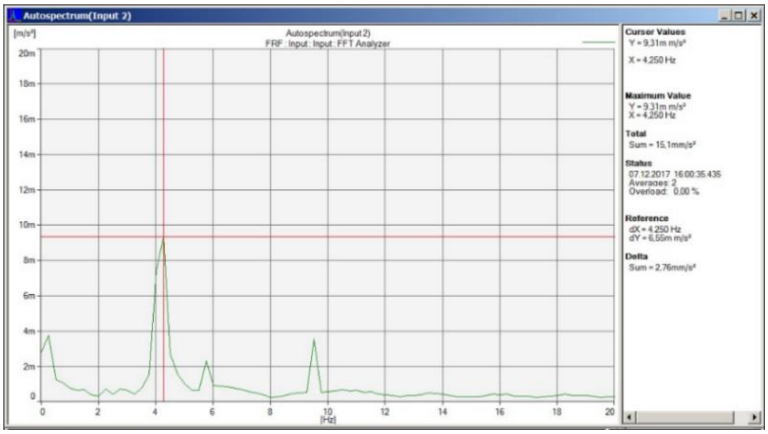

Source: Own source

Figure 56: Frequencies determined for excitation in x-direction, sensor situated in the geometrical centre of the conveying element

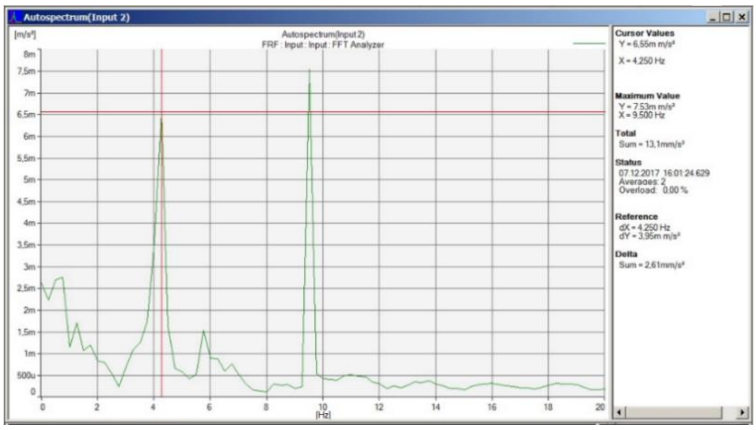

Source: Own source

Figure 57: Frequencies determined for excitation in x-direction, sensor situated next to the hand-over point of the conveying element

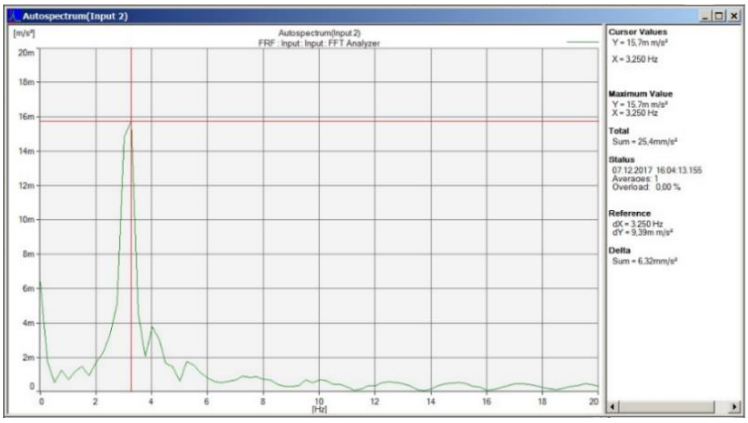

Source: Own source

Figure 58: Frequencies determined for excitation in y-direction, sensor situated in the geometrical centre of the conveying element

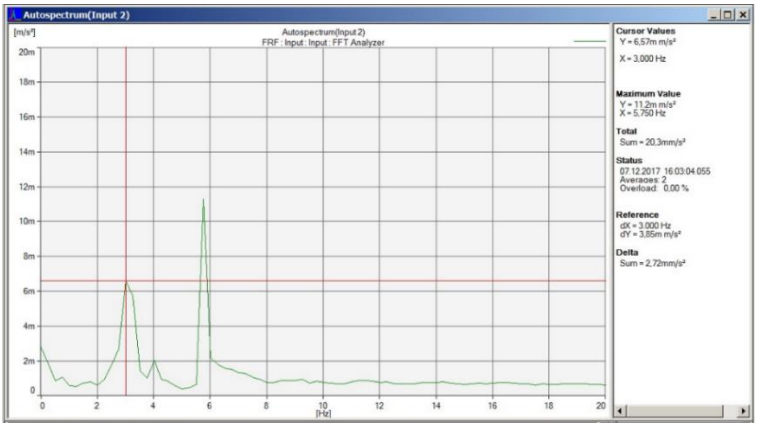

Source: Own source

Figure 59: Frequencies determined for excitation in y-direction, sensor situated next to the hand-over point of the conveying element

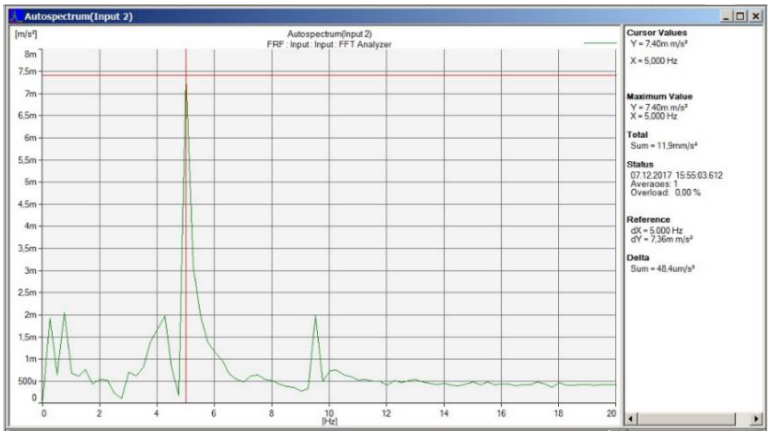

Figure 60: Frequencies determined for excitation in z-direction, sensor situated in the geometrical centre of the conveying element

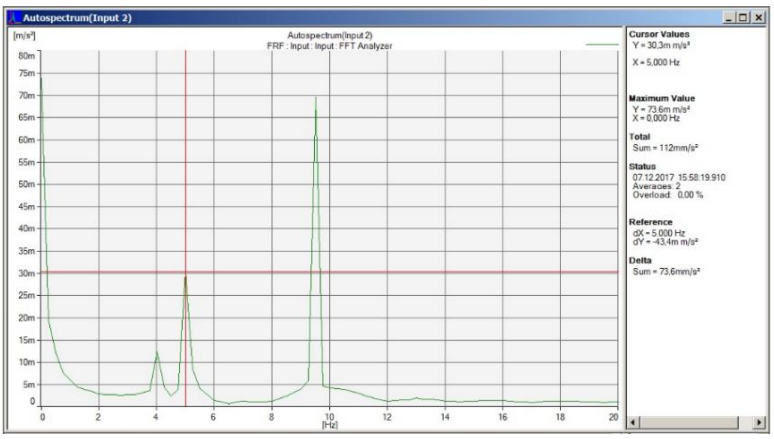

Source: Own source

Figure 61: Frequencies determined for excitation in z-direction, sensor situated next to the hand-over point of the conveying element

With reference to the results of the testes, the new resonance frequencies are determined. To point out the differences to the original assembly, the new values are compared with the original values by the same time. The results are shown in table 3:

Table 3: Resonance frequencies after modification of the system and comparison with original values

	After modification	**Original**
Resonance in x- direction (conveying direction)	4.25 Hz	3.25 Hz
Resonance in y-direction (across conveying direction)	3.25 Hz	3.25 Hz
Resonance in z-direction (vertical)	5.00 Hz	4.25 Hz
Rotation around x-axis (A):	4.00 Hz	3.50 Hz
Rotation around y-axis (B)	9.50 Hz	8.00 Hz
Rotation around z-axis (C)	5.75 Hz	5.25 Hz

Source: Own source

It can be realised, that nearly all values changed compared to the initial situation. The frequencies for the linear motion in x-direction and in z-direction showing increased frequencies of 1.00 Hz, respectively 1.25 Hz, which can be explained by a significant higher stiffness k_B of the new spring pair compared to the original springs, installed close to the back end of the conveyor compared. In addition, the new springs are 50.00 mm shorter, which increases the stiffness in x-direction as well.

The frequency in y-direction is not increased, which only can be explained with a compensation of the stiffness in this direction compared to the original equipment. In any case, this direction is of no importance to the conveying process and will not be analysed any deeper.

The rotation frequencies around the x-axis and the z-axis is increased by 0.50 Hz, while the rotation around the y-axis is increased by 1.50 Hz.

A slight increase of the single frequencies of spectrum is expected due to the total increase of the stiffness of the system in z-direction from $k_{z\,old} = 337304$ N m^{-1} to $k_{z\,new} = 350000$ N m^{-1}and is identified during the tests individually.

The second effect to be determined is the re-situation of the centre of elasticity. For this purpose, again the conveying element is loaded by punctual forces over the full conveying length in x-direction, to identify the point, where only a linear motion with no rotation component can be identified. The same procedure is done in z-direction, beginning at the top end of the conveying element, going stepwise downward into the direction of the ground.

The result of this test is shown in figure 62 and the results are compared anticipant to the original ones in table 4:

Table 4: Resonance frequencies after modification of the system and comparison with original value

Centre of elasticity	From hand-over point	From the top end
After modification	770 mm	300 mm
Original	650 mm	315 mm
Difference	+120 mm	-15 mm

Source: Own source

Source: Own source

Figure 62: New centre of elasticity

As result of the modification, the centre of elasticity moved much closer to the force vector. The major intention for the modification is demonstrated herewith, but unfortunately the centre of elasticity does not match the excitation vector precisely. The centre of elasticity would have to be moved additionally 45 mm into the direction of the back end of the conveyor, do match the force vector.

Explanations for the difference between existing value and calculated value will be found in slight mistake calculating the mass distribution of the conveying element to the spring centre points of the conveyor and production variation in the stiffness of the supplied springs. It can be expected, that the motion of the goods over the full length of the conveying element will be much more uniform, but still a small differences of the amplitudes in z-direction will be found.

In the next step, the motion under operation conditions of the vibratory conveyor has to be analysed. The acceleration sensor is fixed to the geometrical centre of the conveying element in x-direction with its recording orientation in z-direction. This position and orientation is identical to the recording situation during the analysis of the original system and supplies comparable data.

The data record showing again a clear signal of 16.50 Hz as in the first test. Again the expected signal of 16.00 Hz as described in the manual of the vibratory conveyer, is not matched precisely. This confirms the assumption of a slight inaccuracy of the transformer. Due to the smallness of the difference, this inaccuracy is not corrected and the potential influence to the results is neglected.

Figure 63 shows the excitation signal of the conveying element, which is identical to the original signal.

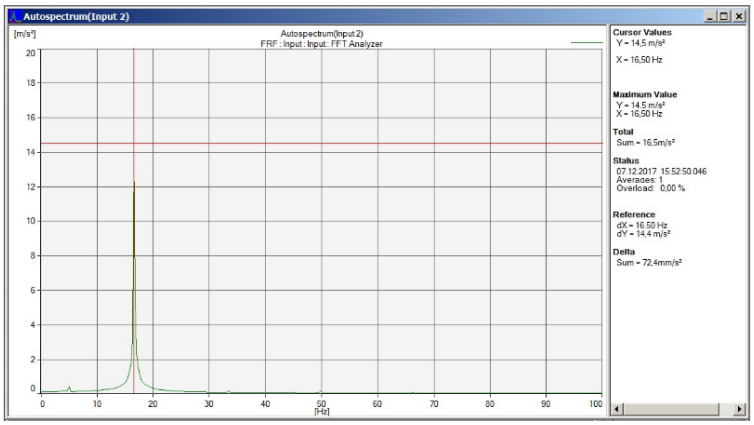

Source: Own source

Figure 63: Excitation frequency of the modified vibratory conveyor

Identical to the test series of the original system, the motion of the reference dots is analysed. The position of the reference dots has not been changed and is recorded by a photo camera using slow shutter speed. Doing this, two important parameters can be identified by the same time. The first parameter is the excitation angle of the different reference dots and the second parameter is the amplitude of the conveying element in area of the reference dots. The focus again is put on the amplitude in z-direction of the conveying element.

The angles of the excited reference dots are shown in figure 64:

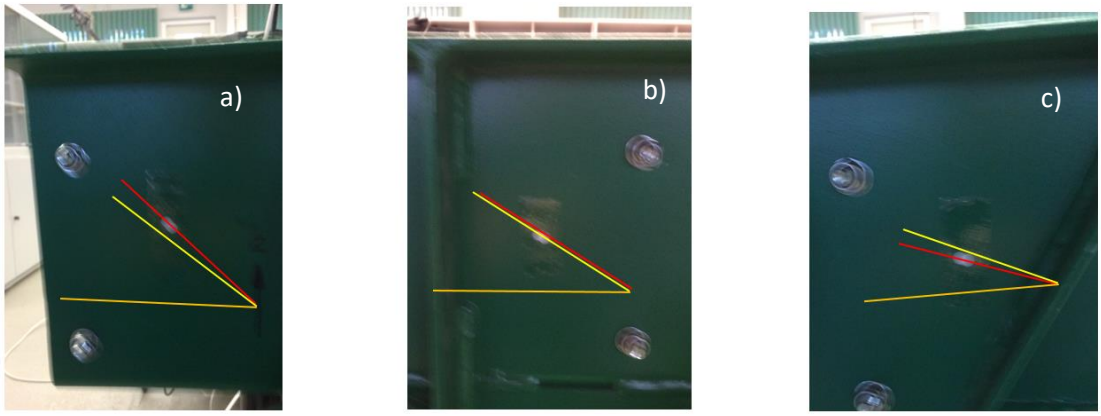

Source: Own source

Figure 64: Motion of reference marks a) close to hand over point, b) close to conveying element centre c) close to back side

Legend corresponding to figure 64:

- The orange Line represents the horizontal (parallel to x-direction)
- The yellow line represents the angle of excitation of 30°
- The red line represents the motion of the considered reference mark

The evaluation of the test shows the following results:

- The motion of reference mark “a” takes place under 34° to the horizontal i.e. +4° to the excitation direction
- The motion of reference mark “b” takes place under 30° to the horizontal i.e. the excitation direction
- The motion of reference mark “c” takes place under 26° to the horizontal i.e. -4° to the excitation direction

The analysis of the amplitude after the modification supplies the following results:

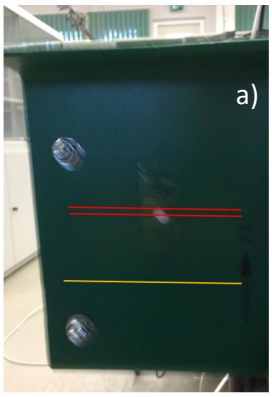

Front
Scale: 0.6:1
(Reference dot: 5 mm)
Amplitude in z-direction: 1.5 mm

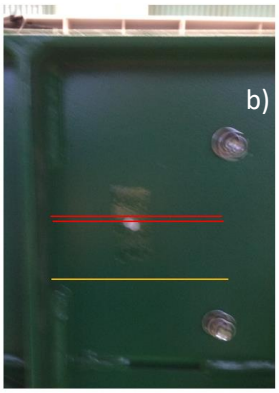

Middle
Scale: 0.6:1
(Reference dot: 5 mm)
Amplitude in z-direction: 1.3 mm

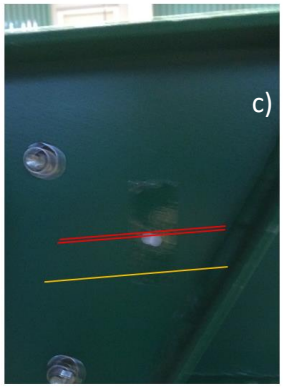

Back
Scale: 0.5:1
(Reference dot: 5 mm)
Amplitude in z-direction: 1.0 mm

Source: Own source

Figure 65: Amplitudes in z-direction of reference marks after modification

The amplitude in z-direction after the modification compared to the original values is almost identical in all referent dot positons. For the selection of the new springs, the intended amplitude has not be pre-defined, due to the intention of using standard springs for the test. The measured amplitudes in z-direction are higher than calculated, but this can be explained with the real situation of the centre of elasticity being closer to the force vector, but still not being touched by it.

The target to generate an even motion of the conveying element is nearly precisely matched by the test. The distance in x-direction between centre of elasticity and force vector centre still results in a slight unevenness of the motion over the full length of the conveying element, but the results are much closer to the ideal motion now.

It can be assumed, that a small modification of either the stiffness k_{Az} or k_{Bz} would result in the intended effect of a completely even motion. Table 5 shows the comparison of the results before and after the modification of the system:

Table 5: Comparison of angles and amplitudes before and after the modification

Reference	Original value	Value after modification	Difference
Angle at hand-over point	42°	34°	-8°
Angle in geometrical centre	30°	30°	0°
Angle at the back end	18°	26°	+8°
Amplitude at hand-over point	2.00 mm	1.50 mm	- 0.50 mm
Amplitude in geometrical centre	1.10 mm	1.30 mm	+ 0.20 mm
Amplitude at the back end	0.80 mm	1.00 mm	+ 0.20 mm

Source: Own source

6.1.5 Improvement of the conveying process

In a further step, the same sample part as in the test sequence of the original equiped vibratory conveyor is used for the representative analysis of the goods motion. As already expected, the good is conveyed showing a bigger amplitude from the beginning of the motion at the back end position in x-direction of the conveying element. But the motion is still smooth and strictly orineted into the direction of the hand over point. Over the full length of the conveying element, only a very slight cahnge of the goods motion occures. The amplitude of the good increases a little bit in the area of the geometrical centre of the conveying element but then remains nearly constant until it reaches the hand-over point. The speed of the good in x-direction is not decreasing anymore and the blocking effect does not occure.

The motion is recorded by a video camera and the video is attached in appendix 5 to this dissertation. A representative outline of the motion is shown in figure 66:

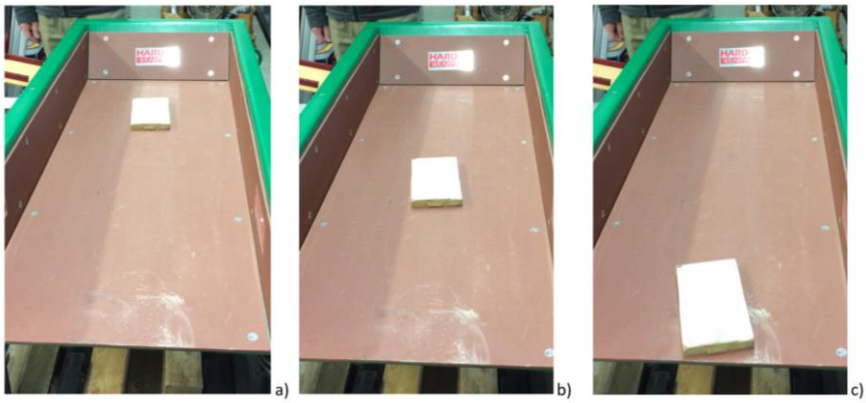

Source: Own source

Figure 66: Recorded motion of an example good after the modification. Position a) near the start point, b) in the area of the geometrical centre and c) close to the hand-over point of the conveying element

6.1.6 Transmission of Vibration to the ground after modification

After the successful optimisation of the conveyors motion, the focus has to be put on the transmission of vibration to the ground of the modified system. For this purpose, the vibration sensor is fixed to one of the two traverse steel bars of the frame, close to its geometrical centre in x-direction. Again it is oriented in z-direction to record the full spectrum of the vibrations transmitted by the conveying element.

Due to the relevance of vibration signals up to 100.00 Hz, the recorded spectrum shown in figure 67 is cut off at this value.

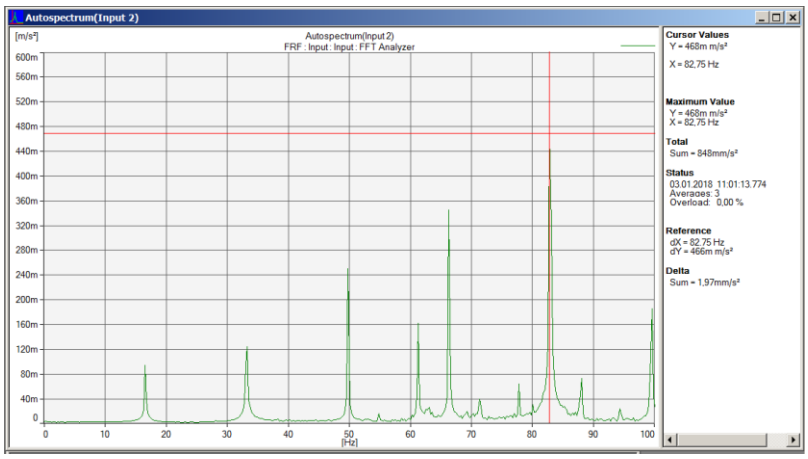

Source: Source Own source

Figure 67: Recorded spectrum of vibrations to the ground from 0 – 100 Hz after the modification

The graph shows again the 16.50 Hz excitation signal and its multiples. The amplitude of the excitation signal is nearly identical to the original installation but the signals of all multiples increased significantly. The third multiple of 66.00 Hz is lower, but the fourth multiple of 82.50 Hz is nearly identical compared to the original application and the fifth multiple of 99.00 Hz is approximately 5 times higher than in the test of the original conveyor.

This small differences of the transmission of vibrations to the ground must be mainly explained by the significant change of the spring stiffness in k_{Az} and k_{Bz} compared to the initial situation. The situation generally is very similar to the initial transmission of vibrations to the subsoil.

This result demonstrates, that the optimisation of the motion and the simultaneous reduction of vibration to the ground of a linear vibratory conveyor designed as a one-mass system is not possible. It will be tested, if a two-mass vibratory conveyor will fulfil this requirements. For this purpose a function model is designed and tested and the results are documented in the following chapter.

6.2 Model of a two-mass system

In chapter 4.2, the design principles and additional possibilities for the modification of a conveyors motion is generally explained. The additional benefit of the specific control of the transmission of forces and vibrations of a two mass linear vibratory conveyor as well is explained and supported by the implementation of general equations. For an easy recall of the principle, figure 68 shows the mechanical model of such a system once again:

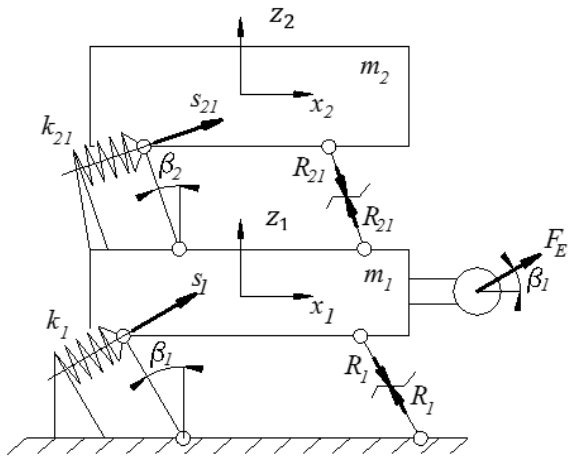

Source: Own source

Figure 68: Observed mechanical model of a two-mass linear vibratory conveyor

For the optimisation of the conveyors motion by the simultaneous elimination respectively lowering of vibration transmission to the ground, the following condition with reference to the modification of the angles β_1 and β_2 of the mechanical model is of highest interest to be observed:

$$\beta_1 = \beta_2$$

Following up equations (39) and (40) already developed in chapter 4.2, the zero displacement s_{10} of mass $m_1$and the maximum displacement s_{20} of mass m_2 can be found with the help of the corresponding equations for the case $\beta_1 = \beta_2$

$$s_{10} = \frac{(k_{21} - m_1\omega^2)F_{E0}}{(k_1 - m_1\omega^2)(k_{21} - m_2\omega^2) - k_{21}m_2\omega^2} \text{ an} \tag{64}$$

$$s_{20} = \frac{k_{21}F_{E0}}{(k_1 - m_1\omega^2)(k_{21} - m_2\omega^2) - k_{21}m_2\omega^2}. \tag{65}$$

Equation (64) can be adjusted in a way that s_{10} will become zero. This will be the case for $k_{21} = m_1\omega^2$. For that case, the minimum transmission of forces to the floor is achieved [28, 30].

To explain the importance of this case for the solution of the described problem, the optimisation of the motion of the conveying element by simultaneous elimination respectively reduction of vibration transmission to the ground, the following general graph for the amplitude s over frequency ω function of a two mass swing system will be observed.

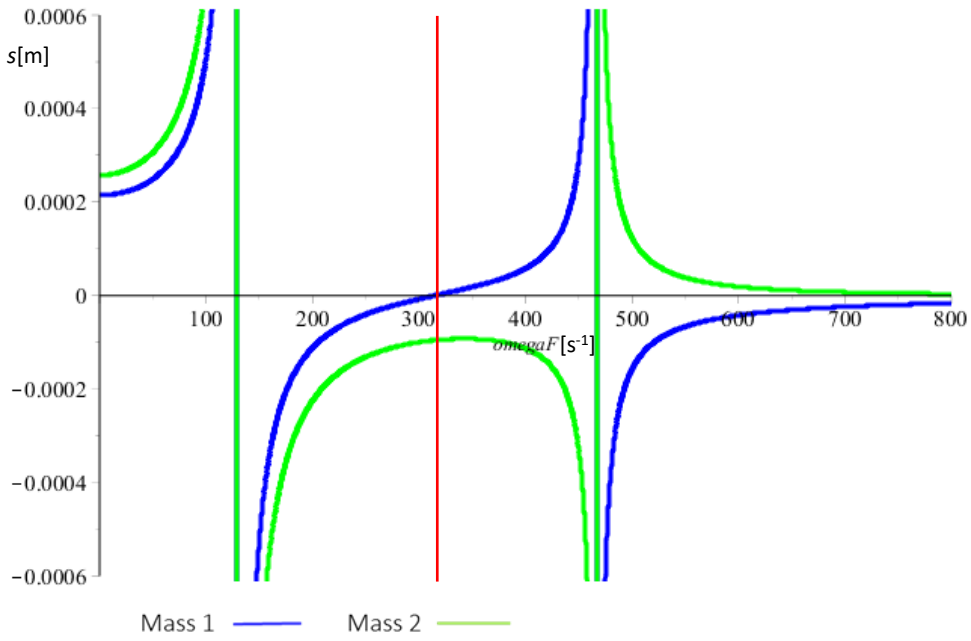

Source: Own source

Figure 69: Amplitude over frequency function of the two-mass swing system

The graph generally describes the amplitude over frequency function of two masses, m_1 with the amplitude s_1 and m_2 with the amplitude s_2. Mass m_1 is excited directly by a drive while m_2 is excited by mass m_1. Observing the area of the red line, the amplitude s_1 of mass m_1 is zero, while the amplitude s_2 of m_2 matches it's maximum.

Matching this point permanently with an excited operating two-mass conveyer would have the effect that mass m_1 remains stationary, receiving the full excitation and mass m_2 will work as absorber, transmitting the full excitation into the maximum amplitude $s_{2\,max}$. Using mass m_2 as conveying element, the optimum motion will be generated to convey the goods under optimum conditions with the maximum capacity of the conveyor. By the same time, any vibration to the ground is eliminated by the excited mass m_1.

Based on this dynamical model, the minimum transmission of vibration and forces to the floor is achieved. As soon as mass m_1 remains stationary, the total excitation is passed over to the absorber mass m_2, supplying the optimum conveying of goods [26]. To achieve the optimum performance of the system, the influence of the mass of the goods has to be taken under consideration, otherwise the conveyor will operate outside his optimum conditions immediately, as soon as the goods touching the conveying element.

This kind of two-mass vibratory conveyor based on the absorber principle has to fulfil the following important conditions very precisely to enable the intended performance:

- Masses, operation frequencies and stiffness of the implanted springs have to be concerted precisely
- The mass with corresponding tolerance field of the goods to be will have to be determined

If these conditions are chosen precisely, the intended performance of the conveyor can be realised. Figure 70 shows an example for the selection of fitting conditions and the resulting function amplitude over time.

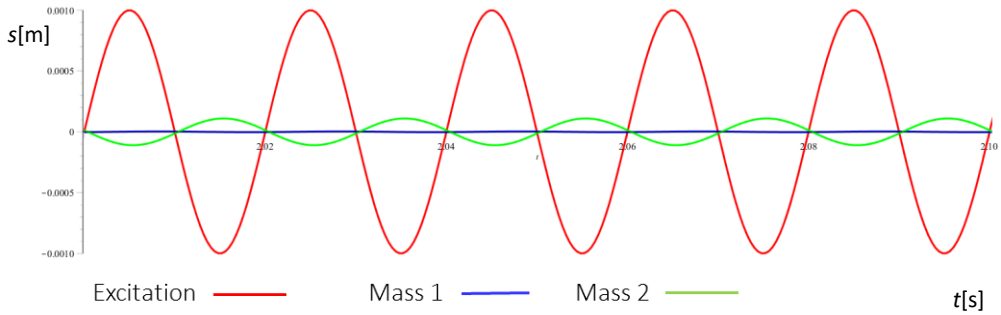

Source: Own source

Figure 70: Amplitude over time function of the implemented two-mass swing system

In the following chapter, the data for a function model for the verification and validation of tests is developed and simulated.

6.2.1 Simulation of the conveying process

As starting point for the calculation and construction of the test model is the selection of the excitation source. An electromagnetic exciter, generating an excitation of $f = 50$ Hz is available.

The intention is to run the model in resonance, to achieve the optimum performance of the conveyor. The necessary spring stiffness and masses can be determined by selecting springs and finding the corresponding masses based on equation (44). This equation is converted to

$$m = \frac{k}{\omega^2}. \tag{66}$$

With

$$\omega = 2\pi f \tag{67}$$

One target for the design of the model is the use of standard springs. To simplify the conditions, it is decided to use the same springs for mass $m_1$and mass m_2.

So the following definition can be made:

$$k_1 = k_{21} \tag{68}$$

Standard springs with a stiffness of 232860 N m^{-1} and a length of 75.00 mm are chosen for the model and two springs are installed per mass, so the total stiffness per mass is 465720 N m^{-1} based on equation (63), the necessary masses $m_1$and m_2 are determined. Doing this, all necessary mechanical parts for the design like levers, springs, screws, bearings etc. have to be dedicated correctly to the masses $m_1$and m_2. For these masses in dependence to the spring stiffness and the frequencies ω_1 and ω_2 can be calculated.

The values used for the test model are the following:

$\omega_1 = 314.16\ s^{-1}$ (corresponding to $f_1 = 50.00\ Hz$),

$m_1 = 25.88\ kg$ and

$\omega_2 = 134.15\ s^{-1}$ (corresponding to $f_2 = 21.35\ Hz$),

$m_2 = 6.45\ kg$.

For the angle is selected:

$\beta_1 = \beta_2 = 30°$

Based on these data, the function model shown in figure 71 is designed. As material steel with the specification S235 JR is selected.

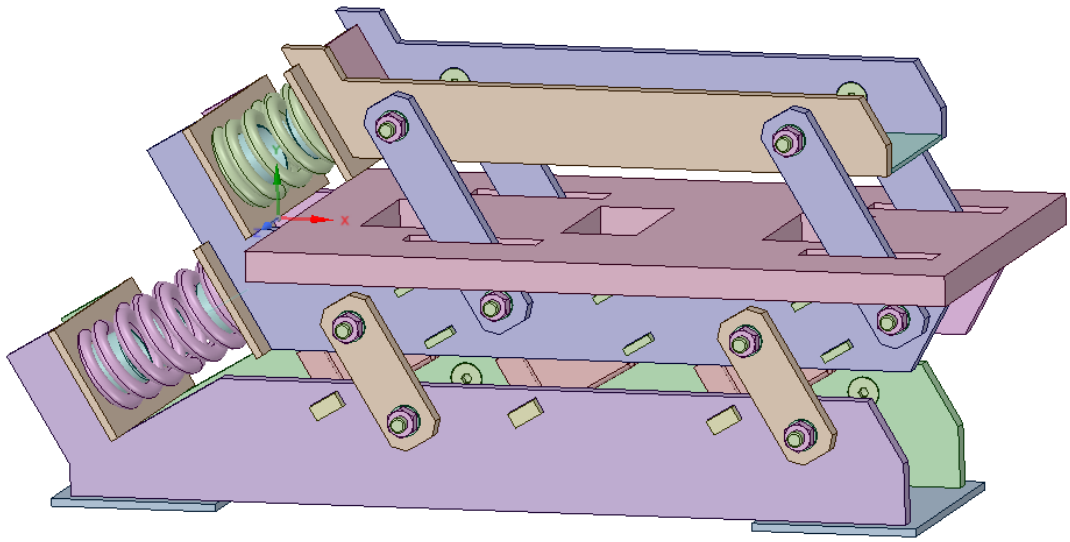

Source: Own source

Figure 71: Function model of a two-mass vibratory conveyor

Mass m_2 is assembled of the conveying element, the half-length of the two springs and the half-length guiding levers. For the calculation of the mass with help of the CAD-model, only one spring and one lever pair is calculated while the second lever pair will be added to mass m_1. This procedure supplies the most precise results. Figure 72 shows the assembled parts involved in the mass calculation of m_2 under use of the sectional view:

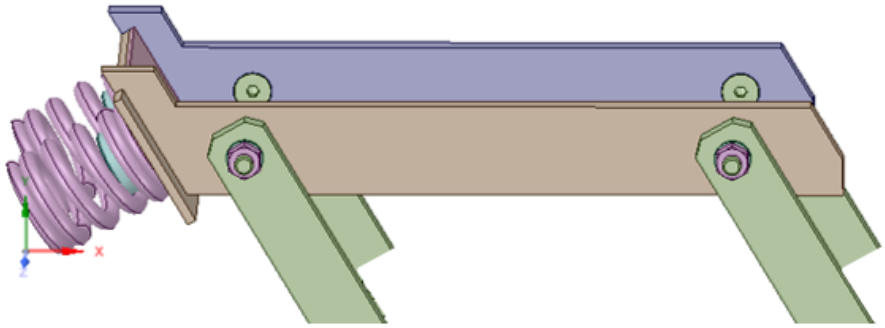

Source: Own source

Figure 72: Components of mass m_2

Mass m_1 consists of the excited mass element, the half-length of the springs connected to mass m_2, the half-length of the springs connected to the frame of the model, the half-length of the levers connected to mass m_2 and the half-length of the levers connected to the frame. For the mass calculation the same method is used, i.e. the calculation of two springs, in total four levers and the excited mass. The parts involved for the calculation of mass m_1 are shown in figure 73, again as sectional view:

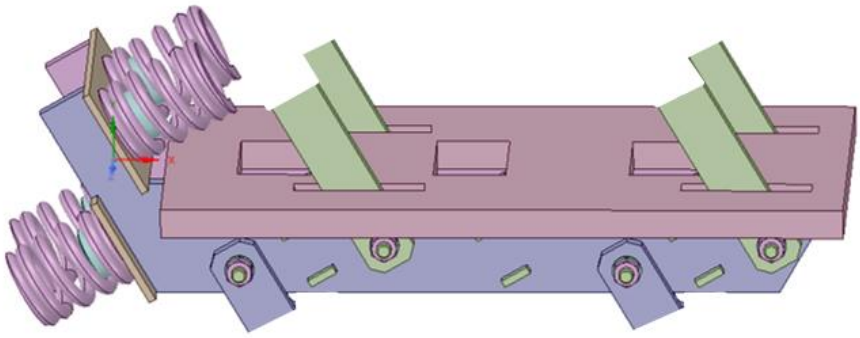

Source: Own source

Figure 73: Components of mass m_1

The frame section consist of the remaining parts and the electromagnetic exciters. It will be put to the ground with no fixation. For the completeness, the frame section with its elements and a total mass of $m_3 = 20.53$ kg is shown as sectional view in figure 74. For the determination of the requested results, the mass m_3 can be neglected.

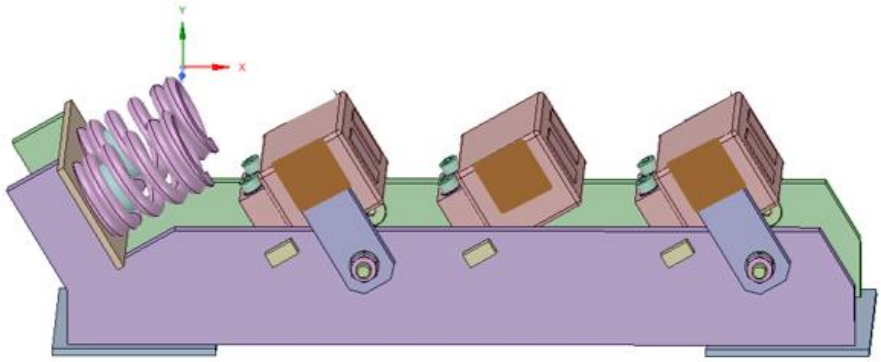

Source: Own source

Figure 74: Components of mass m_3

The motion of the masses m_1 and m_2 now can be described by differential equations. These equations are solved numerical by the use of the mathematical software "Maple". The detailed calculations are attached in the annex to this dissertation.

As result of the calculation, the graph for amplitude over time of the motion, shown in figure 75 is received:

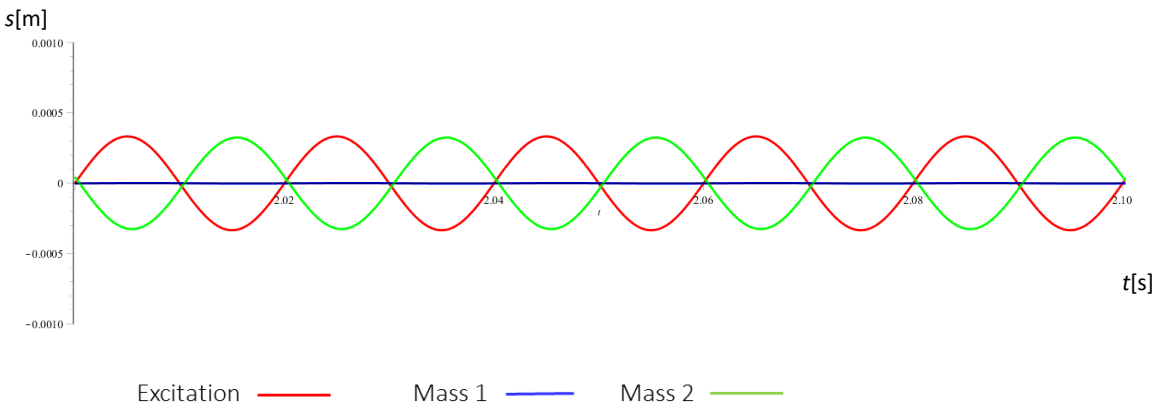

Source: Own source

Figure 75: Graph amplitude over time for the two-mass conveyor model

The graph confirms the intended motions of the masses m_1 and m_2. It shows, that the full excitation is passed over from the excited mass m_1 to the absorber mass m_2, representing the conveying element. Mass m_1 remains stationary and the vibration to the ground is cut off. This simulated motion will be confirmed and evaluated by test in the following chapter.

6.2.2 Experimental determination of the two-mass systems characteristic values

Based on CAD-drawing presented in chapter 6.2.1, the two-mass test conveyor for the verification of the calculation model has been built. It is made of laser cut steel elements using standard steel S235JR. The shape of each element including all necessary drill holes are manufactured using the laser cutting technology. For the manufacturing of the single elements, tolerances based on standard DIN 7168-1 medium have been used. The tolerance ranges defined in this standard are shown in table 6:

Table 6: Tolerances based on DIN 7168-1

Class of tolerance	Limit of deviation in mm for nominal size range in mm						
	0,5-3	**> 3-6**	**> 6-30**	**> 30-120**	**> 120-400**	**> 400-1000**	**> 1000-2000**
f (fine)	+/- 0.005	+/- 0.005	+/- 0.10	+/- 0.15	+/- 0.20	+/- 0.30	+/- 0.50
m (medium)	+/- 0.10	+/- 0.10	+/- 0.20	+/- 0.30	+/- 0.50	+/- 0.80	+/- 1.20
c (rough)	./.	+/- 0.50	+/- 1.00	+/- 1.50	+/- 2.50	+/- 4.00	+/- 6.00

Source: Own source

The medium class of tolerance has been selected due to the manufacturing precision and possibilities of the existent laser in the company manufacturing the steel element. The bearings for the levers are manufactured as bush bearings, as well made of standard steel pipe and shaft elements. Shafts with a diameter of 11.00 mm are pressure-grouted to the conveying element m_2, the excited mass m_1, and the base frame m_3 of the conveyor.

The standard steel pipes with an outer diameter of 15.00 mm as well are pressure-grouted to the already fixed shafts. The drill holes diameters of the levers having diameters between 15.05 mm and 15.08 mm depending on the tolerance manufactured. The arising gaps may are used for the lubrication with oil. The relatively big gaps of 0.025 mm to 0.04 mm will be analysed with regards to impacts on the frequencies and the motion of the conveyor.

To avoid any kind of distortion, stresses and unplanned mass increase to the conveyor, the whole construction is bonded by using a two-component metal bond. Due to the fact, that mainly pressure loads are expected to take effects on the construction, this method will generate sufficient stability to the system.

The selected springs are fit self-centred to the arbores, working by the load of the conveying element m_2 and the excited mass m_1. No additional fixation is foreseen. The electromagnetic exciters are fixed to the base frame m_3 using metric screws M8. The counter elements to the exciters are fixed to the excited mass m_1, as well using metric screws M8. The finished and ready to work installation of the two-mass linear vibratory conveyor is shown in figure 76:

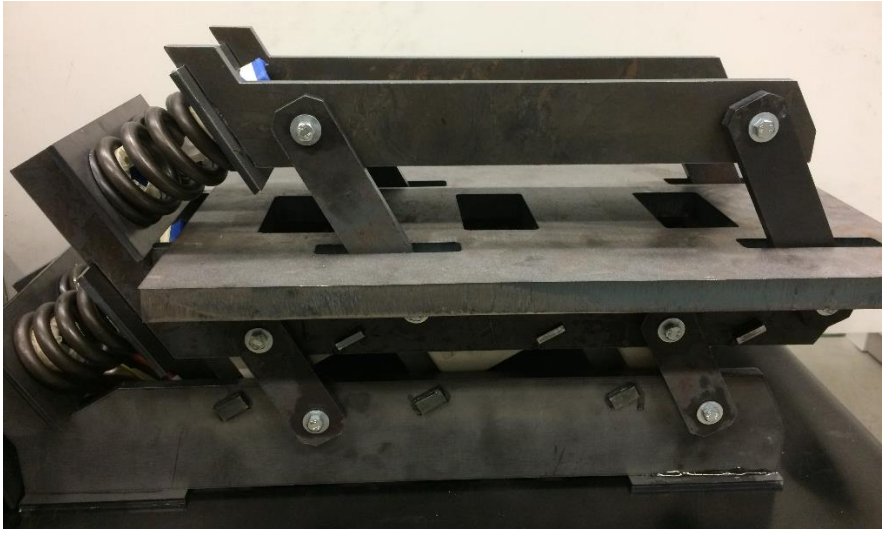

Source: Own source

Figure 76: Two-mass linear vibratory conveyor test model

The electromagnetic exciters of the new conveyor have been taken from a blow feeder type SMB 6 of the German manufacturer Sortimat. This exciter is already described in chapter 6.2.1 and is selected previous to the design of the new conveyor, due to the similarities of the masses to be moved and the stiffness of the springs comparing the new linear conveyor with the bowl feeder. The following additional technical data of the exciter shown in figure 77 are:

- 220 V, 1 pH
- Max. current: 1.13 A
- Max. achievable amplitude: 2.50 mm
- Excitation impulse: 25 Hz

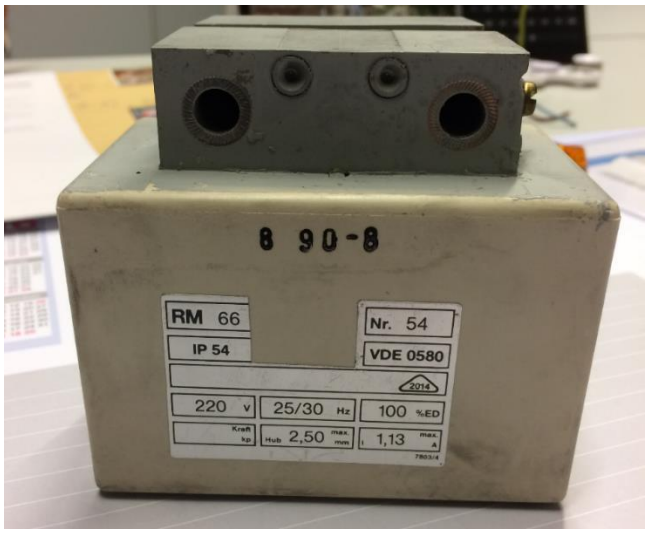

Source: Own source

Figure 77: Electromagnetic exciter and its technical data

The analysis of the two-mass new linear vibratory conveyor starts with the determination of the natural frequencies of the system. In the first test, the sensor is fixed to the conveying element m_2 in x-direction and in z-direction. The excitation occurs in recording direction of the sensor. The recording spectrum is selected from 0 – 1000 Hz to catch all representative frequencies. Figure 78 shows the results recorded in x-direction, the main intended conveying direction:

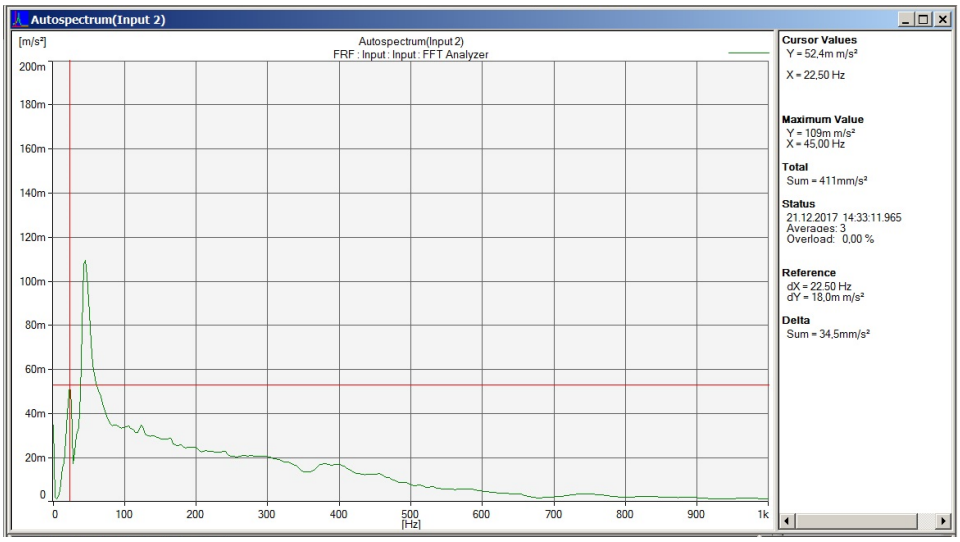

Source: Own source

Figure 78: Frequencies determined for excitation in x-direction of the conveying element mass m_2

The main frequencies identified are 22.50 Hz and 50.00 Hz which represents by far the strongest signal. Between 75.00 Hz and 600.00 Hz, a wide band of not identifiable frequencies occurring. These frequencies have to be seen as random noise caused by the imperfections of the multiple bearings.

The clear 50.00 Hz signal matches precisely the calculated value for f_1 of the excited mass m_1, in correspondence to the stiffness of the selected springs. This demonstrates the preciseness of the manufactured steel parts and of the spring stiffness.

The 22.50 Hz is slightly above the expected frequency f_2 of 21.35 Hz for the conveying element mass m_2. Presuming, that all springs having a similar preciseness, a small difference of the conveying elements mass m_2 supplies the reason for this differences.

To crosscheck the results, the natural frequencies in z-direction of the conveying element m_2 are analysed and the results are shown in figure 79:

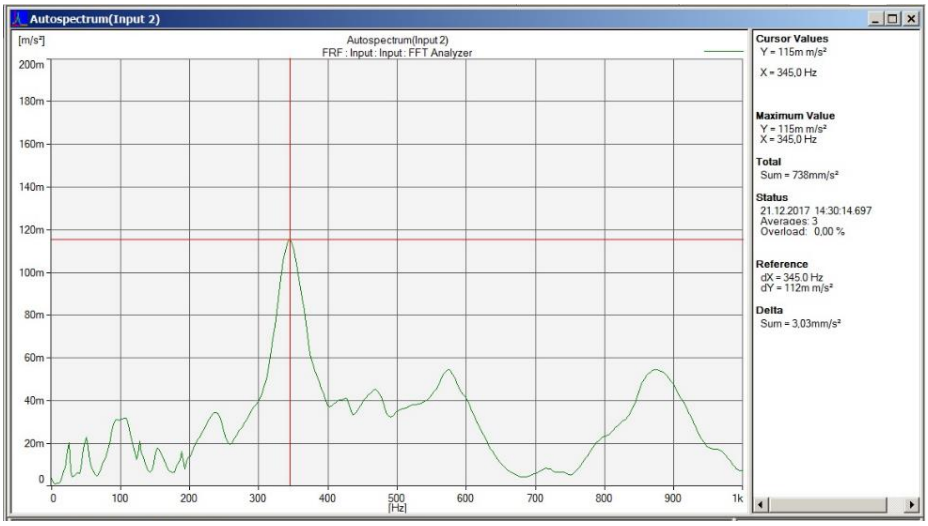

Source: Own source

Figure 79: Frequencies determined for excitation in z-direction of the conveying element mass m_2

The graph of the identified frequencies looks very different compared to the graph recorded in x-direction and frequency peeks now can clearly be identified. The frequencies 22.50 Hz and 50.00 Hz as well as their doubles and triples clearly can be identified, but the following signals cannot be put into any relation to these frequencies. It must be assumed, that in the range over 150.00 Hz, the influence of the various imperfections with regards to the fixation of the springs and the play in the bearings creating strong signals if the system gets excited in z-direction.

It can be expected, that a signal above 100.00 Hz will not have strong impact on the motion of the conveyor and these signals will not be analysed any deeper. For the further analysis on operation, the x-direction as the major conveying direction will be analysed exclusively, to avoid the influence of potentially disturbing signals.

The next analysis is done by fixing the sensor in x-direction to the excited mass m_1 and exciting this mass in x-direction as well. The results of the natural frequencies identified is shown in figure 80:

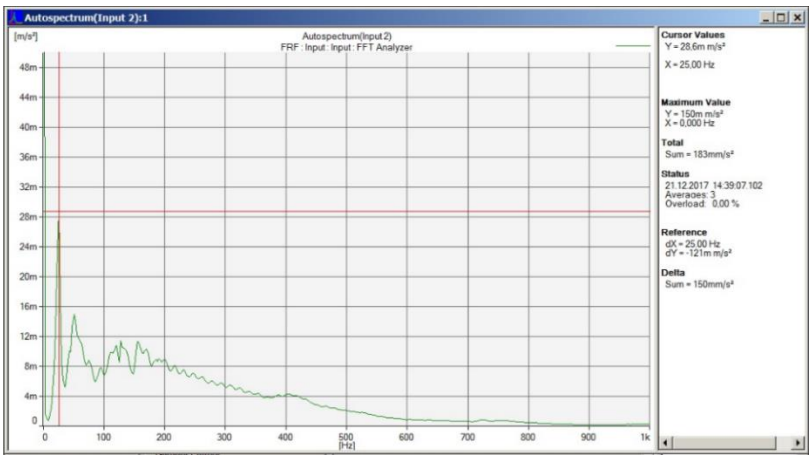

Source: Own source

Figure 80: Frequencies determined for excitation in x-direction of mass m_1

Again the 22.50 Hz and 50.00 Hz signals are identified clearly and the graph shows strong similarities to the graph shown in figure 78. The peaks above 100.00 Hz are appearing more clearly compared to the results recorded on mass m_2, but the general explanation for this random noise, various imperfections in the bearings and the fixation of the springs, has to be confirmed.

The analysis by fixing the sensor in z-direction to the excited mass m_1, exciting this mass in z-direction results in the recording shown in figure 81:

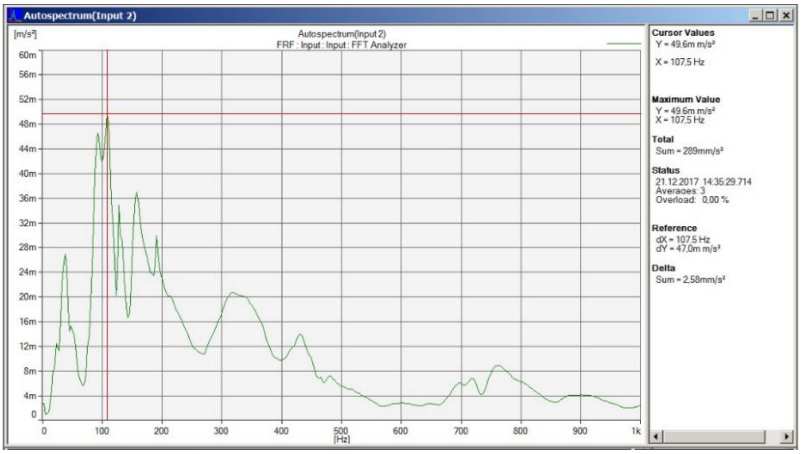

Source: Own source

Figure 81: Frequencies determined for excitation in z-direction of mass m_1

Clearly the 50 Hz signal can be identified, but already the double frequency of 100.00 Hz is surrounded by even stronger interfering signals. The 22.50 Hz signal cannot explicit be identified. This confirms the affiliation of this frequency to the conveying element m_2. The signal is absorbed by the various interfering signals caused by the already named imperfections.

Comparing the graphs shown in figure 79 and in figure 81, only a far similarity can be seen. The random noise as a different effect to the much higher mass m_1 compared to the mass m_2, representing only one quarter of m_1.

For the further analysis, again only the x-direction as the major conveying direction will be analysed exclusively, to avoid the influence of potentially disturbing signals.

In the following step, mass m_1 is excited by the electromagnetic excitation device. Doing some trials to find the best adjustment, the 50 % excitation power of the device, shown in figure 82, turns out to be the optimum operation condition. Below this adjustment, the amplitude generated is too small to supply a significant effect to the conveyor. Above the 50 % position, the imperfections of the conveyor showing effect of strong disruptive vibration effects to the system and the goods to be conveyed.

Source: Own source

Figure 82: Operation controller of 2-mass linear vibratory conveyor on 50 % operation power

On operation only very little amplitudes << 1 mm occur, so only analysis of acceleration over frequency can be done for the verification of the calculation presented in chapter 6.2.

For the first analysis on operation, the sensor for the recording is placed in x-direction to the conveying element m_2, which is the major conveying direction. The results are shown in figure 83:

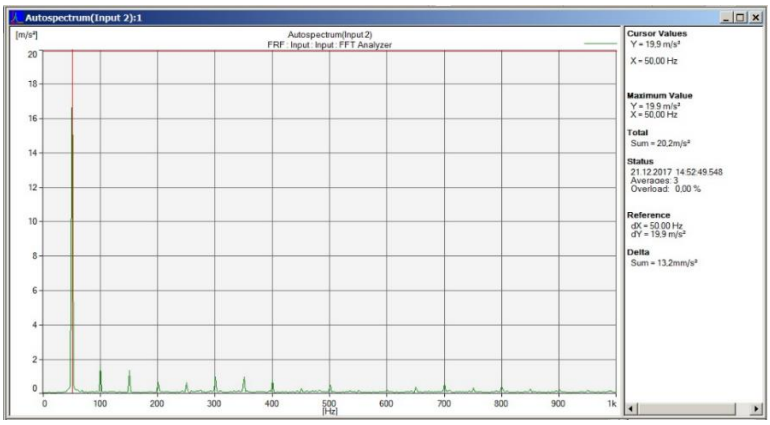

Source: Own source

Figure 83: Excitation frequency during operation in x-direction of the conveying element mass m_2

The graph shows a clear 50 Hz signal and signals of the multiples of this frequency. The acceleration of the 50.00 Hz signal is 19.90 m s^{-2}, the double frequency of 100.00 Hz already shows only 1.50 m s^{-2}. All other multiples of the 50.00 Hz signals up to 1000.00 Hz getting weaker from period to period.

The conveying element m_2 is precisely running in resonance with the excitation signal and the major natural frequency of the excited mass m_1. By the same time, is running over resonant to its own natural frequency of 22.50 Hz. Due to the lower mass of the conveying element m_2 compared to the excited mass m_1, this effect could be expected and will not have negative impact on the capacity of the linear conveyor.

Based on the general equation [1]

$$F(t) = -m \cdot \omega^2 \cdot \mathrm{s}(t) \tag{69}$$

the maximum amplitude of the conveying element can be calculated using the transformed equation

$$s = \frac{F(t)}{-m \cdot \omega^2} \tag{70}$$

with

$$F(t) = m \cdot a(t) \tag{71}$$

the equation can be simplified to

$$s = \frac{a(t)}{-\omega^2}\,. \tag{72}$$

The following parameters are known:

$$m = 6.45\ kg$$

and

$$a = 19.9\ m\ s^{-2},$$

so the calculated absolute value for the maximum amplitude is

$$s_{20} = 0.20\ mm\ .$$

Based on equation (54), an excitation force of $F_E = 90.10$ N can be determined.

The result of this calculation corresponds with the observed motion of the conveying element m_2. The precise determination by measuring is not possible with the instruments being available in the laboratory, so the result from the calculation is taken for the further contemplation.

In a second test, the sensor is installed in x-direction to the excited mass m_1. The result of this test is shown in figure 84:

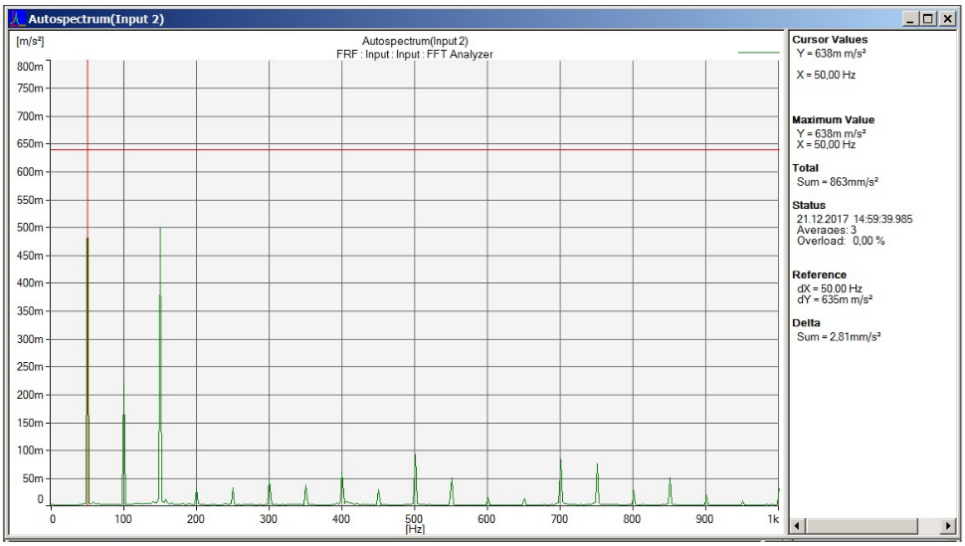

Source: Own source

Figure 84: Excitation frequency during operation in x-direction of mass m_1

Again, a clear and interference-free 50.00 Hz signal is recorded. The acceleration on 50.00 Hz shows a value of 0.638 m s^{-2}. The signals for the double and triple of the excitation frequency showing values in the range of 0.500 m s^{-2}, all further multiples are in the range below
0.100 m s^{-2} and can be neglected.

Based on equation (72), the calculated absolute value for amplitude of the excited mass m_1 is

$$s_{10} = 0.0065\ mm,$$

which is only 3.2 % of the conveying elements acceleration. The real amplitude over time function is shown in the scaled outline graph figure 85:

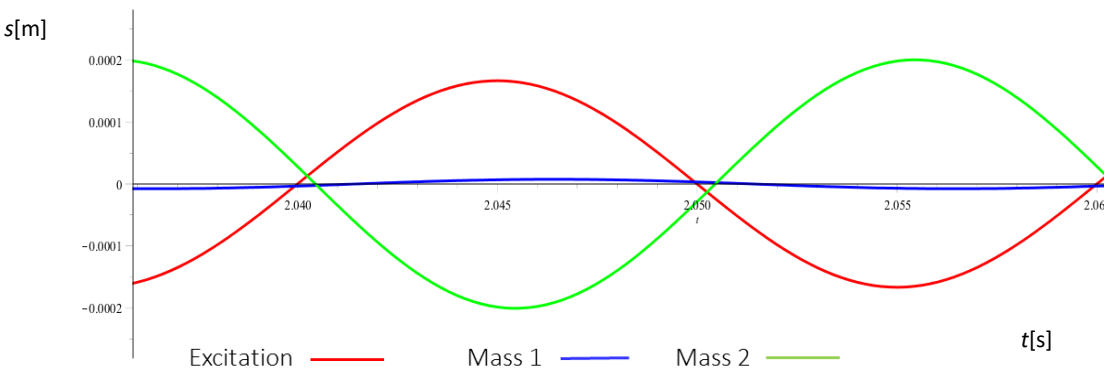

Source: Own source

Figure 85: Graph amplitude over time of the tested real two-mass conveyor

This analysis confirms the correctness of the calculation presented in chapter 6.2 and equations (64) and (65). The excited mass $m_1$is nearly in static condition with very low amplitude, while the conveying element m_2 operates in resonance with a 31.2 times higher acceleration, generating a significant amplitude for the conveying of goods.

The imperfections in manufacturing of the elements the conveyor consists of, the simple bearing type as well as the week fixation possibilities of the springs used in the system are identified to be the reason for the generation of the remaining motion of the excited mass m_1. It can be assumed, that optimized conditions would cause in even better results.

6.2.3 Effect of the conveyed goods on the two-mass system

The last trial is done to find the tolerance range for the loads conveyed by the two-mass vibratory conveyor.

Due to the fact that the conveyor is built under adherence of the optimum masses for the empty system the value of interest will be the maximum mass to be put to the conveying element, avoiding an amplitude generating the risk of destruction of the conveyor. Figure 85 shows the general idea of the test:

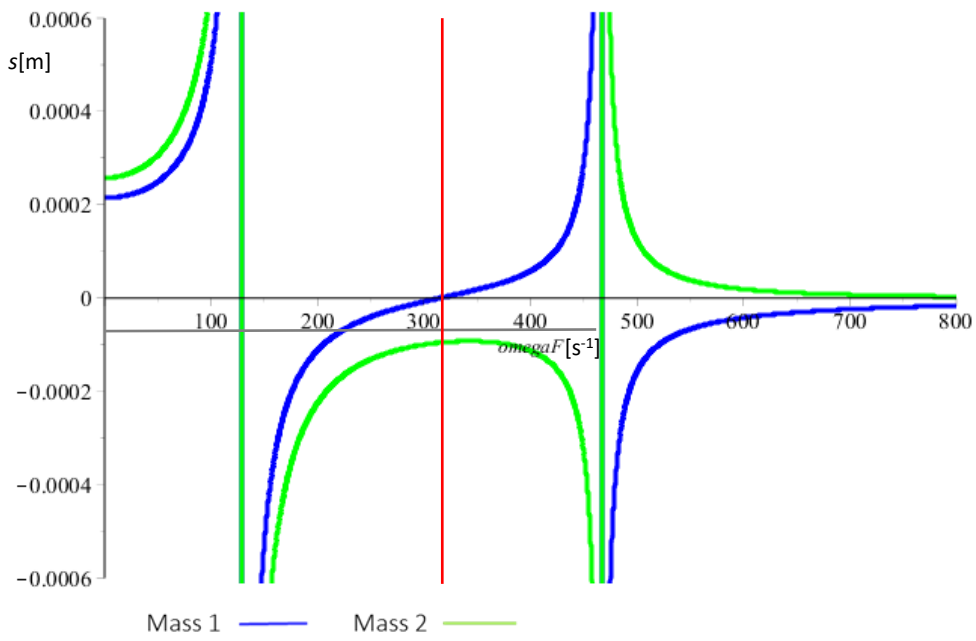

Source: Own source

Figure 86: Amplitude over frequency function of the tested two-mass swing system and its optimum operation point (red line) and its presumed amplitude tolerance range (grey line)

For the determination of the requested range, masses of 0.50 kg, 2.00 kg and 5.00 kg are put to the conveying element of the operating conveyor. The mass of 5.00 kg represents the maximum mass fitting to the conveying element. To receive reference figures for the comparison and evaluation of the test results, the different masses are set into equations (64) and (65) in advance of the tests. The results of these calculations are shown in table 7:

Table 7: Calculated amplitudes s_{10} and s_{20} for different masses on the conveying element m_2

	Case 1	**Case 2**	**Case 3**	**Case 4**
Added mass [Kg]	0.00	0.50	2.00	5.00
Total mass m_2 [Kg]	6.45	6.95	8.45	11.45
Amplitude s_{10} [mm]	0.00	0.0014	0.0018	0.0032
Amplitude s_{20} [mm]	0.204	0.189	0.156	0.110

Source: Own source

For the calculation, an excitation force $F_E = 90$ N has been presumed. The results of the calculation including the mentioned systematic deviation are transmitted into the graphs 87 and 88, showing the amplitude over mass function:

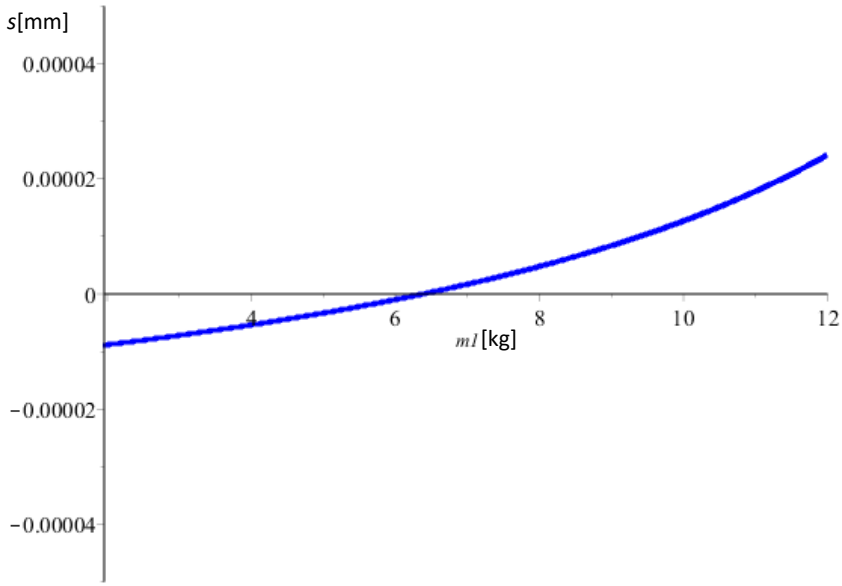

Source: Own source

Figure 87: Amplitude s_{10} for empty conveying element and added masses

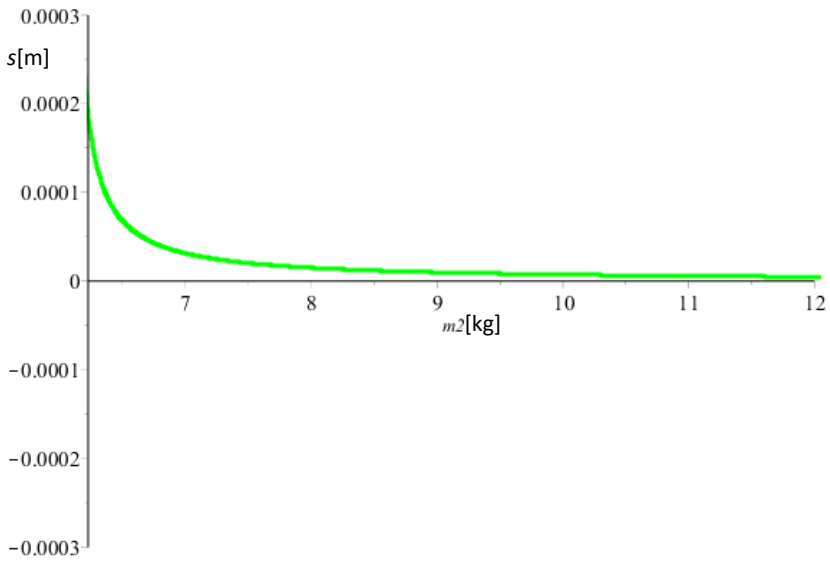

Source: Own source

Figure 88: Amplitude s_{20} for empty conveying element and added mass

The graphs showing the expected behaviour characteristics of the amplitudes, caused by the increase of mass m_2 due to addition of goods. The graphs are corresponding to figures 69 and 86, showing an increase of the amplitude s_{10} and a decrease of the amplitude s_{20} as reaction on the mass load of goods to be conveyed.

The calculated value for $s_{10}$of the unloaded conveyor of 0.0009 mm shows a big difference to the measured value of 0.0065 mm. This difference can only be explained by influences due to imperfections of the manufacturing process of the conveyor, resulting in a higher measurement values. Due to the smallness of the amplitude and the obviously sensitivity to not identifiable perturbations to the recorded real-data, it will be resigned on further tests with sensors mounted to mass m_1, due to the lack of certainty.

In addition, the transformation of the amplitude over frequency function is analysed with regards to its transformation caused by the change respectively increase of the total mass m_2 by loading the conveying element with goods. It can be expected, the characters of both amplitudes m_1 and m_2 will change and the location as well as the maximum value of the amplitude of m_2 will change.

Figure 89 shows a comparison of the characters of the graph of the unloaded system and the system loaded with 5.00 Kg:

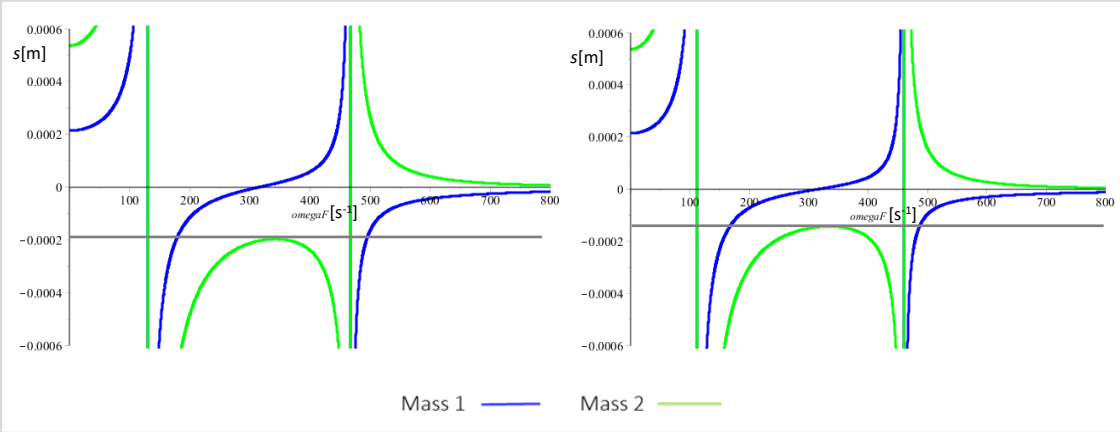

Source: Own source

Figure 89: Amplitude s_{20} for empty and loaded conveying element (left: empty, right: loaded)

It can be seen, that for the loaded system the inflexion points of the curves moved slightly in direction of the zero-point of the ω-axis. By the same time, the gradient of the m_1-curve becomes flatter in the area of crossing the ω-axis and the m_2-curve becomes wider. The maximum amplitude of the m_2-curve is slightly lower (shown by the grey lines). As a result of these graphs, the increase of loads on the system will result in lower amplitudes of the conveying element. These diagrams confirming the results of the graphs for the amplitude to mass correlation, shown in figure 87 and 88. Generally it can be expected, that a load of 5.00 Kg will not cause a strong change in the motions and conveying characteristic.

The described effect can be compensated by increasing the excitation force F_E if necessary, to avoid a decrease of the conveyors capacity. The amplitude of mass m_1 will be increasing by the same time, but due to the expected, very small changes it can be assumed that it will still be very low and of no significant influence to the transmission of vibration to the subsoil.

After the determination of the calculated results, the conveyor is loaded with the different masses as shown in figure 90 and a corresponding video showing the masses in motion is added in the appendix 6 to this dissertation.

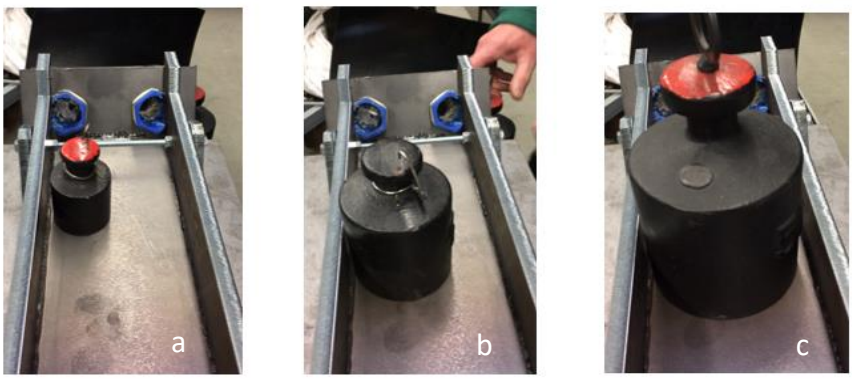

Source: Own source

Figure 90: Goods on conveying element mass m_2 during test; a) 0.50 kg, b) 2.00 kg, c) 5.00 kg

During the test, the acceleration of the conveying element m_2 is measured in x-direction and the result for the maximum load of 5.00 kg is shown in figure 90:

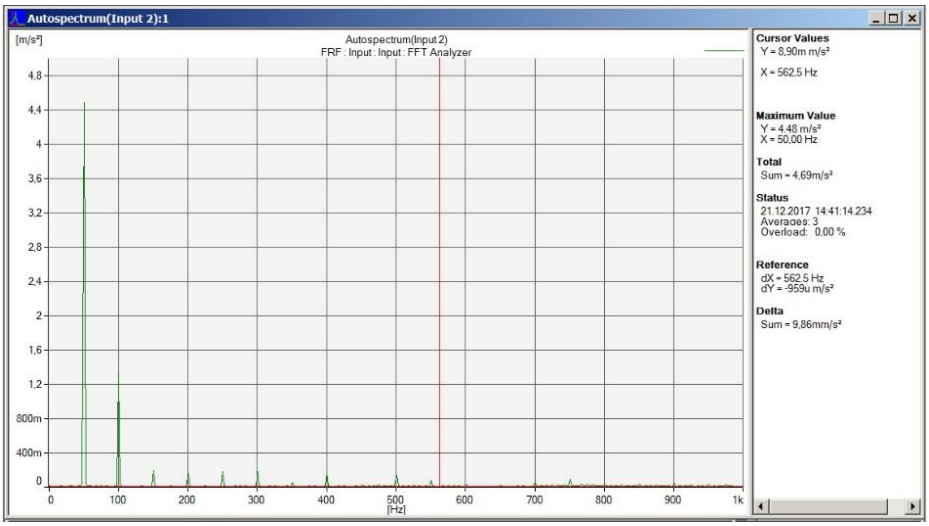

Source: Own source

Figure 91: Excitation frequency during operation in x-direction of the conveying element mass m_2 including 5.00 kg mass element

The identification of differences in the conveying velocity, documented in the video of appendix 6, is very difficult. All masses are conveyed by approximately the same speed. The result of the recorded acceleration graph for the mass of 5.00 kg shows a maximum acceleration value of 8.90 m s^{-2}, which is a significant difference to the empty conveyor. Based on equation (69), the amplitude of the loaded conveying element is now:

$$s_{20} = 0{,}09\ mm$$

Comparing the test result with the calculated result for the total added mass of 5.00 kg to the conveying element of $s_{20} = 0.11$ mm, a difference between calculated and measured value of only 0.02 mm occur. This difference can be explained by the real excitation force, being slightly smaller than the presumed 90 N, respectively some friction in the bearings of the whole system.

The result generally confirms the expectations of the test. The observed motion characteristics of the goods to be conveyed demonstrating, that the two-mass vibratory conveyor in practice does not react very sensitive to an increase of the mass by 5.00 kg, which is already 78 % increase to the mass of the conveying element. By the same time, the transmission of vibration to the ground still is massively reduced, compared to a one-mass linear vibratory conveyor.

6.2.4 Evaluation of the Two-mass system

It surely can be expected, that two-mass vibratory conveyors based on the tested design principle will be able to convey a multiple mass of goods compared to the mass of its conveying element. They will show a smooth and stable conveying characteristics by very low transmission of vibration to the ground.

Unfortunately it is not possible to match a maximum tolerance value for the permissible loadings of the tested conveyor. But due to the dimensions of the conveying element, it's mass and its support the conclusion can be done, that this type of design will allow the transport of high loads without the risk of damages or even destruction of the conveyor or parts of it.

The expected, measureable increase of the maximum amplitude by increasing the loads in the range of the test conveyors possibilities, unfortunately cannot be verified. Increasing the load by 78 %, not a decrease of the amplitude can be detected on the conveying element, having no big influence on the capacity of the conveyor.

Based on the tests it can be presupposed, that even rapid load changes, caused for example by filling up the conveying element sequential, will not have a significant impact on the conveying characteristics of the linear vibratory conveyor. This result confirms the suitability of a two-mass vibratory conveyor based on the calculated design principle for the efficient use in industrial applications.

With reference to the reduction respectively isolation of vibrations to the ground, caused by the linear vibratory conveyor and its goods, the test confirms totally the expectations. The excited mass m_1 is nearly coming to static condition and the forces are passed over to the conveying element m_2, operating as absorber mass.

Herewith, the general objective of this dissertation, the optimisation of the conveying process by simultaneous reduction of vibrations to the ground is achieved and the correctness of the developed equations and the industrial applicability is achieved and confirmed.

6.2.5 Recommendations

For future designs of linear vibratory conveyors based on the introduced and scientifically proven principle of this dissertation, the following recommendation are worth to be considered:

- The calculation introduced in this dissertation is open to be using different possibilities regarding the selection of individual spring stiffness, excited and conveying element masses and excitation frequencies. By the selection of springs with the individual stiffness, different masses or different excitation frequencies, equal or very similar results will be achieved with reference to the performance of a conveyor and the reduction of vibration to the ground. Designers will have to choose the optimum conditions for each individual system in dependence of shape and mass of the goods to be conveyed.
- Based on the experiences with the test conveyor, it has to be put special attention to the bearing technology and individual design of a conveyor. Probably the best possibility is the use of fitting and shock resistant roller bearings, to avoid the generation of additional, unwanted vibrations to the system.
- The fixation of the springs to the vibratory conveyor is of additional importance. Here as well unwanted vibrations could occur. The springs should be selected with regards to a proper pre load condition generated especially by the conveying element, to avoid unwanted bouncing effects.
- Designing and calculating the conveying element, it can be of use to pre assume a certain base load of goods to be conveyed to the conveying element, to increase the capacity range with reference to the maximum upper tolerance limit of the load.

An additional positive effect on a two-mass linear vibratory conveyor operating on the analysed type can be generated by the additional implementation of pneumatic springs to such a system. Doing this, a systematic increase of stiffness can be generated and mass variations will be compensated due to the relation presented in equation (47). A linear vibratory conveyor can easily be adjusted to convey for example coal or coke, having significant different specific masses. By a simple pressure adjustment, the same conveying conditions can be generated for the different materials. Figure 92 shows an example of a pneumatic spring element.

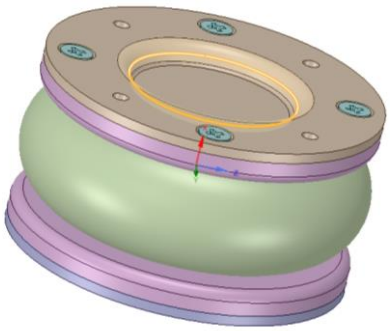

Source: Own source

Figure 92: Pneumatic spring element

Fitting this kind of pneumatic spring into a two mass linear vibratory conveyor between mass m_1 and mass m_2 in a way that the pneumatic force F_{p12} will affect the levers as shown in figure 93, the intended impact on mass variations of goods can be generated.

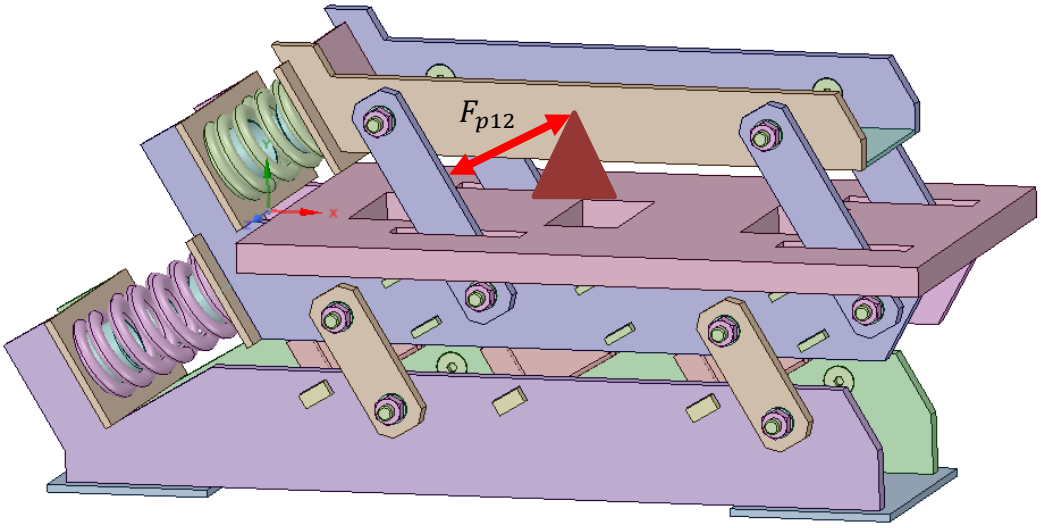

Source: Own source

Figure 93: Effective force F_{p12} caused by a pneumatic spring element

Taking all these aspects under consideration, a two-mass linear vibratory conveyor based on the principles presented, will operate under stable conditions and with very low generation of vibration to the ground.

7 Conclusion

This dissertation deals with the function and performance optimisation of linear vibratory conveyors. Target of the dissertation is to introduce equations of common validity, enabling the optimisation of the motion of existing linear vibratory conveyors and linear vibratory conveyors in the stage of their design development with regards to the optimum performance and capacity and simultaneously the reduction of transmission to the ground.

Initially, different typical designs of linear vibratory conveyors are introduced, their operating principles are explained and representative excitation devices are described. Four conveyor types are identified, where later the three most common linear vibratory conveyor design types are selected for further analysis.

Two dynamical models for linear vibratory conveyors operating on the principle of one-mass being excited and working as conveying element by the same time are set up. The corresponding equations to these principles are developed and with help of mathematic software numerical simulated. In a next step, a dynamical model for a linear vibratory conveyor consisting of an excited mass and an absorber mass, operating as conveying element is introduced. The corresponding equations for the determination of the motion forms of these types of conveyors are developed and three cases of general interest are described. A short introduction of potential goods to be conveyed by linear vibratory conveyors and the corresponding effects between conveyor and goods is given, followed by a description of the conveyors´ effect to the subsoil.

In the next step, an existing linear vibratory conveyor is deeply analysed with regards to its motion characteristics and the transmission of vibration to the ground. This is done by a detailed experimental determination of the characteristic values in the laboratory. A verification of the developed equations follows by developing an individual dynamical model of the particular linear vibratory conveyor and the numerical simulation using the determined data of the analysis. Based on the results of the numerical simulation, the parameters for the optimisation of the conveyor are calculated. The determined modifications are implemented to the linear vibratory conveyor and verified by an addition analysis of the conveyors motion and vibration transmission.

Due to the expected, unsatisfactory results regarding the transmission of vibration to the subsoil, a two-mass test vibratory conveyor is designed. It is operating based on the results of the developed equation for the use of an excited mass, passing over the full excitation to an absorber mass, with the intention to work as conveying element. By the same time, the excited mass is intended to come to rest position and isolating the vibration to the subsoil.

The idea is verified and validated by building the two-mass linear vibratory conveyor and the experimental analysis of the conveyors motion and emission of vibration.

The calculated result is matched nearly perfectly and the calculation can be used for general design purposes. Only due to some imperfections in the bearings and the fixation of the springs, the isolation of vibration to the ground is not isolated totally.

Finally, the effect of the conveyed goods mass is analysed experimentally by a stepwise increase of mass elements to the linear vibratory conveyor. As result of the limited test can be recorded, that two-mass linear vibratory conveyors built on the principle of the determined equations are operation under very stable conditions, even under the condition of heavy load changes.

The target of the dissertation, function and performance optimization of linear vibratory conveyors is fully achieved and equations as well numerical calculation tools for the general, reproducible design of linear vibratory conveyors are developed.

Literature

(In alphabetical order of the authors)

[1] ASSMANN, B. *Technische Mechanik Band 3, Kinematik und Kinetik*. Oldenbourg Verlag, 1987, ISBN: 978-3-486-58072-3.

[2] BUJA, H.O.: *Praxishandbuch Ramm- und Vibrationstechnik*. Berlin: Bauwerk Verlag, 2007. 336s. ISBN 978-3-410-21584-4.

[3] BROCH, J. T. *Mechanical vibration and shock measurements*,
Functional and power optimization of vibration conveyors, 1984. ISBN 978-8787355346

[4] DECKER, K.-H.: *Gestaltung und Berechnung*, Carl Hanser Verlag GmbH & Co. KG, 2014 ISBN 978-3-446-43856-9

[5] DRESIG, Hans, HOLZWEIßIG, Franz. *Maschinendynamik*. 8. Auflage. Berlin: Springer-Verlag, 2007. 526s. ISBN 978-3-540-72032-4.

[6] DRESIG, H.; VUL´FSON, I. I.: *Dynamik der Mechanismen*. Berlin: VEB Deutscher Verlag der Wissenschaften, 1989. ISBN 3-326-00361-7

[7] GRIEMERT, R., RÖMISCH, P.: *Fördertechnik*, Springer Fachmedien Wiesbaden, 2015. ISBN 978-3-658-09083-8

[8] GRIFFIN, M. J. *Handbook of human vibration*. 1st edition. London: Academic Press, 1996. ISBN 978-0123030412.

[9] HARRIS, C.M.: *Shock and Vibration Handbook.* Fifth edition. McGraw-Hill. NewYork, 2005. ISBN 0-07-137081-1

[10] KNAEBEL, M., JÄGER, H., ROLAND MASTEL (2009), R., Technische Schwingungslehre, 7.Auflage, Vieweg+Teubner Verlag, Wiesbaden. ISBN 978-3-8349-9435-6

[11] LANETS O.S., Kachmar R. Ya., Borovets V.M. (2016), *Jusitification of parameters of the vibratory hopper feeder with an electromagnetic drive*, Industrial Process Automation in Engineering Instrumentation, 50, 54-76.

[12] MATA, A.S., (2016): *Fundamentals of Machine Theory and Mechanisms-Kinematic Analysis of Mechanisms*, Springer International Publishing. ISBN 978-3-319-31970-4

[13] PEŠÍK, M. *Movement of the Object on Vibrating Conveyor with Respect to its Friction on the Oscillating Surface*. In *Transactions of the Universities of Košice : Research reports from the Universities of Košice*. 3st edition. Košice: [s.n.], 2012. ISSN 1335-2334.

[14] PEŠÍK, M. *Air Suspension of Vibratory Conveyors*. Young scientists 2012. VI. International Conference of Young High School Scientists of the Nysa Euroregion. Jelenia Gora. 2012. s. 96-103. ISBN 978-83-62708-66-6.
Functional and Performance Optimization of Vibration Conveyors

[15] PEŠÍK, M. *Function and Performance Optimization of Vibration Conveyors*, Liberec 2013, Dissertation.

[16] SEBULKE, J.: *Handbuch Maschinenbau*, Springer Vieweg, Wiesbaden, 2017. ISBN 978-3-319-31970-4

[17] STURM, M.: *Two-mass linear vibratory conveyor with reduced vibration transmission to the ground*. Publication for 27th International Conference on VIBROENGINEERING September 26-28, 2017 in Katowice, Polen, publicated in Vibroengineering PROCEDIA

[18] STURM, M., PESIK, L.: *Determination of a Vibrating Bowl Feeder Dynamic Model and Mechanical Parameters*, publication in technical magazine "Acta Mechanica et Automatica", ISSN 2300-5319

[19] STURM, M., PESIK, L.: *Two-Mass Linear Vibratory Conveyor*, sent for publication to 58th International Conference of Machine Design Departments ICMD 2017, 06.09.-08.09.2017, ISBN 978-80-213-2769-6

[20] STURM, M., PESIK, L.: *The Vibrating Bowl Feeder Dynamic Model*. Publication for 55th conference on experimental stress analysis EAN 2017, 30.05.-01.06.2017, ISBN 978-80-553-3166-6

[21] THEISEN, M. R.: *Wissenschaftliches Arbeiten*. 14. Auflage. München: Verlag Franz Vahlen GmbH, 2008. 303s. ISBN 978-3-8006-3596-2

[22] VETTER, G.: *Handbuch Dosieren*. Essen: Vulkan-Verlag, 2001. 473s. ISBN 3-8027-2199-3.

[23] VIBROS s.r.o.: *Manual for vibratory conveyors type FO*, 261 01 Příbram, Příbram V – Zdaboř, Česká republika, 2016.

[24] WEIGAND, A.: *Einführung in die Berechnung mechanischer Schwingungen*. Berlin: VEB Verlag Technik, 1955.

Internet sources

[25] NENDEL, K.: *Zweidimensionale Bewegungsformen bei Vibrationsförderern* [online]. 2008. [Cit.03.01.2018] Available from http://www.vibrationsfoerdertechnik.de /Download/2DBewegungsformen_WGTL_Tagungsband08.pdf.

[26] PEŠÍK, M. *Kinematics of Objects in Vibratory Conveors*. In ACC JOURNAL. 1st edition. Liberec: Technická univerzita v Liberci, 2012. [Cit. 03.01.2018] Available from http://acc-ern.tul.cz/cs/journal/item/root/acc-journal-xviii-12012>. ISSN 1803-978.

[27] PEŠÍK M. (2012), *Kinematics of Objects in Vibratory Conveyors*, ACC Journal, 1st edition, Liberec: Technical University of Liberec, [Cit. 03.01.2018] Available from http://acc-ern.tul.cz/cs/journal/item/root/acc-journal-xviii-12012.

[28] PEŠÍK, M. *A Mechanical Model of the Vibrating Conveyor*. In ACC JOURNAL. 1st edition. Liberec: Technická univerzita v Liberci, 2011. [Cit. 03.01.2018] Available from http://acc-ern.tul.cz/cs/journal/item/root/acc-journal-xviii-12011>. ISSN 1803-978.

[29] RHEIN-NADEL AUTOMATION GmbH: *Zufuhrtechnik*. [online]. [Cit. 03.01.2018]. Available from http://rna.de/Zufuehrsysteme_Basisgeraete.mfpx?ActiveID=1023

[30] RISCH, T.: 2D-*Vibrationsformen bei Vibrationsförderern*. [online]. 2008. [Cit. 03.01.2018] Available from http://www.vibrationsfoerdertechnik.de/Download/2D Bewegungsformen_WGTL_Poster08.pdf

[31] RISCH Thomas. [online]. [Cit. 03.01.2018] Available from http://www.vibrationsfoerdertechnik.de *Functional and power optimization of vibration conveyor*

[32] VIBROS s.r.o. [online]. [Cit. 13.02.2017]. Available from http://www.vibros.cz/vibracni-stroje/

Pictures

[33] Rhein-Nadel Automation GmbH [online]. [Cit. 13.02.2017]. Available from http://www.rna.de/zufuehrsysteme/

[34] Vibroprocess SrL [online]. [Cit. 03.01.2018]. Available from http://www.vibroprocess.it/en/products/7-power

[35] Action Equipment Inc. [online]. [Cit. 03.01.2018]. Available from http://www.actionconveyors.com/products/rutteltische/?lang=de

[36] Cyrus GmbH Schwingtechnik [online]. [Cit. 03.01.2018]. Available from https://www.cyrus-germany.com/de/produkte/produkt/show/schwingfoerderer-mit-schubkurbelantrieb.html

[37] Xijie Vibration Machinery Manufacturing Co. ,Ltd. [online]. [Cit. 03.01.2018]. Available from http://www.vibroxj.com/news/characteristics-of-linear-vibrating-screen

[38] PRAB Inc. [online]. [Cit. 03.01.2018]. Available from http://www.directindustry.de/industrie-hersteller/vibrationsfoerderer-71561.html

[39] Berger Maschinenbau GmbH [online]. [Cit. 03.01.2018]. Available from http://www.bergermb.de/silo-schuettgut-ruetteltisch/ruettler-silo-schuettgut/ruettler-gleichstrom.html

[40] Tekanmotor Sp. z o.o. [online]. [Cit. 03.01.2018]. Available from http://www.teknamotor.pl/oferta-szczegoly/38-transporter-wibracyjny.html

[41] JVI Vibratory Equipment [online]. [Cit. 03.01.2018]. Available from http://www.jvivibratoryequipment.com/products/electromechanical-feeders/vibrating-conveyors

[42] Action Equipment Inc. [online]. [Cit. 03.01.2018]. Available from http://www.actionconveyors.com/products/vibratory-feeders/

List of Authors Publications

[1] STURM, M., PESIK, L.: Experimental Determination and Simulation of Spring-Tensions under Working Conditions of a Vibrating Bowl Feeder. Publication for 12. International Scientific Conference Optimisation of Mechanical Systems and Machineries, 8.-10.06.2016. ISBN 978-80-553-2573-6

[2] STURM, M., PESIK, L.: *The Vibrating Bowl Feeder Dynamic Model*. Publication for 55th conference on experimental stress analysis EAN 2017, 30.05.-01.06.2017, ISBN 978-80-553-3166-6

[3] STURM, M., PESIK, L.: *Determination of a Vibrating Bowl Feeder Dynamic Model and Mechanical Parameters*, published in "Acta Mechanica et Automatica", ISSN 2300-5319

[4] STURM, M., PESIK, L.: *Two-Mass Linear Vibratory Conveyor*, sent for publication to 58th International Conference of Machine Design Departments ICMD 2017, 06.09.-08.09.2017, ISBN 978-80-213-2769-6

[5] STURM, M.: *Two-mass linear vibratory conveyor with reduced vibration transmission to the ground*. Publikation für 27th International Conference on VIBROENGINEERING September 26-28, 2017 in Katowice, Poland, published in Vibroengineering PROCEDIA

Appendix

(On attached CD)

[1] Dissertation as PDF-file:
"Dissertation_Martin_Sturm".pdf

[2] CAD-model of the tested one-mass linear vibratory conveyor:
"1 1_mass_system_asm.stp"

[3] CAD-model of the tested two-mass linear vibratory conveyor:
"2 2_mass_system_asm.stp"

[4] Video of the one-mass linear vibratory conveyors´ original motion:
"3 1_mass_original.mov"

[5] Video of the one-mass linear vibratory conveyors´ motion after the modification:
"4 1_mass_modified.mov"

[6] Video of the two-mass linear vibratory conveyors´ motion with different masses:
"5 2_mass_different_goods.mov"

[7] Maple calculation folder including:
"6 amplitude_stiffness_original_conveyor.mv"
"7 amplitude_time_original_conveyor.mv"
"8 amplitude_stiffness_simplified_model.mv"
"9 amplitude_time_simplified_model.mv"
"10 amplitude_time_lever_model.mv"
"11 amplitude_time_variant_B_conveyor.mv"
"12 amplitude_stiffness_modified_conveyor.mv"
"13 amplitude_time_modified_conveyor.mv"
"14 2_mass_system_30_30_testmodell_realfedern_v5b_k21b_fuer_modell.mv"